ENHANCEMENT OF MECHANICAL AND PHYSICAL PROPERTIES OF SILICATE BASED EPOXY NANOCOMPOSITES

BY

YASIR ABDELHAFIZ ALI ELNAIEM

A Thesis Presented to the
DEANSHIP OF GRADUATE STUDIES

KING FAHD UNIVERSITY OF PETROLEUM & MINERALS

DHAHRAN, SAUDI ARABIA

In Partial Fulfillment of the
Requirements for the Degree of

MASTER OF SCIENCE

In

MECHANICAL ENGINEERING

May 2014

KING FAHD UNIVERSITY OF PETROLEUM & MINERALS

DHAHRAN- 31261, SAUDI ARABIA

DEANSHIP OF GRADUATE STUDIES

This thesis, written by **YASIR ABDELHAFIZ ALI ELNAIEM** under the direction of his thesis advisor and approved by his thesis committee, has been presented and accepted by the Dean of Graduate Studies, in partial fulfillment of the requirements for the degree of **MASTER OF SCIENCE IN MECHANICAL ENGINEERING.**

Dr. Nesar Merah
(Advisor)

Dr. Zuhair M. Gasem

Department Chairman

Dr. Numan Abu-Dheir
(Member)

Dr. Abdul Samad Mohammed
(Member)

Dr. Salam A. Zummo
Dean of Graduate Studies

4/6/14

Date

عمادة الدراسات العليا
DEANSHIP OF GRADUATE STUDIES

Dedication

To My Parents

ACKNOWLEDGMENTS

I would like to thank King Fahd University of Petroleum & Minerals for giving me this opportunity to pursue my master of science. I would also like to thank my advisor Dr. Nesar Merah for his continuous advice, understanding, help and support throughout my master program. Special thanks are due to Dr. Muneer Alqadi for his guidance and encouragement and my committee members Dr. Numan Abu-Dheir and Dr. Abdulsamad Mohamed and not to forget my colleague Ahmed Rafiq who worked with me during this research.

TABLE OF CONTENTS

LIST OF TABLES

LIST OF FIGURES

ABSTRACT (ENGLISH)

Full Name : Yasir Abdelhafiz Ali Elnaiem

Thesis Title : Enhancement of Mechanical and Physical Properties of Silicate Based Epoxy Nanocomposites

Major Field : Mechanical Engineering

Date of Degree : May 2014

Epoxy-clay nanocomposites containing different clay loadings (1, 1.5, 2, 3 and 5wt %) were synthesized using high shear mixing technique. The optimized curing conditions for DGEBA epoxy cured with IPDA hardener were used.

The effect of degassing time and temperature on nanoclay dispersion and distribution within epoxy matrix was investigated to find the optimum degassing parameters. The morphology of the resultant nanocomposites was characterized using DSC, SEM, XRD and the Dynamic Viscometer. The enhancement of mechanical properties was investigated by performing flexural and fracture toughness tests.

The effect of nanoclay addition on water uptake at different immersion temperatures was studied. The variation of mechanical properties with nanocomposite moisture absorption was determined.

The results showed that the optimum nanoclay dispersion was achieved for a degassing temperature of 120ºC. Analysis of the XRD showed that the morphology of the resultant nanocomposite was either disordered intercalation or exfoliation.

The DSC results showed that the addition of I.30E clay led to slight decrease in glass transition temperature (T_g) with about 6% reduction for nanocomposite containing 5 wt% nanoclay.

The flexural strength of the developed nanoclay/epoxy composite was found to increase by 15% for 1.5 wt% and due to the high stiffness of the clay, as compared with epoxy resin, flexural modulus improved continuously with clay loading.

Fracture toughness improvement up to about 35% was observed for addition of 3wt% clay loading. The fractographic analysis showed that the improvements in flexural strength and fracture toughness are due to the rough corrugated surfaces of nanocomposites as compared with epoxy resin.

The diffusion of water molecules and maximum moisture uptake at ambient temperature and at 80ºC of epoxy are reduced considerably by the presence of nanoclay particles.

The glass transition temperature (T_g) for neat epoxy and nanocomposites, after water uptake, was decreased due to the plasticizing effect of water molecules which diffused into epoxy matrix.

The mechanical properties of neat epoxy and nanocomposites were affected by water uptake at different immersion temperatures. Both flexural and fracture toughness properties were found to be lower after water absorption.

ABSTRACT (ARABIC)

ملخص الرسالة

الإسم الكامل : ياسر عبدالحافظ على النعيم.

عنوان الرسالة : تحسين الخواص الميكانيكية والفيزيائية للمركبات الإيبوكسية ذات الطابع النانو سيليكاتى.

التخصـــــص : الهندسة الميكانيكية.

تاريخ الدرجة العلمية : مايو 2014 م.

فى هذه الرسالة تم تصنيع مركبات إيبوكسية ذات طابع نانوسيليكاتى تحتوى على كميات مختلفة من الحشوات النانوطينية (1,1.5,2,3 و 5 فى المائة) بإستخدام تقنية الخلط بالقص العالى . أستخدمت أفضل ظروف المعالجة للراتنج الإيبوكسى فى هذه الرسالة.

تمت دراسة تأثير زمن وحرارة التفريغ على درجة توزيع الحشوات النانوطينية فى الإيبوكسى النقى لإيجاد أفضل عوامل التفريغ . بنية المركبات التى تم إنتاجها فحصت بإستخدام الميكروسكوب الإلكترونى الماسح وأشعة إكس والماسح التفاضلى لقياس الكالورى ومقياس اللزوجة الحركى. لوحظ التحسن فى الخواص الميكانيكية بإستخدام إختبارى الإنحناء وكسر الصلابة.

تم دراسة تأثير إضافة الحشوات النانوطينية على درجة إعاقة إمتصاص الماء عند درجات حرارة مختلفة . أيضا تم دراسة تأثير إمتصاص الماء على الخواص الميكانيكية.

أظهرت النتائج أن أفضل درجة توزيع للحشوات النانوطينية كانت عند 120 درجة مئوية. أشعة إكس أظهرت أن درجة توزيع الحشوات النانوطينية كانت مختلطة بين تشتت عالى ومتوسط.

أظهرت نتائج المسح التفاضلى لقياس الكالورى أن إضافة الحشوات النانوطينية للإيبوكسى النقى أدت لإنخفاض درجة حرارة التحول الزجاجى بمقدار 6 فى المائة مع إضافة 5 فى المائة من الحشوات النانوطينية.

أظهرت نتائج إختبار الإنحناء أن إضافة 1.5 فى المائة من الحشوات النانوطينية حسنت إجهاد الإنحناء بمقدار 15 فى المائة أيضا نتيجة لصلابة الحشوات النانوطينية مقارنة بالراتنج الإيبوكسى لوحظت زيادة مستمرة لمعامل الإنحناء مع إضافة الحشوات النانوطينية.

تحسنت إجهادات صلابة الكسر بمقدار 35 قى المائة مع إضافة 3 فى المائة من الحشوات النانوطينية و أظهرت النتائج أن إضافة الحشوات النانوطينية حسنت خصائص المركب الإيبوكسى فى حجز وإعاقة إمتصاص وإنتشار الماء عند درجة حرارة الغرفة و 80 درجة مئوية . نتائج الميكروسكوب الإلكترونى الماسح أظهرت أن التحسن فى كل من إجهاد الإنحناء وإجهاد كسر الصلابة كان نتيجة لخشونة وتموج سطح المركب الإيبوكسى ذى الطابع النانوسيليكاتى مقارنة مع الإيبوكسى النقى.

إنخفضت درجة حرارة التحول الزجاجى للإيبوكسى النقى والمركب الإيبوكسى ذى الطابع النانوسيليكاتى نتيجة لتأثير جزيئات الماء التى أمتصت بواسطة الإيبوكسى.

الخواص الميكانيكية للإيبوكسى النقى والمركب الإيبوكسى ذى الطابع النانوسيليكاتى تأثرت بإمتصاص الماء عند درجات حرارة مختلفة حيث إنخفض كل من إجهاد الإنحناء وإجهاد كسر الصلابة بعد إمتصاص الماء.

CHAPTER 1

INTRODUCTION

1.1 Background

Nanocomposites contain the matrix (the continuous phase) and the reinforcement which is called the filler (the discontinuous phase) in the nanometer scale (less than 100nm).

In Polymer Matrix Composites (PMC), the load is transferred from the matrix (Polymer) to the filler (Clay or other fillers) which has high modulus of elasticity as well as high strength. Therefore the overall mechanical properties are improved. The main drawback of the addition of these fillers is their negative impact on fracture toughness because stress concentration regions will be initiated in the form of cracks which may enlarge to a critical crack size causing composite failure. To overcome this problem matrices are reinforced by adding clays of nanometer scale sizes less than the critical crack size.

Epoxy resins are thermoset polymers that are frequently used as a matrix for advanced composite materials. Their extensive use is primarily due to their superior mechanical properties, excellent adhesion, good processibility, low cure shrinkage and low cost [1]. These have made them the material of choice in some automobile, aircraft structures, Glass Fiber Reinforced Pipes (GFRP) and anticorrosion coatings.

The addition of clay into epoxy usually improves the mechanical, thermal and physical properties of the nanocomposites. It is also found to reduce the ability of moisture to penetrate in the matix. The properties improvement of these nanocomposites depends mainly on the type of polymer and clay used, clay loading and the dispersion of layered

silicate nanoclay in the epoxy matrix [2-4]. Therefore, various mixing techniques and different process parameters are used to mix the clay with epoxy and control the morphology of the resultant nanocomposite in order to achieve an exfoliated morphology which is found to have the best overall properties. Without proper dispersion of the nanoclay, defects will be created in the form of clay aggregation that develop high stress concentration regions especially with higher clay loadings [5]. During nanoclay dispersion, the basal spacing between the clay layers should be increased and the epoxy molecules go between the interplanar spacings.

The need to investigate the effect of processing parameters on the final morphology and the properties of epoxy/nanoclay system is therefore a must. For instance, degassing is considered to be an important process that helps produce nanocomposites that are free of air bubbles which form during hand and High Shear Mixing (HSM) of clay and epoxy. Proper degassing may improve the diffusion of epoxy molecules into the intergallery between the clay layers. The diffusion process depends on the degassing parameters (temperature and time). The degassing temperature and time have to be controlled to increase the interplanar spacing of the layered silicate clay and enhance the nanoclay dispersion. This will result in improvement in the nanocomposite morphology, for that either a disordered intercalation or an exfoliated morphology will form.

Water uptake is considered one of the main reasons that cause polymer degradation. For this reason, researchers are trying to add layered silicate nanoclays to epoxy resins to enhance the barrier properties and to decrease liquid absorption and diffusivity.

The water temperature greatly affects the moisture uptake because it increases the diffusion of water molecules in polymer matrices especially in such harsh environments like Saudi Arabia in which the temperature can reach up to 60ºC and the relative humidity can go up to 90% in summer.

This work will focus on preparing epoxy-clay nanocomposites with optimized degassing parameters and finding the optimum clay loading that have the best overall flexural, fracture toughness and barrier properties.

1.2 Objectives

The main objective of the proposed work is to prepare a nanoclay/epoxy composite with optimized degassing process and study the effect of adding five different loadings of Nanomer I.30E nanoclay (1, 1.5, 2, 3 and 5wt%) on flexural, fracture toughness and physical properties (water uptake at different temperatures) of epoxy resin.

The specific objectives of this research work will be:

1. To study the effect of degassing temperature and time on the morphology of epoxy-clay nanocomposites.
2. To investigate the effect of clay loadings on flexural and fracture toughness properties of epoxy-clay nanocomposites.
3. To determine how the water temperature affects the barrier property of the epoxy resin and its nanocomposites.
4. To study the effect of water uptake at different temperatures on flexural and fracture toughness properties of epoxy-clay nanocomposites.

1.3 Motivation and Justification

Because of its high mechanical and chemical properties epoxy resin is one of the most popular thermosets which is used as a matrix for Glass Fiber Reinforced Pipes (GFRP) and anticorrosion coatings. However, it is observed that liquid uptake degrades the functional, structural, and mechanical properties of epoxy-based composites. Developing epoxy resins with high resistance to moisture uptake will greatly help the manufacturers of GFR pipes, pipe fittings in Saudi Arabia (such as Future Pipe and Amiantitt-Bondstrand companies) and steel pipe coatings (like Alqahtani pipe coatings company). The current trend in the kingdom of Saudi Arabia is to use (GFRP) pipes instead of carbon steel pipes in water, seawater and crude oil transportation due to the high first cost, operation, maintenance costs of carbon steel pipes and corrosion problems associated with it as well as the availability and low cost of (GFRP) pipes. The addition of nanoclays is expected to greatly improve both matrix barrier properties as well as mechanical properties (such as fracture toughness, flexural strength, tensile strength and modulus of elasticity). The aim of this work is to find the right processing parameters and clay loadings that will result in an epoxy/nanoclay composite with optimal flexural, fracture toughness and barrier properties. The outcome of this research will benefit the companies that working in GFRP industry.

1.4 Research Methodology

The plan to fulfil the objectives mentioned above contains the following: (1) Literature review, (2) nanocomposite preparation with optimized degassing parameters, (3) exposure to water at different temperatures, (4) determination of the mechanical

properties before and after water exposure, (5) characterization of epoxy and nanocomposites.

The details of the plan mentioned above are outlined in the following sections:

1.4.1 Literature review

A complete literature review was performed in the area of epoxy-clay nanocomposites which includes the different types of epoxy and nanoclays used, the various fabrication and characterization techniques. The literature review concentrated on the mechanical tests that were performed to obtain the mechanical properties such as flexural and fracture toughness tests.

1.4.2 Nanocomposite preparation with optimized degassing parameters

For preparing epoxy- clay nanocomposites the equipment that are available in advanced materials science laboratory in the mechanical engineering department were utilized. High shear mixing method using model L5M-A Mixer was chosen to disperse the clay in epoxy matrix with the optimized mixing speed and times. The proper curing parameters (temperature and time) optimized in earlier work [6] were used.

Degassing is considered an important process that helps to enhance the diffusion of epoxy monomer into the intergallery between clay layers which improve the nanocomposite morphology and also helps in air bubbles elimination. To determine the optimum degassing parameters three different temperatures (80,100 and 120^{o}C) and two different degassing durations (2 and 4 hours) were selected.

1.4.3 Exposure to water at different temperatures

To investigate the effect of nanoclay addition and water temperature on moisture uptake, neat epoxy and epoxy/nanoclay composites were immersed in water at two different temperatures (23ºC and 80ºC) according to ASTM D570 standards. The weight gain of the samples with time, measured and recorded periodically was used to determine the variation of diffusivity and water uptake of neat epoxy and the nanocomposites.

1.4.4 Mechanical Properties

a) Effect of clay loading on fracture toughness and flexural properties

To determine the clay loading that lead to optimum improvement in the nanocomposite mechanical properties, five different clay loadings were used (1, 1.5,2,3 and 5 wt%). Flexural and fracture toughness tests were performed according to ASTM standards.

b) Effect of water uptake on fracture toughness and flexural properties

To investigate the influence of water moisture at different immersion temperatures on the mechanical properties of neat epoxy and nanocomposites, flexural and fracture toughness tests were performed after four months of immersion in tap water at (23ºC and 80ºC).

1.4.5 Characterization

Different characterization techniques such as X-Ray Diffraction (XRD), Scanning Electron Microscopy (SEM), Differential Scanning Calorimeter (DSC) and the Dynamic Viscometer have been used to study the resultant nanocomposite morphology, viscosity and fractography.

XRD analysis was performed to study the nanocomposite structures. SEM has been used to study the fracture surfaces of flexural and fracture toughness tests. DSC was employed to obtain the glass transition temperature (T_g) of neat epoxy and nanocomposite before and after water uptake at two different immersion temperatures. The Dynamic Viscometer was utilized for measuring the viscosity of neat epoxy and nanocomposites containing different clay loadings.

CHAPTER 2

LITERATURE REVIEW

2.1 Introduction

Nanocomposite materials have been widely utilized to obtain desired performance in materials for many years. They are defined as any combination of different materials, at least two, in which one of the components acts as a reinforcing element and is incorporated into another matrix material.

Reinforcing materials are typically added because they are much stronger than the matrix material. In Polymer Matrix Composites, the most popular reinforcing materials are inorganic materials such as metals or ceramics in the form of fibers, sheets, or particles whereas matrix phase is composed of natural or synthetic organic materials.

When the nanocomposite materials are processed appropriately, they combine the advantages of the inorganic material with the basic properties of the organic matrix materials to achieve required properties that are different from those of each material individually.

The main objective of processing nanocomposites is improving material properties such as tensile strength, modulus, fracture toughness, flexural strength, impact strength, reduction in moisture absorption of certain polymers.

Polymers nowadays are the most commonly and widely used synthetic materials for many applications of nanocomposites. They have the potential for applications in a number of industries such as renewable energy, desalination, electronic, automotive and

aerospace industries because of their lighter weight, low cost and high strength-to-weight ratio.

The final morphology and properties of the resultant nanocomposites depends on a number of factors such as the materials used, mixing techniques, degassing parameters and curing conditions. So the need to investigate the effect of processing parameters on the final morphology and the properties of epoxy/clay nanocomposites is a must. The main controlling factor in the properties of polymer nanocomposites in general, and epoxy in particular is the level of dispersion of the clay phase in the epoxy matrix for that two different morphologies are found to describe the state of nanoclay dispersion in polymers which are exfoliation and intercalation morphologies.

2.2 Nanocomposites Morphologies

The main objective during processing of polymer-clay nanocomposites is to have effective dispersion of the nanoclay in epoxy matrix. Without proper dispersion and distribution of the nanoclay, the advantage from high surface area of these clay particles is compromised and when they aggregate can act as defects. The agglomeration of clay particles will be locations of high stress concentration. Distribution of nanoclays describes the homogeneity throughout the sample, and the dispersion describes the level of clay layers dispersion and agglomeration in the resultant nanocomposites [6].

According to the processing steps, the polymer-clay nanocomposite has two types of morphology, i.e., intercalated or exfoliated form as shown in Figure 2.1. In the intercalated form, matrix polymer molecules are introduced between the ordered layers of clay resulting in an increase in the interlayer spacing. In the exfoliated form, clay layers

are separated and distributed within the matrix. If the basal spacing between clay layers does not increase during mixing with polymer and no polymer molecules were introduced between the ordered layers of clay then the resulting composites are conventional composites. The improvement in properties depends on a number of factors including the degree of exfoliation and the types of clay and epoxy utilized to synthesize nanocomposites [6]. The degree of exfoliation depends mainly on the processing technique used to disperse the nanoclay into epoxy. It has been found by many researchers [5, 7-9] that exfoliated nanocomposites show better material properties than their intercalated counterpart. Therefore, the interest of the majority of research is to achieve exfoliated morphology, because its structure makes available maximum surface area for interaction and load bearing.

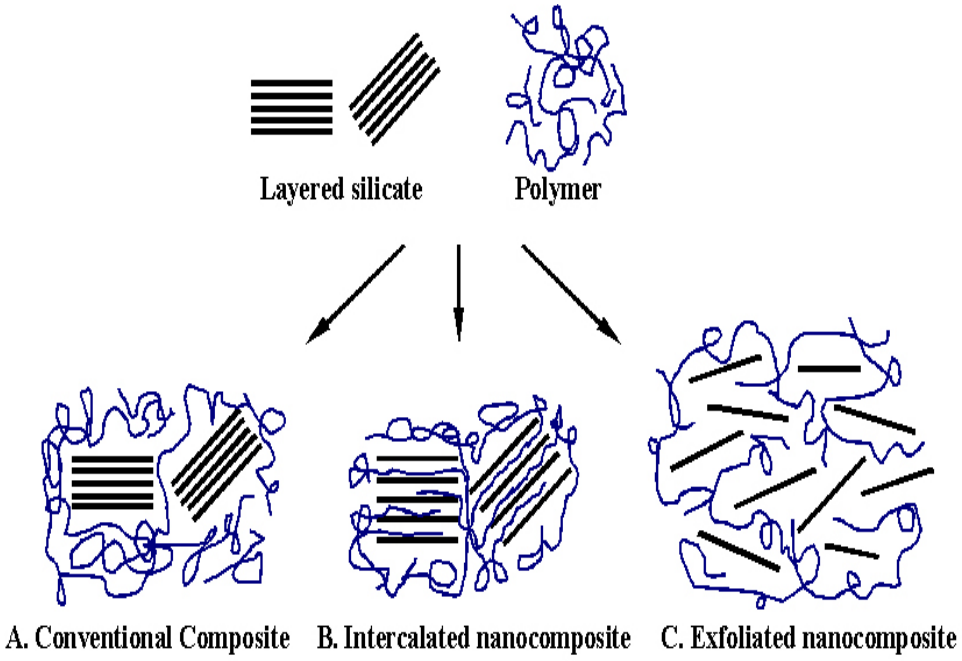

Figure 2.1: Scheme of different nanocomposite structures A) conventional composite B) intercalated nanocomposite and C) exfoliated nanocomposite [10].

2.3 Mechanical Properties of Epoxy-Clay Nanocomposites

Mechanical properties are considered to be one of the most important criteria in deciding the type of materials to use in various applications. Mechanical properties also help in the design step to predict and evaluate the performance of the material. They can be obtained by using some standardized test methods to quantify their behavior. The results of the tests are used to make a decision for suitability of a material for a specific application. In this study, fracture toughness and flexural tests were performed to compare the mechanical properties of the neat epoxy resin with those of produced nanocomposite materials.

In this section, the literature dealing with the mechanical properties of epoxy-clay nanocomposites is reviewed and discussed. Different types of nano-clay particles are considered.

Many researchers studied the effect of adding different clay types on the flexural and fracture toughness properties of different types of epoxies using various fabrication techniques. However, contradictory results have been reported with some studies showing improvement in fracture toughness due to clay addition [4, 11-18] while other researchers reported a reduction in fracture toughness [19, 20]. Similar conflicting results are reported for flexural strength, some authors found enhancement in flexural strength due to nanoclay incorporation [4, 11-13] while others reported reduction in flexural strength with clay addition [18, 21]. The reasons behind these contradictory results in both fracture toughness and flexural strength are due to the different materials (epoxy resins and nanoclays), mixing techniques, degassing process and curing cycles used.

2.3.1 Flexural Strength

Flexural test measures the force required to bend a beam under three or four point loading conditions. Li et al [11] have prepared completely exfoliated epoxy/organo-montmorillonite nanocomposites (Nano-SiO2) and found dramatic improvements in mechanical properties compared with reported traditional epoxy/o-MMT nanocomposites. The authors observed that the tensile modulus and tensile strength increased by 63% and 53%, respectively. They also reported that the flexural modulus was enhanced by 6%, flexural strength by 13.2% and notch impact strength by 36.1% at approximately 3.33 wt% clay loading (Figure 2.2).

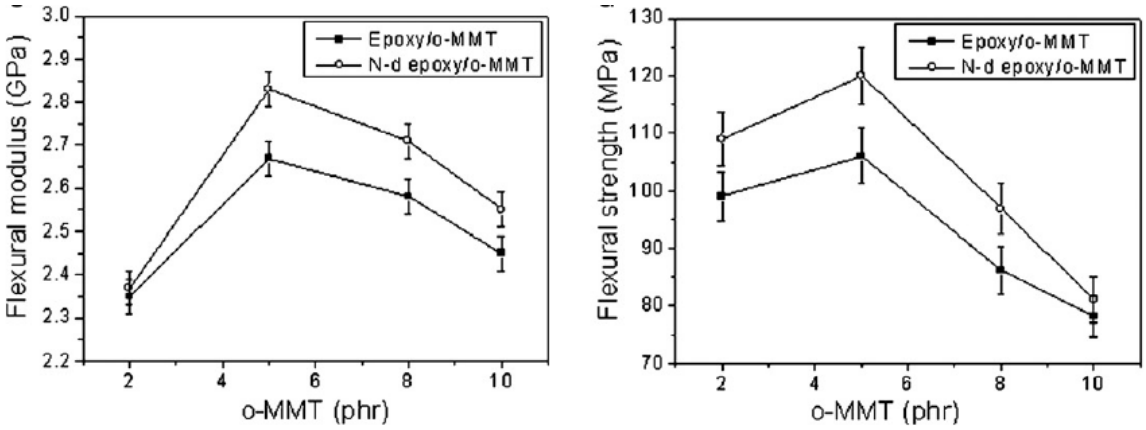

Figure 2.2: Flexural modulus and flexural strength properties of traditional epoxy/o-MMT nanocomposites and N-d epoxy/o-MMT nanocomposites [11].

Zulfli and Chow [13] synthesized hybrid epoxy composite reinforced by glass fiber and Nanomer 1.28E. Significant enhancement in flexural modulus and flexural strength as shown in Figure 2.3 were achieved. It was concluded by the authors that these improvements in mechanical properties were due to the good exfoliation of the clay in the reinforced nanocomposites, the reinforcement of the fibers as well as the interfacial bonding of the layered silicate clay and their good stiffness ability. They also observed

that at higher clay loadings the strengthening effect and the interfacial interactions were decreased with the formation of clay agglomeration this led to a reduction in flexural strength and flexural modulus.

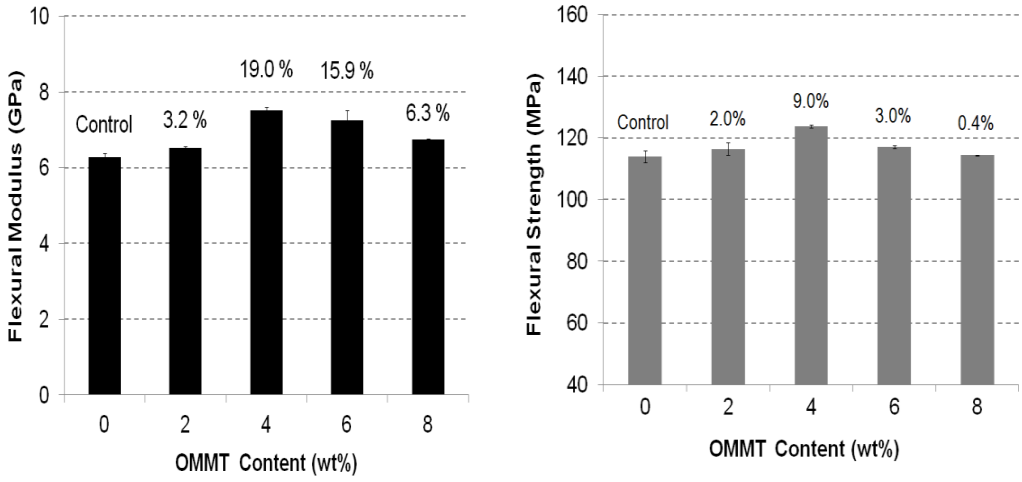

Figure 2.3: The effect of clay loadings on flexural strength, flexural modulus [13].

Akbari et al [21] prepared nanocomposites using organophilic montmorillonite (MMT) clay. Three loadings were used (1.5, 3 and 5 wt%) to investigate the effect of clay addition on both the compressive stress and the flexural strength they observed that both of the aforementioned properties of nanocomposites were lower than that of the neat epoxy. The authors claimed that the gradual decrease in both the flexural strength and the compressive stress with higher clay contents were due to the nature of clay adhesion to the epoxy layers, the ease of plastic deformation due to the presence of nanoclay particles as well as the formation of voids.

Mahmood et al [18] investigated the Cloisite 30B clay concentration's effect on the mechanical Properties. The tensile modulus was found to increase with the clay loading

but the ultimate tensile strength decreased with clay loadings higher than 1 wt%. Flexural modulus increased because of the high modulus of the nanoclay as compared to the epoxy resin. Flexural stress was found to decrease with clay loading addition. They explained that clay aggregation and the incomplete dispersion of nanoclay with higher clay loadings as well as the formation of microvoids which raised the stress concentration in the nanocomposite were the reasons behind the reduction in ultimate tensile and flexural strengths.

Kusmono et al [22] manufactured and tested epoxy-clay nanocomposites using polymerization techniques. Epoxy resin (DGEBA) and Nanomer (1.28E) modified by quaternary trimethylstearylammonium-ions nanoclay particles were used to fabricate the nanocomposites. The results showed encouraging improvements in tensile, flexural and impact strengths with respect to the pure epoxy as shown in Figure 2.4. The tensile strength, flexural strength and impact strength were increased by 41, 20 and 95%, respectively. The improvement in these properties was mainly attributed to the formation of an exfoliation morphology in the nanocomposites.

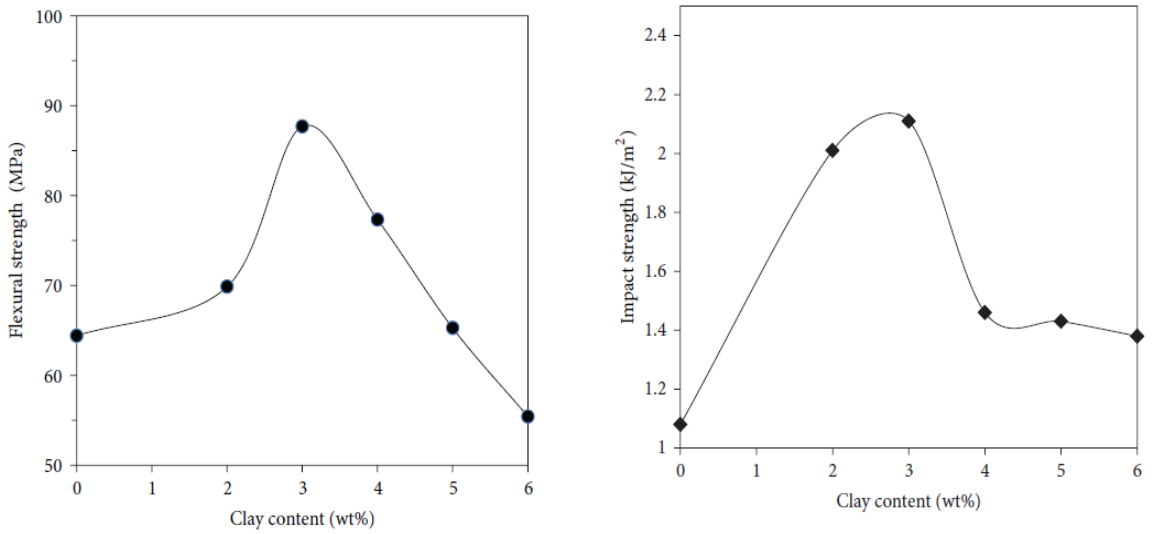

Figure 2.4:Effect of clay content on flexural and impact strength of epoxy/clay nanocomposites [22].

2.3.2 Fracture Toughness Test

The fracture toughness is a property which describes the ability of a material containing crack to resist fracture. Hong et al [12] synthesized nanocomposites using silica (SX) and rubber nano-particles (R6SX) reinforcements in order to investigate their effect on fracture toughness and Young's modulus of epoxy resin they observed a significant enhancement in both properties due to the silica nano-particles incorporation as shown in Figure 2.5.

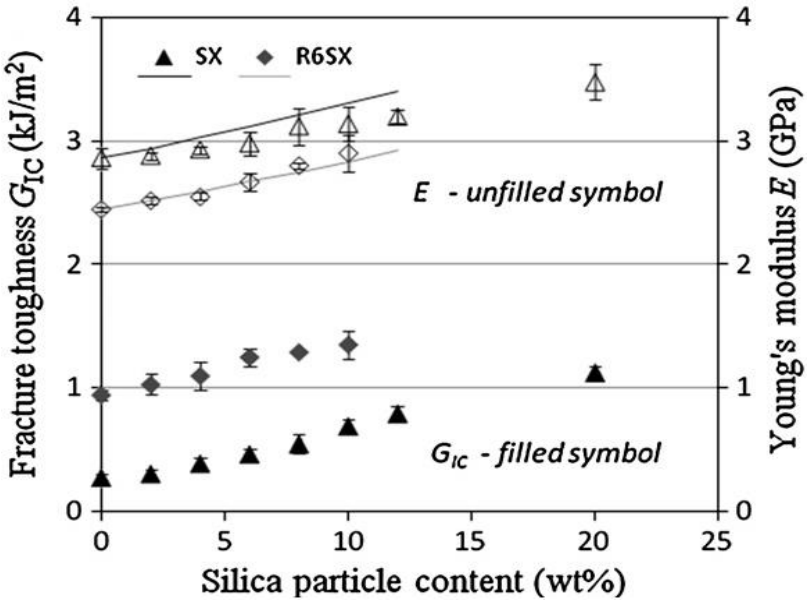

Figure 2.5: Fracture toughness and Young's modulus of nanocomposites containing different nano-silica particles loadings [12].

Improvements in fracture toughness were also observed by Zulfli and Chow [13]. They found that the fracture toughness was improved by 110% when the nanoclay content was 4 wt% as shown in Figure 2.6. They claimed that the good interfacial adhesion of the fiberglass and epoxy due to the presence of the nanoclay improved fracture toughness but at higher clay loadings clay aggregation decreased fracture toughness. Similar to Zulfli and Chow findings, Marino et al [23] prepared nanocomposites using DGEBA-based epoxy resin (EC157) reinforced by fiberglass and Cloisite 30B nanoclay. They indicated a significant enhancements in fracture toughness and crack propagation threshold of clay modified epoxy.

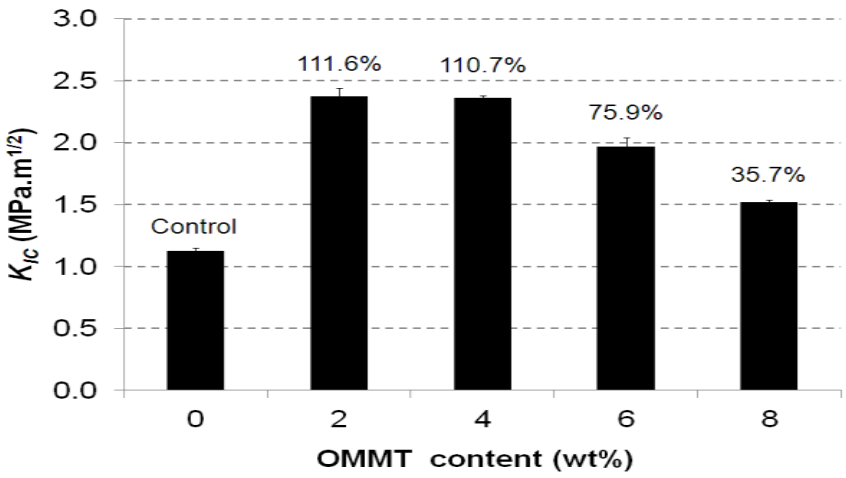

Figure 2.6: The effect of clay loadings on fracture toughness properties [13].

Zaman et al [14] conducted tensile and fracture toughness tests on epoxy and nanocomposites to investigate the effect of nanoclay addition on Young's modulus, tensile strength and fracture toughness of epoxy resin. They prepared the nanocomposite using three different types of clay modifiers to enhance the interfacial bonding strength and the exfoliation dispersion. The modifiers were ethanolamine (denoted ETH), Jeffamine M2070 (M27) and Jeffamine XTJ502 (XTJ). Improvement in both the modulus of elasticity and plane strain fracture toughness were observed with 1.3 wt% clay loading but the tensile strength was found to decrease with nanoclay addition. Also Ma et al [17] synthesized nanocomposites using two different types of curing agents (Jeffamine D230 and 4,40-diaminodiphenyl sulfone) a relatively high clay loadings were used to reinforce epoxy resin (10 and 20 wt%) enhancement in Young's Modulus, tensile strength and fracture toughness were observed due to the uniform dispersion of nano silicate.

Yao et al [15] carried out Single Edge Notch Bending (SENB) test to investigate the effect of nanoclay addition on the fracture toughness of epoxy systems. They found that the fracture load of the nanocomposites increased continuously with increasing silicon dioxide (SO_2) loading up to 3 wt%, which was considered to be the optimal clay loading. At 3 wt% clay loading an improvement of about 15.4% in fracture toughness, as shown in Figure 2.7, was observed in comparison with neat epoxy samples. The authors related the improvement in fracture toughness up to 3 wt% clay loadings to the good dispersion of the silicone dioxide in the epoxy matrix. Similar findings were reported by Kusmono et al [22]. The authors found that the fracture toughness increased by about 19% with increasing clay loading up to 3 wt%, after which the fracture toughness started to decrease. Wang et al [24] also studied the toughening effect of the addition of Nanomer PGW nanoclay in to DER 332 epoxy resin and found that the fracture toughness increased by about 77% with a clay loading of 2 wt%, after that it decreased (Figure 2.8) The micrographs for neat epoxy image was smooth and featureless surface, on the other hand, nanocomposites showed rough and corrugated surfaces (Figure 2.9).

.

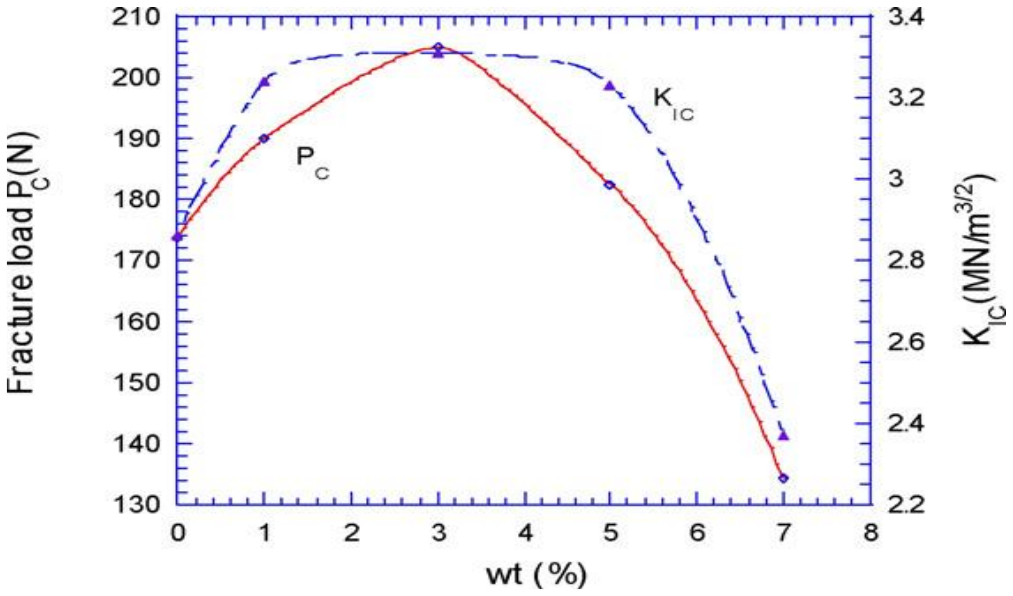

Figure 2.7: The variation of fracture load and fracture toughness with clay loadings[15].

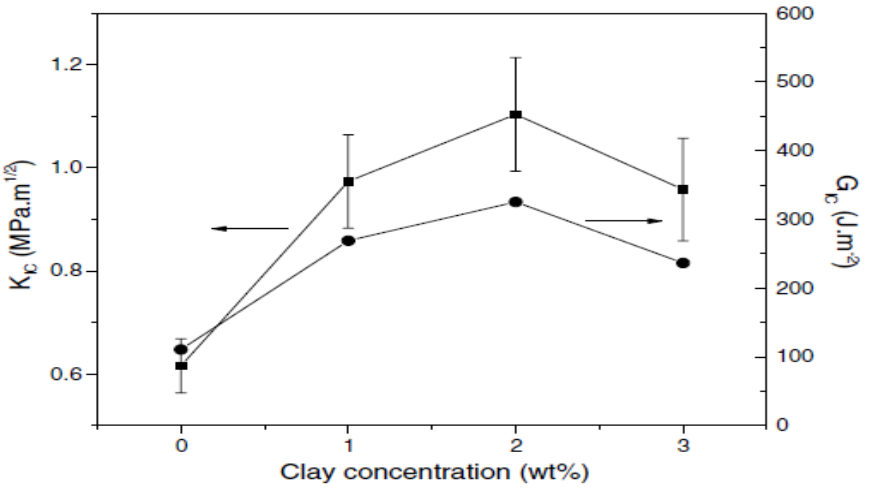

Figure 2.8: The variation of fracture toughness and the critical strain energy release rates with clay concentration [24].

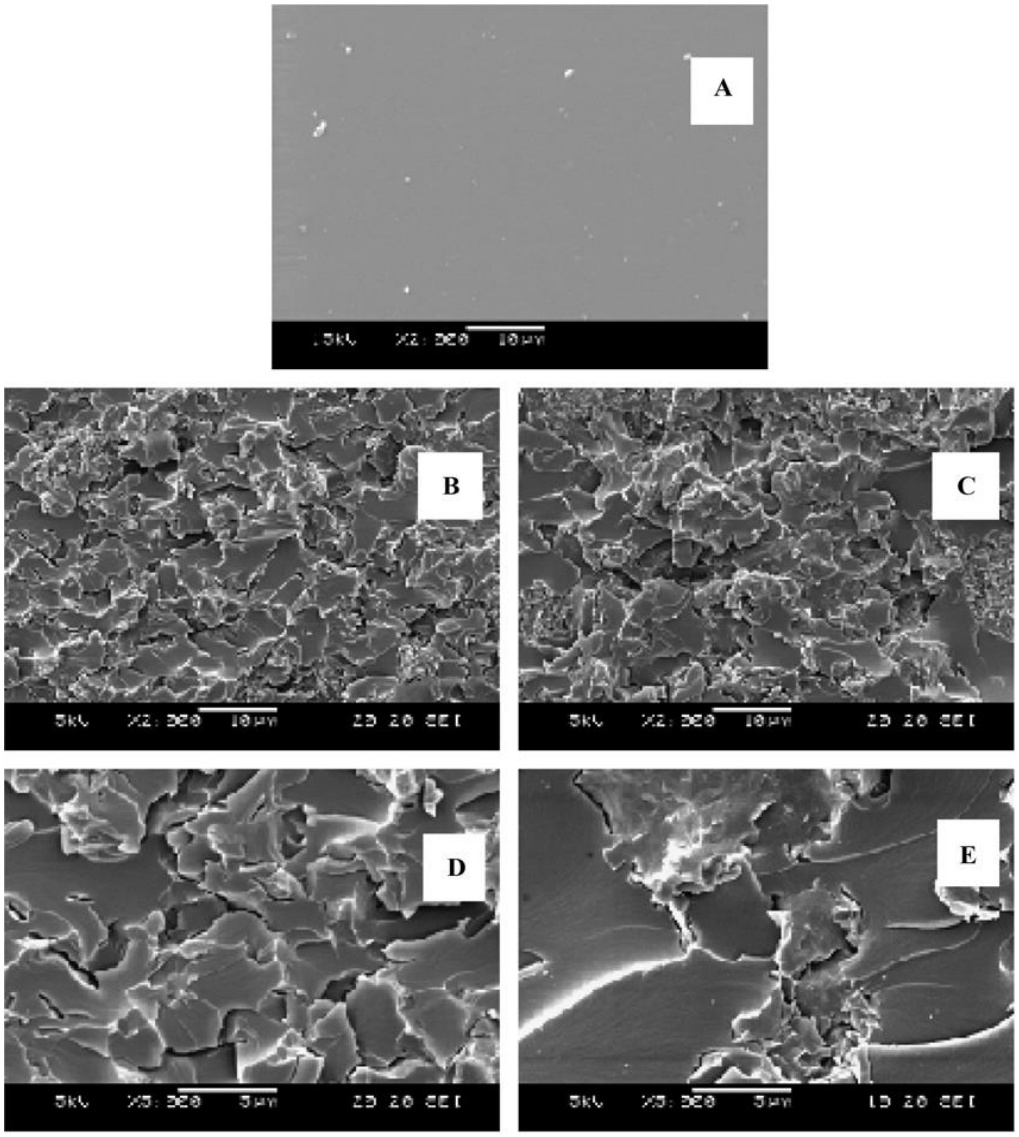

Figure 2.9: SEM micrographs for (A) pure epoxy, composites with (B) 1 wt% and (C) 3 wt% (X2000); and composites with (D) 1 wt% and (E) 3 wt% (X5000) [24].

Brunner et al [16] studied the toughening effect of the addition of functionalized organosilicate clay to epoxy resin. The authors found that the fracture toughness increased by about 50% for the nanocomposites containing 10 wt % silicate loading. The authors attributed this enhancement in the fracture toughness to the corrugated fracture surfaces which was confirmed using Scanning Electron Microscope (SEM). Mahmood et al [18] observed that fracture toughness increased linearly with clay loading up to 5wt%

with almost 25% enhancement, these improvements were explained by the increase in the roughness of the fracture surfaces with clay loading addition (Figure 2.10).

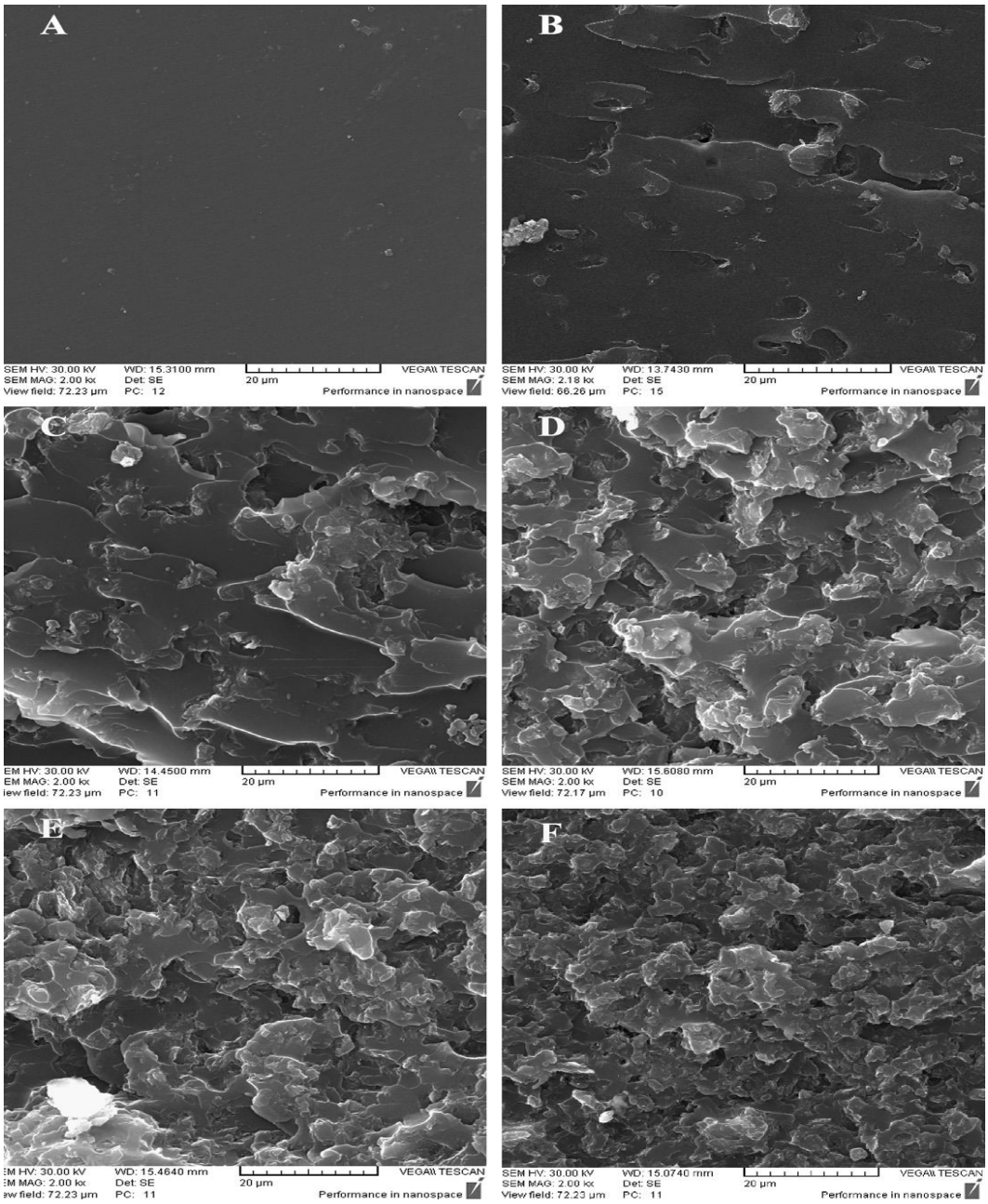

Figure 2.10: SEM micrographs of the fracture surfaces for (A) neat epoxy, nanocomposites with (B) 1 wt%, (C) 2 wt% (D) 3 wt%, (E) 4 wt% and (F) 5 wt% clay [18].

Some researchers reported a reduction in fracture toughness, for instance Arun et al [19] prepared a nanocomposites by shear blending and sonication using two reinforcements for making three different nanocomposites, at first, they used 5wt% I30.E nanoclay, 5wt% core rubber shell (CSR) reinforcement and a combination of both reinforcements (3% I30E and 2wt% CSR). The notched specimens test results showed that the neat epoxy has the highest value of fracture toughness as shown in Figure 2.11. The authors explained the reduction in fracture toughness for the nanocomposites to the formation of voids which was confirmed from the SEM micrographs.

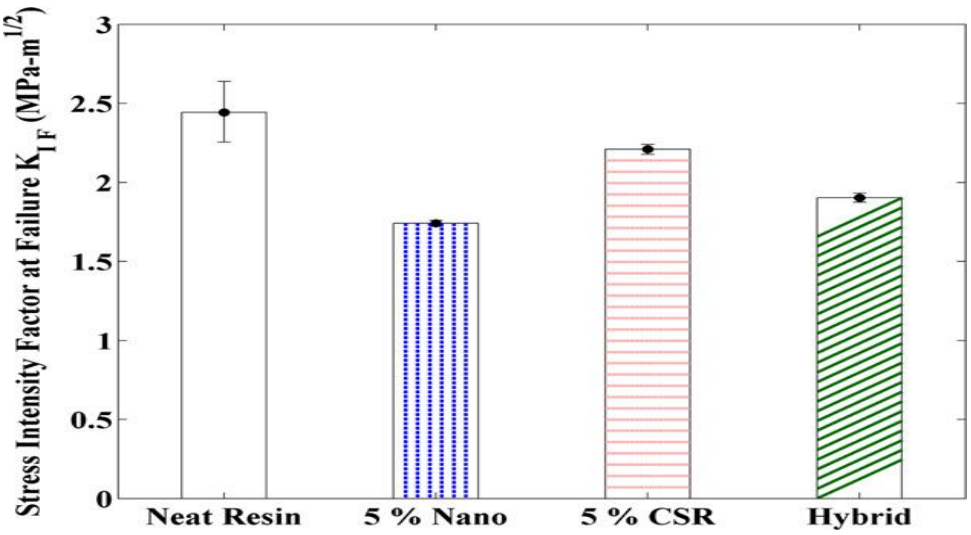

Figure 2.11: Stress intensity factor comparison for notched specimens[19].

Sung et al [20] carried out three point bending test for DGEBA epoxy and nanocomposites reinforced with surface modified MMT clay using mechanical stirring technique. Loadings of up to 10 wt% were used. The authors observed a decrease in fracture toughness as shown in Figure 2.12. They explained this deterioration by the increase in the brittleness of the nanocomposites and the presence of voids and debonding between MMT clay and epoxy.

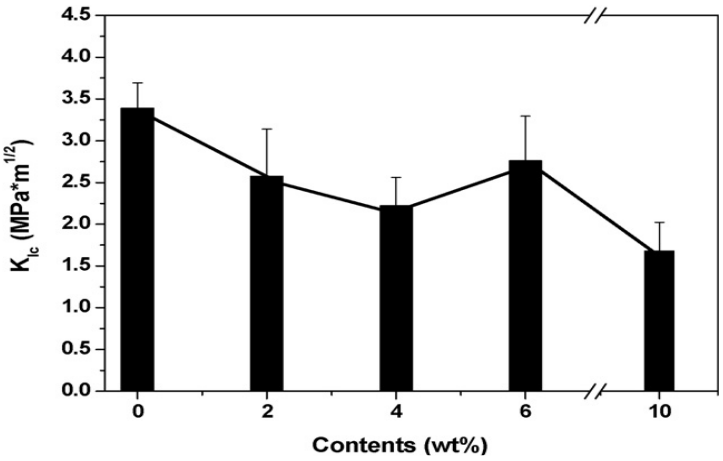

Figure 2.12: The variation in of the maximum fracture load and fracture toughness as a function of clay concentration [20].

2.4 Characterization of Epoxy-Clay Nanocomposites

Different characterization techniques have been used to characterize polymer nanocomposites. In the following sections, X-Ray Diffraction (XRD), Dynamic Viscometer (DV), Differential Scanning Calorimetry (DSC) and Scanning Electron Microscopy (SEM) will be briefly discussed.

2.4.1 X-Ray Diffraction

X-Ray Diffraction (XRD) is a widely used technique in nanocomposites research to obtain the interplaner spacing (d-spacing) using Bragg's law. So it gives an idea about the type of nanocomposite structure. The XRD can only detect the periodically stacked montmorillonite layers; disordered or exfoliated layers cannot be detected. Therefore, only the intercalated structures where individual silicate layers are separated by less than 7 nm, give a peak in XRD while no peak appears in the disordered or exfoliated structures [6].

Zulfli and Chow [13] synthesized an exfoliated hybrid composites. X-ray diffraction analysis revealed that no peaks were observed in all the nanocomposites prepared with different clay loadings as seen in Figure 2.13, Similar to Zulfli and Chow [13], Jan and Andrzej [25] prepared an exfoliated or disorder intercalation structures which was confirmed using XRD analysis.

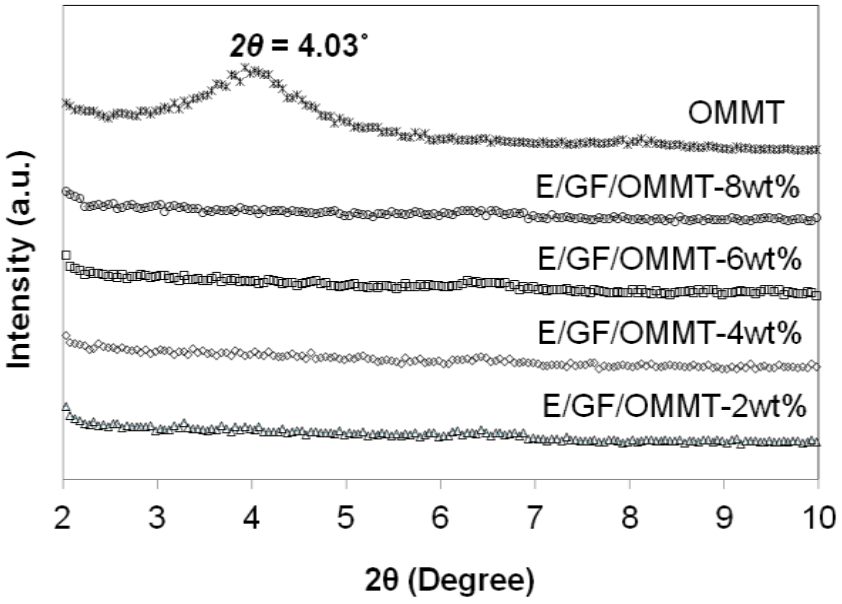

Figure 2.13: X-ray diffraction for the clay powder and composites containing different loadings [13].

Emrah et al [2] prepared Epoxy clay nanocomposite using unmodified (MMT) and modified (OMMT) clay reinforcements mixed with epoxy (DGEBA). To investigate the degree of dispersion, XRD technique was utilized. The analysis showed that an exfoliated or disorder intercalation structures were formed.

2.4.2 Differential Scanning Calorimetry

DSC characterization technique is mainly used to obtain the glass transition temperature (T_g), the melting temperature (T_m), crystallization the energy required to crystalize and

resin curing. Generally, DSC is a thermal technique that shows the endothermal and exothermal peaks assigned to T_g and T_m respectively so the degree of polymer stability is determined using DSC technique.

Andre et al [26] and Emrah et al [2] performed DSC analysis on neat epoxy and nanocomposite samples in order to investigate the effect of clay addition on T_g. The authors found that the addition of nanoclays has almost no effect on T_g . Carsten et al [27] prepared epoxy clay nanocomposites with different clay loadings they tried to study the effect of modifying the layered silicate nanoclay using different amines. They showed that the glass transition temperature of neat epoxy and its nanocomposite depend on the degree of the crosslinking density and the addition of nanoclay particles reduced the value of T_g . On the other hand Dong et al [28] showed a linear increase in glass transition temperature with clay loading addition with an improvement of about 30% at 40 wt% MMT clay the authors claimed that the improvement in T_g is due to the heat-insulation effect of MMT clay particles.

2.4.3 The Dynamic Viscometer

The dynamic viscosity expresses the substances resistance to distortion when a shear effort is being applied. The Dynamic Viscometer is used to estimate the viscosity of neat epoxy and nanocomposites containing different clay loadings. Because, if the viscosity of epoxy-clay mixture increased, higher mixing force will be required to properly mix the clay and hardener with epoxy resin, as a result more air bubbles will form. So viscometers are used to assess the dynamic viscosity to see the rate of change in viscosity with nanoclay incorporation.

Mohan et al [29] prepared a nanocomposites using two different reinforcements the unmodified clay-UC- (Na^+ montmorillonite nanoclay) and the organo-modified montmorillonite. The second reinforcement (OC) was an alkyl-ammonium based nanoclay they were added to DGEBA epoxy polymer resin. The authors found that the addition of OC and UC reinforcements increased the viscosity of neat epoxy resin. There where around 93% and 91% increase in viscosity on addition of 10 wt% OC and UC reinforcements respectively.

Ngo et al [30] synthesized epoxy clay nanocomposites using epoxy (EPONTM 828) and Cloisite 30B as nanoclay filler using high-speed mixing technique. They studied the effect of temperature, mixing time and the speed of mixing on viscosity they showed that increasing all these parameters led to an increase in the value of viscosity as shown in Figure 2.14 they related the increase in viscosity to the improvement in the level of clay dispersion as the mixing temperature, time and speed increased.

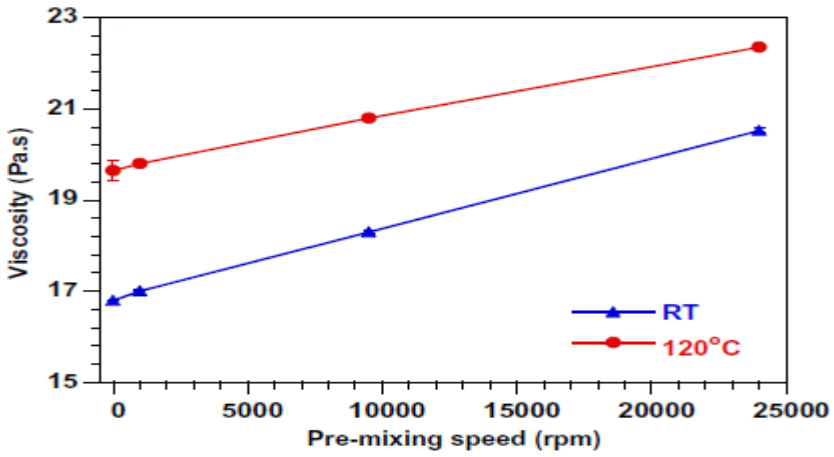

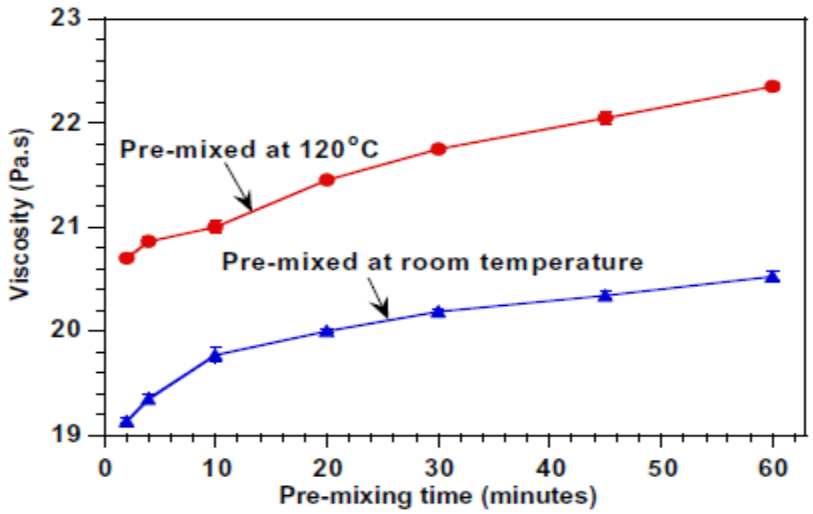

Figure 2.14: the effect of mixing speed and time at two different mixing temperatures (room temperature and 120ºC) in viscosity [30].

2.5 Water Uptake of Epoxy and Epoxy-Clay Nanocomposites

Nanoclay reinforcements are added to epoxy resins to enhance their barrier properties. Although many researchers studied the effect of nanoclay addition on diffusivity and water exposure of polymers, contradictory results have been reported. Al-Qadhi et al [5] studied the effect of I.30E clay addition on water uptake of epoxy (DGEBA) they found that the addition of nanoclay improved the barrier properties of epoxy resin and the diffusivity was found to decrease by about 51 % for 1 wt% clay loading. The increase in the tortuous path because of clay layers was the reason behind the reduction in the diffusivity. They also showed that the maximum water uptake after 300 days immersion in tap water decreased by about 22% with 5 wt% loading.

Liu el at [31] synthesized epoxy clay nanocomposites using High pressure mixing technique to study the effect of adding I.30E clay to TGDDM/DDS epoxy resin on water absorption at different exposure temperatures (23,50 and 80ºC). They concluded that the water uptake of neat epoxy and nanocomposites was linearly proportional to the square

root of time and the maximum water absorptions of the nanocomposites decreased with increasing clay loading. The observed significant reductions in the diffusivity of the epoxy resin with increasing nanoclay loading, was attributed to the tortuosity effect. Furthermore, they reported that the nanocomposites at higher environment temperatures (50 and 80ºC) were nearer to full saturation than those at a lower environment temperature (23ºC) for the same immersion time.

Alamri and Low [32] prepared epoxy clay nanocomposites using three different types of nano-fillers such as nano-clay platelets, halloysite nanotubes (HNTs) and nano-silicon carbide (n-SiC) particles to see their effect on barrier and mechanical properties. They observed that the maximum water absorption and the diffusion coefficient of neat epoxy and nanocomposites containing different types of reinforcements and loadings decreased due to the nanoparticles incorporation as compared to pure epoxy. The diffusivity was reduced by (30, 31.7 and 36.3%) with the addition of 5 wt% of nanoclay particles, HNTs and nano-SiC content, respectively. Similar to Liu el at [31] and Al-Qadhi et al [5], they concluded that tortuosity was the reason behind the reduction in the diffusivity. Similar findings were reported by Kim et al. [33] and Becker et al [34] in which they found that the addition of clay nanoparticles decreased the diffusivity and water uptake of pure epoxy. For mechanical properties the addition of 1wt% reinforcement showed better flexural strength, flexural modulus and fracture toughness than other filler content as listed in Table 2.1 and Table 2.2 before and after water exposure for about 130 days. Fracture toughness for nanocomposites after water exposure was found to be higher than the nanocomposites before water uptake. The authors claimed that the enhancement in fracture toughness can be attributed to the increased resistance to crack propagation due

to crack deflection and plastic deformation. In contrast flexural strength and flexural modulus for nanocomposites after water exposure were found to be lower than before water uptake. Many researchers have noticed the reduction in flexural strength of epoxy based nanocomposites as a result of water exposure. Similar to Alamri and Low [32], Abacha et al [35] has observed a drop in both flexural strength and flexural modulus of epoxy clay nanocomposites due to water uptake. Also Buehler et al [36] reported a reduction in flexural strength of two different composites reinforced by carbon fiber-epoxy and fiberglass-epoxy systems as a result of water moisture.

Table 2.1: Flexural strength and modulus of epoxy and its nanocomposites before and after water exposure [32].

Samples	Before placing in water		After placing in water	
	Flexural strength (MPa)	Flexural modulus (GPa)	Flexural strength (MPa)	Flexural modulus (GPa)
Epoxy	58.5 ± 2.6	0.9 ± 0.1	51.4 ± 3.1	0.7 ± 0.2
+1% nanoclay	85.2 ± 2.5	1.6 ± 0.4	52.6 ± 4.3	1.3 ± 0.2
+3% nanoclay	58.7 ± 3.9	1.5 ± 0.1	52.7 ± 4.3	1.3 ± 0.2
+5% nanoclay	61.2 ± 3.5	1.4 ± 0.2	53.0 ± 3.9	1.3 ± 0.2
+1% HNT	70.7 ± 6.2	1.5 ± 0.2	55.8 ± 6.5	1.4 ± 0.2
+3% HNT	68.2 ± 8.1	1.3 ± 0.1	52.5 ± 4.9	1.3 ± 0.2
+5% HNT	64.5 ± 4.7	1.4 ± 0.1	53.1 ± 3.5	1.4 ± 0.2
+1% n-SiC	71.1 ± 3.2	1.6 ± 0.3	59.8 ± 4.3	1.4 ± 0.3
+3% n-SiC	66.3 ± 2.9	1.4 ± 0.2	56.5 ± 5.8	1.3 ± 0.3
+5% n-SiC	61.9 ± 3.2	1.4 ± 0.1	54.5 ± 3.4	1.4 ± 0.3

Table 2.2: Fracture toughness and impact strength of epoxy and its nanocomposites before and after water treatment [32].

Samples	Before placing in water		After placing in water	
	Fracture toughness (MPa $m^{1/2}$)	Impact strength (kJ/m^2)	Fracture toughness (MPa.$m^{1/2}$)	Impact strength (kJ/m^2)
Epoxy	0.9 ± 0.1	5.6 ± 0.7	1.3 ± 0.2	6.2 ± 1.4
+1% nanoclay	1.1 ± 0.1	6.1 ± 1.3	1.4 ± 0.3	7.4 ± 1.5
+3% nanoclay	0.9 ± 0.1	6.9 ± 1.4	1.4 ± 0.2	6.6 ± 1.5
+5% nanoclay	1.0 ± 0.2	7.8 ± 2.7	1.3 ± 0.3	7.3 ± 1.7
+1% HNT	1.3 ± 0.2	5.6 ± 1.1	1.7 ± 0.2	6.5 ± 1.8
+3% HNT	1.0 ± 0.1	6.4 ± 0.7	1.6 ± 0.5	6.3 ± 1.8
+5% HNT	1.2 ± 0.1	7.0 ± 0.9	1.3 ± 0.3	6.2 ± 1.5
+1% n-SiC	1.6 ± 0.3	7.5 ± 1.1	2.2 ± 0.3	9.1 ± 1.8
+3% n-SiC	1.2 ± 0.2	7.0 ± 0.8	2.1 ± 0.3	7.9 ± 2.2
+5% n-SiC	1.1 ± 0.1	7.6 ± 1.2	1.9 ± 0.3	8.2 ± 1.4

Zainuddin et al [37] studied the water uptake of nanocomposites fabricated using epoxy (SC-15) resin reinforced with I.28E nanoclay. All the samples were immersed in hot water at two different temperatures (60 and 80ºC) for a round 90 days. The authors reported a significant decrease of about 48% in weight gain for specimens containing 2 wt% of nanoclay over neat epoxy these improvements in barrier properties was related to nanoparticles incorporation. Also they studied the effect of immersion temperatures (60 and 80ºC) on the weight gain they observed that the maximum water uptake was higher for all the wet conditions specimen's when exposed to water at (60 and 80ºC) as compared with the samples immersed in water at room temperature.

Kornmann et al [38] prepared epoxy-layered silicates nanocomposites to study the effect of the addition of organosilicate clay to epoxy resin on water uptake properties at different immersion temperatures (23 and 50ºC) for about 84 days. They showed that the water uptake at 23ºC of the neat epoxy and the nanocomposite containing 10 wt% layered silicate nanoclay were almost the same as shown in Figure 2.15 but at 50ºC the water uptake for nanocomposite was almost twice that of the neat epoxy.

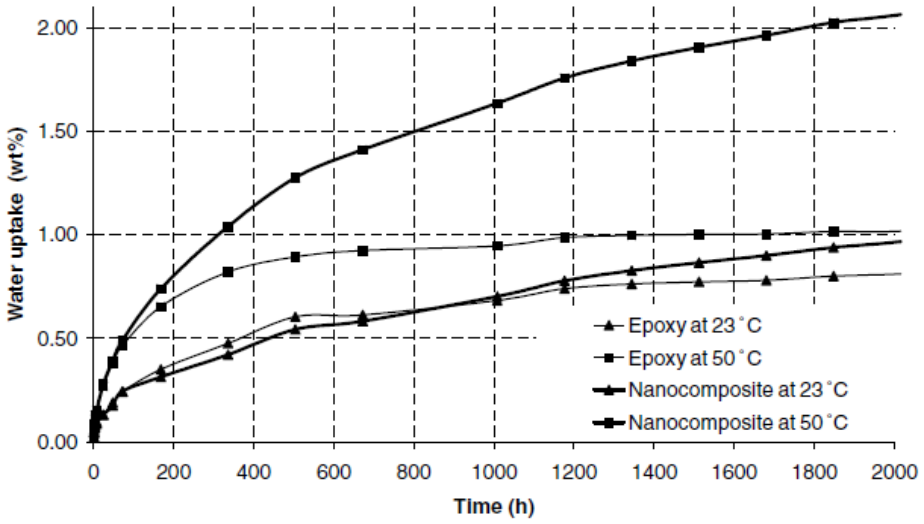

Figure 2.15: Water uptake of the epoxy and the epoxy-layered silicate nanocomposite samples at 23 and 50°C [38].

To summarize the literature review, the addition of nanoclay platelets at relatively low loadings has been shown to enhance the physical, thermal and mechanical properties of epoxy resins. Many researchers tried to look at the different factors that help to enhance the aforementioned properties. They showed that the improvement in the properties depends on types of materials (the epoxy and nanoclay), the different processes to synthesize these nanocomposites such as the mixing technique employed, which determine the final morphology of the nanocomposite with the main aim to obtain an exfoliated structure. The enhancement in the properties also depends on the degassing which helps to produce a nanocomposite that is free of voids and air bubbles. It also helps improve the diffusion of epoxy molecules into the intergallery between the clay layers. It was found that curing which converts the liquid mixture of epoxy monomer and hardener to a hard infusible three-dimensional network also helps to improve the degree of crosslinking. Furthermore contradictory results have been reported on the effect of nanoclay addition on fracture toughness, flexural and barrier properties of neat epoxy and

nanocomposites containing different clay loading at different immersion periods and temperatures. For that more work is required to determine the appropriate process parameters that lead to improved overall properties.

CHAPTER 3

EXPERIMENTAL PROCEDURE

3.1 Introduction

The focus of this chapter is to highlight the experimental procedures followed to prepare neat epoxy and epoxy-clay nanocomposites for flexural, fracture toughness and water uptake tests. It includes the various equipments used to prepare, characterize and test the produced specimens.

3.2 Materials

All nanocomposites produced were made with epoxy resin as matrix system. The epoxy is a viscous liquid made of two parts, resin and hardener. The nanoparticle used as reinforcement was montmorillonite layered silicates.

3.2.1 Epoxy

The epoxy used in this work is Araldite GY6010 supplied by JANA, KSA which is an unmodified liquid epoxy resin based on bisphenol A (DGEBA). It is liquid, clear colour and slight odour with an average weight per epoxide 186 g/eq, the viscosity at 25ºC is 11 pa.s and the density is 1.16 g/cm^3 [6]. It is insoluble in water with the following chemical structure shown in Figure 3.1. The curing agent is isophoronedimine (IPDA) supplied by Bondstrand, Dammam. This IPDA is a product of HUNTSMAN, USA. It is liquid with a clear colour and ammoniacal odor. Its viscosity and density at 25ºC are 15 MPa.s and 0.92 g/cm^3 [6]. The Chemical structure of this hardener is shown below in Figure 3.2.

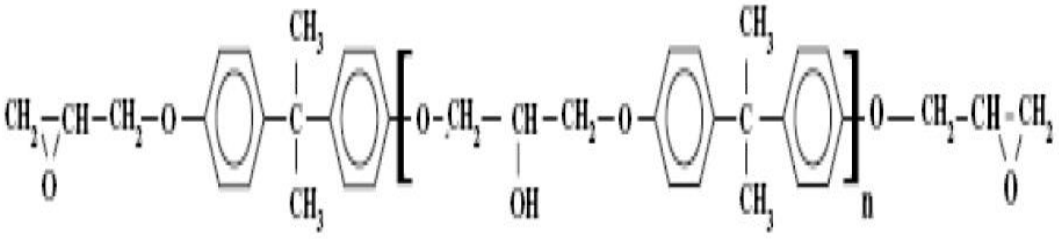

Figure 3.1: The chemical structure of DGEBA epoxy [6].

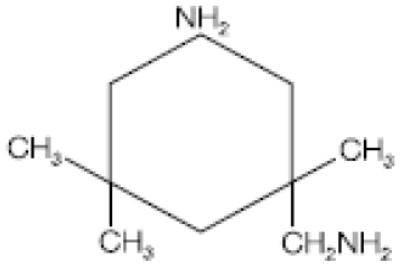

Figure 3.2: The chemical structure of IPDA hardener [6].

3.2.2 The Reinforcement (Nanomer I.30E)

The nanoclays used for this work are montmorillonite nanoclays, commercially known as Nanomer I.30E. Nanomer ® I.30E nanoclay is a surface modified montmorillonite mineral which will disperse to nanoscale in epoxy resin systems. It is an inorganic material with the chemical composition of ½ crystalline unit cell as $[Al_{1.67}\ Mg_{0.33}\ (Na_{0.33})]$ $Si_4O_{10}\ (OH)_2$. The clay layer is usually about 1 nm thick with other dimensions being between 100-1000 nm, giving the clay an aspect ratio in the range of 100 to 1000. Each layer, or platelet, in the clay particle is made up of an octahedral sheet sandwiched between two opposing tetrahedral sheets as shown in Figure 3.3. The layer is usually negatively charged, and the space between two adjacent layers is occupied by anhydrous cations whose position depends on the layer charge location. Common tetrahedral site ions are Si^{4+}, Al^{3+} and Fe^{3+}, however, ions such as Al^{3+}, Fe^{3+}, Fe^{2+}, Mg^{2+}, Zn^{2+}, and Li^{+} are found in the octahedral sites. The ions in both the octahedral and tetrahedral sheets

are coordinated to oxygen ions which gives the layer its net negative charge. The interlayer spaces are generally occupied by Na^+, K^+, Ca^+, and Mg^+ ions which are readily exchangeable. The modulus of an individual layer is in the range of 170 to 180 GPa. The composition of the clay particles (ionic and polar in nature) generally makes it hydrophilic, which means its interaction with organic substance is quite difficult. However, the inorganic cations in the interlayer space can be replaced by organic cationic molecules which change the clay from being hydrophilic to organophilic. Primary octadecyl ammonium is used as an organic modifier for I30.E Nanomer and the chemical structure of organic modifier is shown in Figure 3.4.

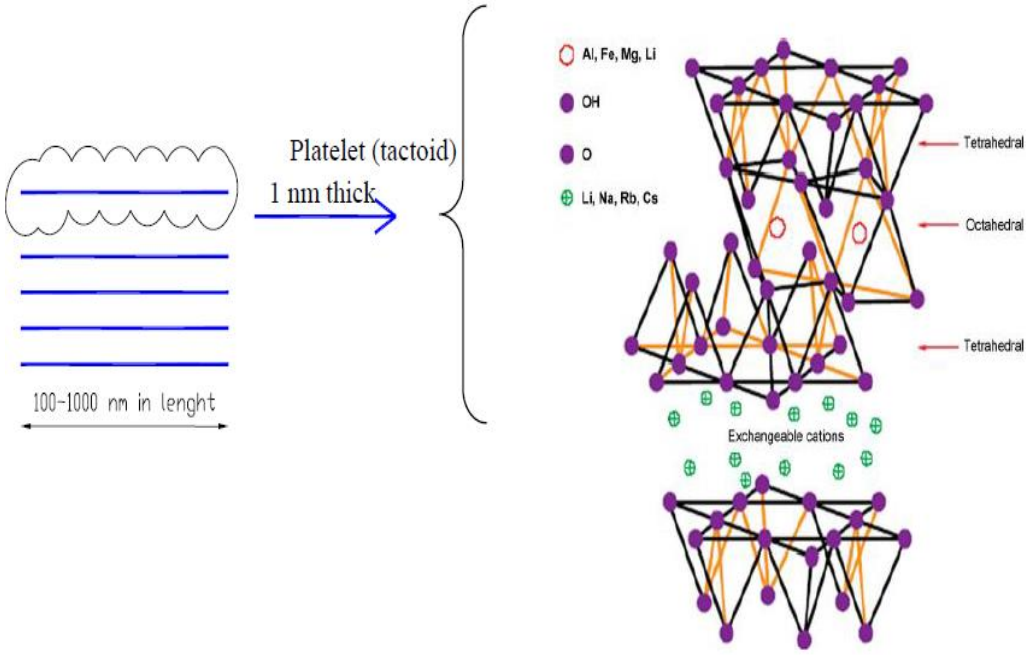

Figure 3.3: Schematic of the layered and chemical structure of an unmodified montmorillonite clay particle [6].

Figure 3.4: Primary octadecyl ammonium [6].

3.3 Preparation of Neat Epoxy Samples

The procedure followed is that described in Al-Qadhi et al [5]. The fabrication of neat epoxy started by pouring a specific amount of epoxy monomer into a beaker and then degassed to eliminate air bubbles at 65ºC using a Shellab vacuum oven connected to a vacuum pump (Figure 3.5). After full degassing, which took about three hours, a stoichiometric amount of curing agent was added to the beaker. The stoichiometric ratio of the hardener and the liquid epoxy was 24 g of hardener for each 100 g of epoxy monomer. The measured epoxy and hardener were then gently mixed together using a stirring rod for 5 minutes to ensure proper mixing of the epoxy with the hardener followed by 10 minutes degassing to remove the air bubbles generated during mixing. After that, the mixture was poured into an aluminum mold, shown in Figure 3.6 that consists of two parts: a base solid plate of dimension 230 x 200 x 12 mm and an upper hollow section of outer dimension 230 x 200 x 10 mm and 200 x 170 x 10 mm inner dimension [6]. The base plates provide the platform for the upper sections which define the dimension of the intended polymer sheet to be cast. The two-part mold was assembled by bolting the sections via 5 mm-diameter holes drilled through the mold plates. During assembling, a replica of the hollow part was made from a thin polymer film (image projector slide sheet) of 0.12 mm thickness and placed between the parts to prevent leakage of material from the mold during the curing process. To prevent sticking

of the cured component to the mold, the latter was polished with abrasive paper and the surface thoroughly cleansed with WD40 cleansing chemical before pouring the epoxy-clay-curing agent mixture [6]. The mould was transferred to the oven for pre-curing at 100ºC and post-curing at 170ºC for one hour each. These curing conditions were found to be optimum for epoxy and hardener used in this study [39]. After that the mold was left to cool down to room temperature inside the vacuum oven. Finally the mold was opened and the sheet of epoxy is removed and is ready for subsequent testing and characterization.

Figure 3.5: Vacuum oven and pump for degassing and curing.

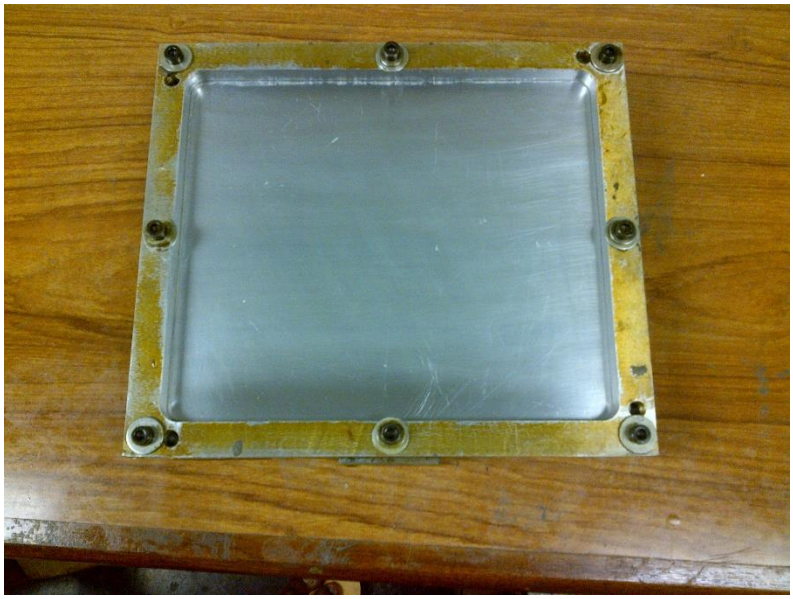

Figure 3.6: The aluminum mold used to prepare neat epoxy and nanocomposites.

3.4 Preparation of Epoxy-Clay Nanocomposites

In this work, high shear mixing technique was used to disperse I.30E nanoclay into the epoxy matrix.

3.4.1 Optimization of Degassing Process

The preparation of nanocomposites used to optimize the degassing process started with manually mixing of 3wt% of I.30E nanoclay into epoxy monomer for 5 min to ensure good distribution of the clay particles in the epoxy. This initial mixing is important to properly blend the clay powder into the epoxy resin and prevent the clay powder from 'flying away' during the subsequent high shear mixing. After stirring, the mixture of the clay and epoxy was moved to the high shear mixer and placed under the mixing assembly as shown in Figure 3.7 with the mixer frame completely immersed. Model L5M-A high shear mixer having maximum mixing speed of 10000 rpm supplied by Silverson, UK, was used to disperse the nanoclay into the epoxy matrix for 60 minutes and 6000 RPM

which were found to be the optimum HSM parameters for this mixer to disperse the nanoclay into the epoxy matrix [40]. During high shear mixing the mixture temperature was maintained between 25-45ºC by using a water bath as shown in Figure 3.7. This maintains the viscosity of the mixture and prevents excessive temperature from being induced into the material which could lead to material degradation or outright burning. The temperature of the mixture during mixing was monitored using a thermocouple. After that the mixture was fully degassed. Three different temperatures (80,100 and 120ºC) and two degassing periods (2 and 4 hours) were chosen to optimize the degassing process. The hardener was then added to the mixture and completely mixed for 5 minutes and then poured into the aluminum mold. Finally, the mixture was pre-cured and post-cured at100ºC and 170ºC respectively for one hour each. A total of six samples were prepared to determine the optimum degassing parameters (temperature and time) for the nanocomposite.

Figure 3.7: Set-up of high shear mixing.

3.4.2 Synthesis of Epoxy-Clay Nanocomposites

The synthesis of nanocomposites started by hand mixing the nanoclay into the epoxy resin for 5 minutes using a stirring rod. The mixture was high shear mixed for 60 minutes and 6000 RPM. The epoxy-clay mixture was then degassed with the optimized degassing parameters first it was degassed for 10 hours at 65ºC followed by 4 hours degassing at 120ºC to remove air bubbles generated during hand and high shear mixing. After degassing, the curing and degassing after adding the hardener were done as mentioned previously in section 3.3. The steps for the production of the epoxy clay nanocomposites are described in Figure 3.8.

To investigate the effect of clay loading on the properties of the resultant nanocomposites, five nanocomposites have been synthesized using different I.30E clay loading, namely: 1, 1.5, 2, 3 and 5 wt%.

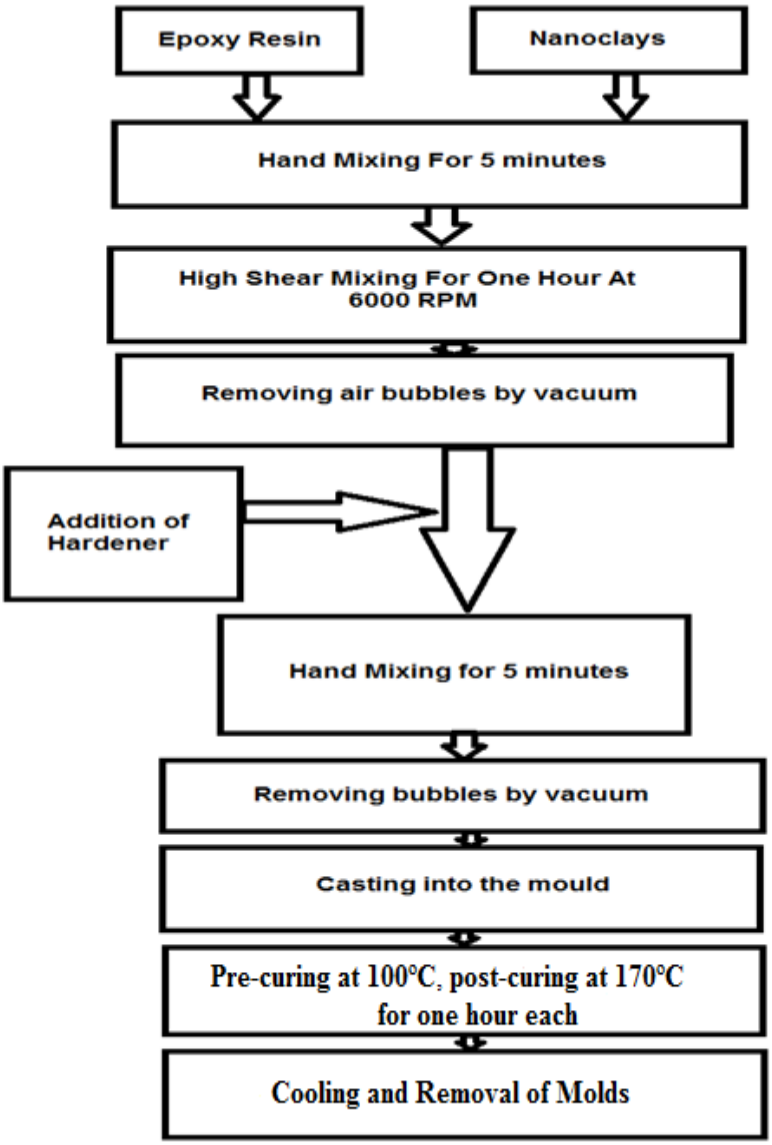

Figure 3.8: Procedure for the production of the epoxy-clay nanocomposites.

3.5 Characterization

To determine the needed physical and thermal properties of neat epoxy and nanocomposites, various techniques were used. These included X-ray diffraction (XRD), Scanning Electron Microscopy (SEM), Differential Scanning Calorimeter (DSC) and the dynamic viscometer.

3.5.1 X-ray Diffraction (XRD)

X-ray diffraction has become a powerful tool for the analysis of nanocomposite structure especially in polymer-clay nanocomposites research. In this work, Shimadzu wide angle X-ray diffraction equipment shown in Figure 3.9, was utilized to analyze the nanocomposite structure. This machine has a voltage rating of 40kV and a current rating of 30mA. The source of the X-ray is Cu Kα radiation having a wavelength of 1.5406Å. Scanning was performed at room temperature with the diffraction angle ranging from 2 to 10º, and step size of 0.02º. The X-ray diffraction analysis was conducted on the pure nanoclay, neat epoxy and nanocomposites. The sample of nanoclay was in the powder form, while small pieces in the form of blocks (10 x 10 x 4 mm) were cut from the sheets of neat epoxy and nanocomposites and placed in sample holders and mounted in the sample chamber of the X-ray diffraction equipment. The X-ray diffraction is used to determine the interplaner spacing (d-spacing) between clays using Bragg's law (Eq.3.1) and hence the type of nanocomposite morphology. The d-spacing depends on the peak angular positions which are called the diffraction angles; lower angular position means higher d-spacing.

$$d = \frac{\lambda}{2 \sin \theta} \tag{3.1}$$

where:

λ is the wavelength of X-rays,

d is the d-spacing between clay layers, and

θ is half of the diffraction angle.

Figure 3.9: Shimadzu Wide Angle X-Ray Diffraction Equipment.

3.5.2 Scanning Electron Microscope (SEM)

Microstructural examinations of the fractured surfaces of flexural and fracture toughness specimens were performed using the JEOL Scanning Electron Microscopy (SEM) shown in Figure 3.10. Due to the very narrow electron beam, SEM micrographs have a large depth of field yielding a characteristic three-dimensional appearance useful for understanding the surface structure of a sample. The SEM used is a high resolution scanning electron microscope with a magnification range of X10 to X300, 000. The electron gun of this SEM has a voltage between 0.3 to 30 kV. Before mounting the specimen on the stub for scanning in the SEM chamber, the fractured surfaces for analysis were coated with gold on a JEOL Fine Coat Ion Sputter JFC-1100 sputtering equipment to make the surface of the sample electrically conductive and prevent it from being charged.

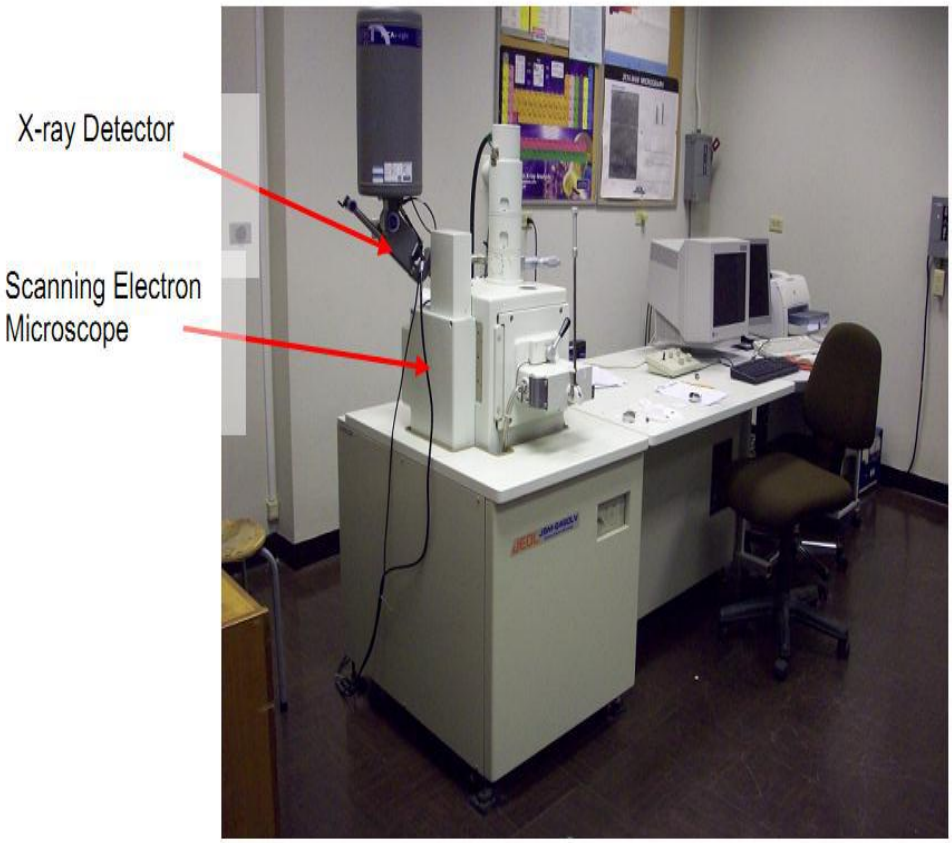

Figure 3.10: Scanning Electron Microscopy.

3.5.3 Differential Scanning Calorimetry (DSC)

DSC-822^e supplied by Mettler TOLEDO was used to determine the glass transition temperature (T_g) of neat epoxy and nanocomposites before and after exposure to water at different immersion temperatures (Figure 3.11). This DSC has a maximum heating capacity of 400 W and a temperature range from room temperature to 700ºC with a maximum heating rate of 100 ºC/min. Thin samples weighing between 4-8 mg were cut from specimens and placed in an aluminum crucible (pan) of 40 µl and covered with its lid. The pan containing the sample was then placed next to a reference pan in the heating chamber of DSC and heated from 25ºC to 200ºC at a heating rate of 10ºC/min in an argon

gas inert environment flowing at 100 ml/min. Cooling was provided by liquefied nitrogen gas.

Figure 3.11: Differential Scanning Calorimetry (DSC) Equipment.

3.5.4 The Dynamic viscometer

The rotational viscometer was used for measuring the dynamic viscosity of epoxy and nanocomposites. Viscosity is measured by establishing the necessary force (shear effort) to move the particles of material with a particular distortion speed. The viscosity is obtained as a result of the ratio between the shear effort and the speed gradient according to the following equation

$$\tau = \mu * \frac{du}{dy} \qquad (3.2)$$

Where:

τ is the shear stress.

μ is the dynamic viscosity.

$\frac{du}{dy}$ is the speed gradient.

The Dynamic viscometer (Figure 3.12) has maximum power supply of 15V and 1.2A and viscosity range from 0.1 to 600 Pa.s. For measuring viscosity neat epoxy and nanocomposites samples with different clay loadings were poured into a 1000 ml beaker after hand and high shear mixing then it was placed under the dynamic viscometer and the spindle for viscometer measurement was moved down till the spindle mark arrives to the sample level.

Figure 3.12: Dynamic Viscometer equipment.

3.6 Water Uptake of Epoxy and Nanocomposites

Neat epoxy and nanocomposite specimens were prepared according to ASTM D 570 standard [41] and completely immersed in glass containers and plastic box filled with tap water at room temperature (23ºC) and 80ºC as shown in Figure 3.13 and Figure 3.14 respectively. The heating was provided using a Shellab vacuum oven. The change in the specimen's weight with time was periodically recorded. According to ASTM D570 standard the specimen should be 80 mm long and 30 mm wide, the thickness of the specimen prepared was around 4 mm.

Figure 3.13: specimens prepared for water uptake at room temperature.

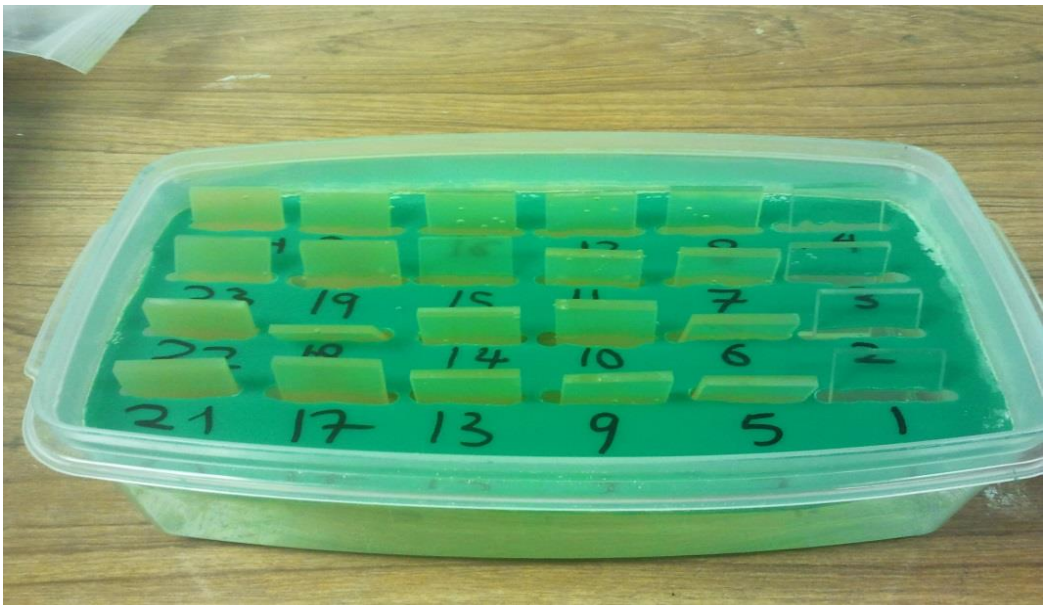

Figure 3.14: specimens prepared for water uptake at 80°C temperature.

3.7 Mechanical Testing

After obtaining the optimum degassing conditions and using the optimized mixing and curing parameters, nanocomposites with different nanoclay loadings were prepared to investigate the effect of clay addition and water uptake on flexural and fracture toughness properties. The following section describes the specimen preparation and the testing procedures for both types of tests.

3.7.1 Flexural Strength test

The three point flexural setup was used to measure the flexural properties of the epoxy resin and its nanoclay composites. The flexural tests were performed according to ASTM D790 standards [41] using Instron testing machine. Block shape configuration was used since the specimens dimensions of this type can be developed from the specimens of water exposure tests to make the flexural tests after water uptake. According to this standard the dimension of block shaped flexural test specimen should be 80 mm in

length, 10 mm in width and 4 mm in thickness. The specimens were prepared using CNC milling machine and the surfaces of the specimens were smoothened using silicon carbide abrasive paper. The specimens were then mounted on the Instron testing machine the support span was set to 64 mm while the cross head speed was set at 1.7 mm/min until the specimen fractures as shown in Figure 3.15. The maximum flexural strength was recorded. Four specimens were prepared and tested for each type of neat epoxy and nanocomposites before and after exposure to water at room temperature and 80ºC.

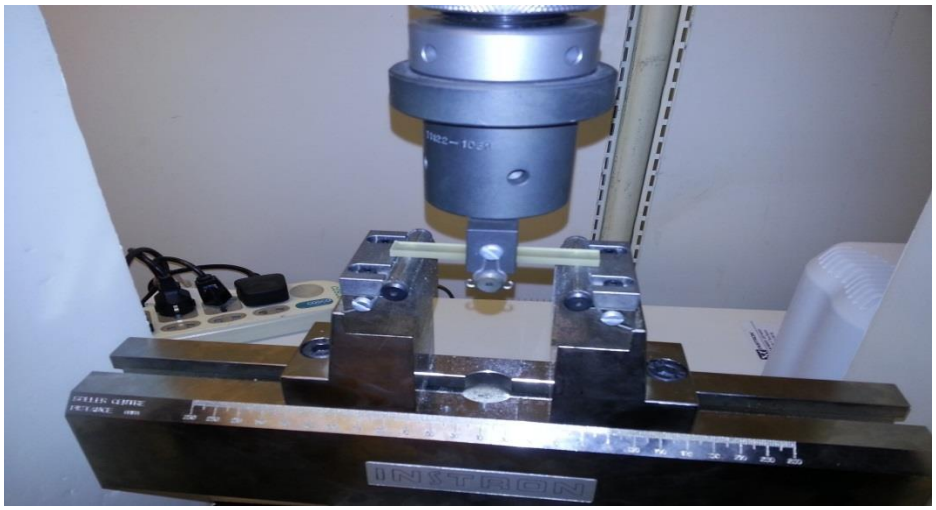

Figure 3.15: set up of flexural test.

3.7.2 Fracture Toughness test

The fracture toughness is a property which describes the ability of a material containing crack to resist fracture. Fracture Toughness tests were performed using Instron testing machine according to ASTM D5045 standard [41]. Single notch edge bending configuration was selected. Since the specimens dimensions of this type can be developed from the specimens of water exposure tests to make the fracture toughness tests after water uptake. According to this standard the dimensions of Single notch edge

bending fracture test specimen should be 80 mm in length, 16 mm in width and 4 mm in thickness with 8 mm pre-crack as shown in Figure 3.16.

The specimens were also prepared using CNC milling machine and the sharp notch was machined using a fresh razor blade. After that the specimens were mounted on the Instron machine the support span was set to 64 mm while the cross head speed was set at 0.5 mm/min until the specimen fractures as shown in Figure 3.17.

As for flexural test four specimens were prepared and tested for each type of neat epoxy and nanocomposites before and after exposure to water at room temperature and 80ºC.

Furthermore, the value of the stress intensity factor was obtained and plane strain fracture toughness test criteria were satisfied.

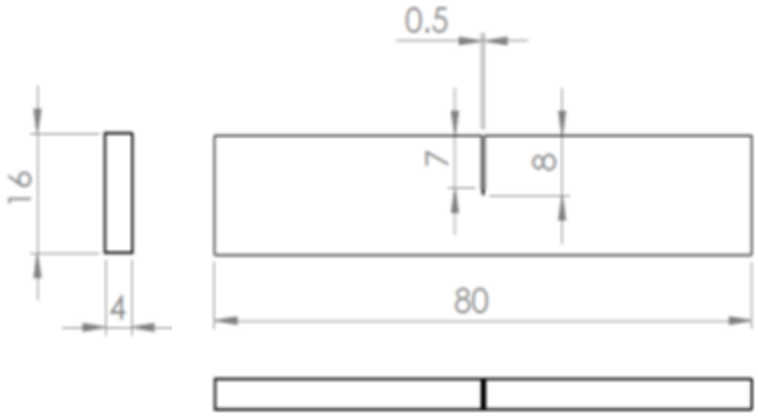

Figure 3.16: Shape and dimensions of fracture toughness specimens, single edge notch bending type, the dimensions are in mm.

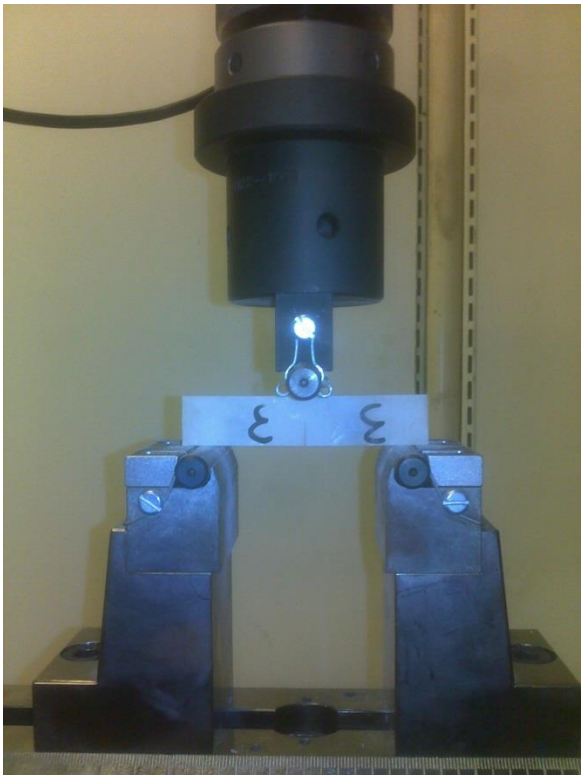

Figure 3.17: set up of Fracture Toughness test.

CHAPTER 4

RESULTS AND DISCUSSION

4.1 Introduction

This chapter sheds the light on optimizing the degassing process which is considered to be an important process that helps to produce nanocomposites free of air bubbles and improves the nanocomposite morphology. And to study the effect of I.30E nanoclay addition and water uptake at different immersion temperatures on flexural, fracture toughness, thermal and barrier properties.

4.2 Optimizing the Degassing Process

The degassing process is considered to be an important step to have a nanocomposite that is free of air bubbles. The formation of these air bubbles is due to the use of different mixing techniques such as, high shear mixing to disperse nanoclays in epoxy which is recently receiving high concentration to improve the degree of clay dispersion in nanocomposites.

The high shear force induced during mixing decreases the size of the nanoclay particles by splitting the particles and increases the interlayer spacing in the clay particles by forcing the epoxy monomer into the galleries between the clay layers. Due to this high shear force, large number of air bubbles is formed and degassing is needed to remove them. The two main parameters of the degassing process are temperature and time. Degassing temperature may affect the diffusion of epoxy between clay platelets and higher degassing temperatures are expected to accelerate the rate of diffusion. This will

increase the interplaner spacing of the clay layers producing a nancomposite with either a disordered intercalation or an exfoliated morphology.

To investigate the optimum degassing parameters six plates were prepared having 3wt% clay loading with three degassing temperatures (80,100 and 120ºC) and two times (2 and 4 hours). From each plate two samples were cut and tested. XRD technique was used to determine the optimum combination of temperature and time that will produce a nanocomposite free of air bubbles with disordered intercalation or an exfoliated morphology.

The XRD spectra of Figure 4.1, show that as the degassing temperature increased the XRD peaks shift to the left according to Bragg's law (Eq.3.1) the change in the peak position indicates a change in the interplaner spacing. The shift to the left means that the diffraction angle of the peaks decreased and the interplanar spacing increased as listed in Table 4.1. No peak was observed in the X-ray spectrum for the sample degased at 120ºC. Because XRD can only detect the periodically stacked montmorillonite layers; disordered or exfoliated layers cannot be detected. Therefore, only the intercalated structures where individual silicate layers are separated by less than 7 nm, give a peak in XRD while no peak appears in the disordered or exfoliated structures [42]. The diffusion process of epoxy matrix between layered silicate nanoclay was enhanced and clay layers were separated and distributed within the matrix indicating disordered or exfoliated morphology were obtained [5, 43]. The effect of degassing time is translated by a shift to the left in the peaks as the degassing time increased from 2 to 4 hours also indicating an increase in the inter-planar spacing.

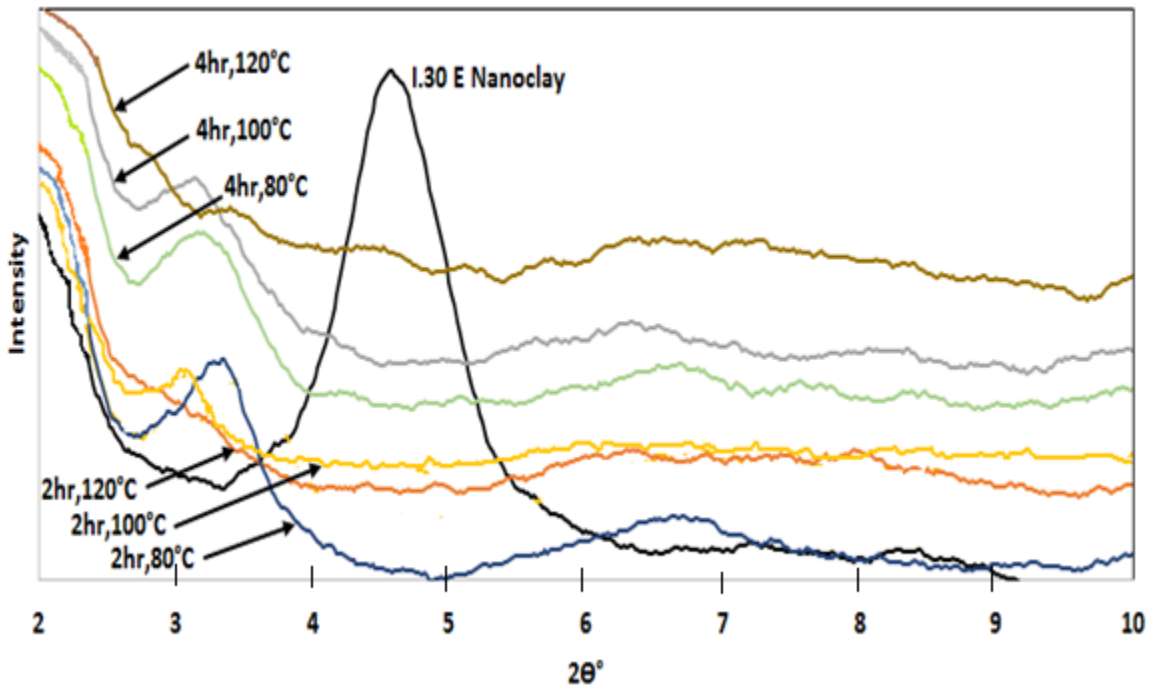

Figure 4.1: X-Ray Diffraction for the clay (I30.E) and nanocomposites with different degassing temperatures and times.

Table 4.1: Diffraction angles and interplaner spacing for nanocomposites with different degassing parameters.

Time (hr)	Sample	Diffraction angle (2Θ)	Interplaner Spacing (A˚)
	Clay I30E	4.4	20.08
2	2 hr at 80ºC	3.24	27.27
	2 hr at 100ºC	3.01	29.31
	2 hr at 120ºC	-	No peak
4	4 hr at 80ºC	3.06	28.88
	4 hr at 100ºC	2.88	30.68
	4 hr at 120ºC	-	No peak

Based on XRD analysis it was found that the optimum degassing temperature was 120ºC which gave the better dispersion. As indicated by the results of Table 4.1 degassing for 4 hours at 120ºC resulted in a relatively higher d-spacing and thus this combination was selected for further processing.

4.3 Effect of Clay Loading

After determining the optimum degassing time and temperature at clay loading of 3wt%, the work focused on studying the effect of clay loading on the mechanical and thermal properties of the nanocomposites. To study the effect of clay loading, five plates of 200×170 mm were prepared with clay loadings of 1, 1.5, 2, 3 and 5 wt% of I.30E nanoclay in addition to the neat epoxy sample. During the preparation of these samples the optimum degassing temperature and time (120ºC for 4 hours) were used. The optimum high shear mixing (HSM) and curing parameters for these types of epoxy and nanoclay determined in earlier work were used [6].

XRD analysis was performed (Figure 4.2) in order to check the resulting morphology of the nanocomposite material. No peaks were observed in all the XRD spectra indicating disordered intercalation or exfoliated morphologies were obtained at all clay loadings. This further indication that the selected process was optimal for the employed materials.

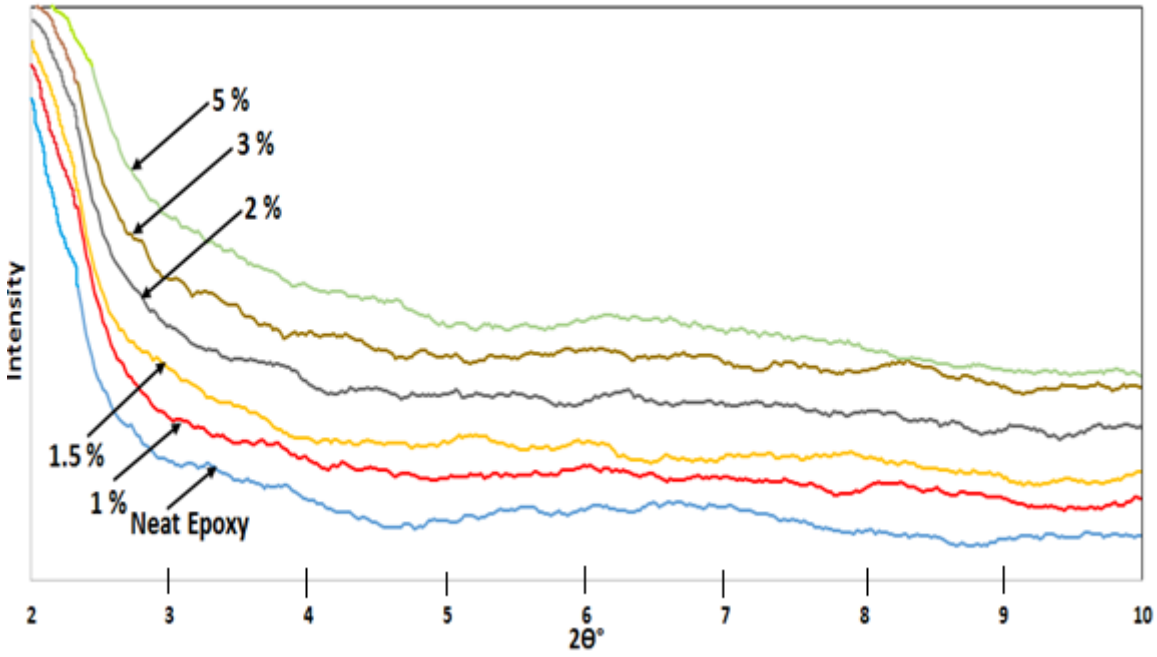

Figure 4.2: X-Ray Diffraction spectra for Neat epoxy and the nanocomposites with different clay loadings (1, 1.5, 2, 3 and 5 wt%).

4.3.1 Effect of Clay Loading on the Dynamic Viscosity

The rotational viscometer was used for measuring the dynamic viscosity by establishing the necessary force (shear effort) to move the particles of material with a particular distortion speed. The viscosity was obtained as a result of the ratio between the shear effort and the speed gradient (Eq.3.2).

Table 4.2 lists the resulting dynamic viscosity for neat epoxy and nanocomposites having (1.5, 3 and 5 wt%) clay loadings. The variation of the dynamic viscosity with the clay loading after hand and high shear mixing is illustrated in Figure 4.3. The dynamic viscosity after hand mixing (HM) was found to rise from 17.96 Pa.s for neat epoxy to 23.86 Pa.s for nanocomposite containing 5 wt% of clay with about 33% increase. Similar trend was observed for the dynamic viscosity after high shear mixing (HSM) with about

120% increase for the sample containing 5 wt% of clay as compared with neat epoxy sample. The linear increase in the dynamic viscosity for the nanocomposites is related to the existence of nanoclay in epoxy resin. The dynamic viscosity of nanocomposites after high shear mixing was higher than the viscosity after hand mixing (Figure 4.3). This is because high shear mixing forces was applied by the high shear mixer to properly mix the nanoclay with epoxy resin so clay layers were separated and distributed within the matrix. The increase in the dynamic viscosity with increasing clay loading have been reported by a number of authors [29, 30] as mentioned previously in section 2.4.3.

Table 4.2: Dynamic viscosity for neat epoxy and nanocomposites (NC) containing different clay loadings.

Sample	Viscosity (Pa.s) After Hand Mixing	Viscosity (Pa.s) After High Shear Mixing
Neat Epoxy	17.95	19.92
NC 1.5% Clay	18.99	24.25
NC 3% Clay	22.02	32.42
NC 5% Clay	23.86	41.80

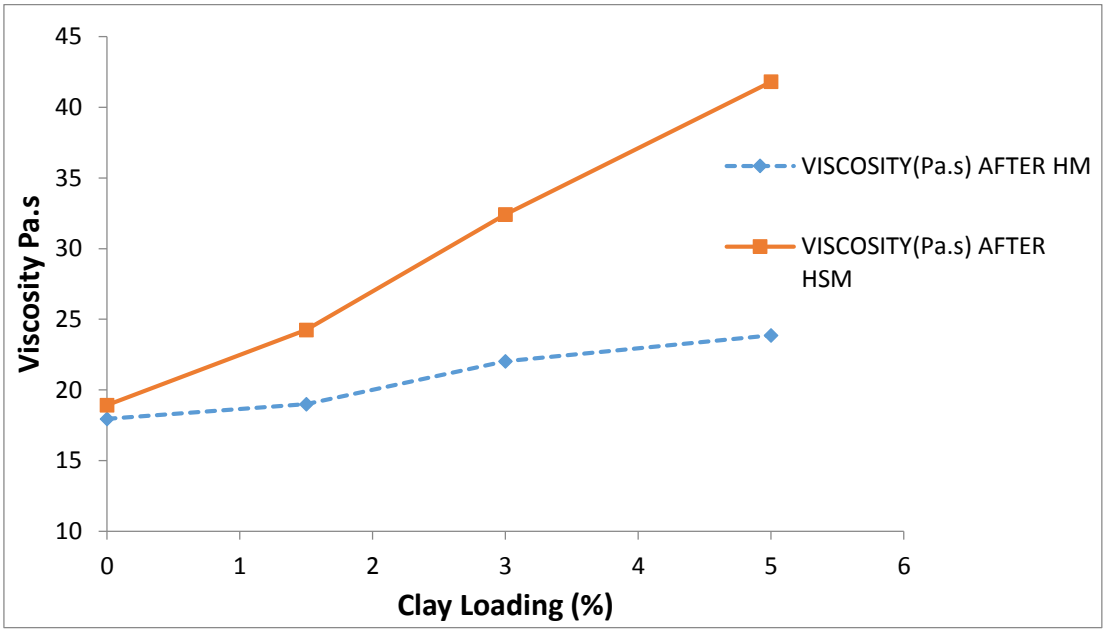

Figure 4.3: The Change of Viscosity for neat epoxy and nanocomposites containing different clay Loadings after Hand Mixing (HM) and High Shear Mixing (HSM).

4.3.2 Effect of Clay Loading on Flexural Properties

Flexural tests have been performed to determine the mechanical properties of the neat epoxy and nanocomposites prepared with optimum degassing, mixing and curing parameters. Table 4.3,Table 4.4 and Table 4.5 list the average values and standard deviations of flexural strength, flexural modulus and flexural strain for neat epoxy and nanocomposites, respectively. The variations of flexural strength with clay loading are illustrated in Figure 4.5. The results show that the flexural strength increased from 100.20 MPa for neat epoxy to about 114.47 MPa for nanocomposite containing 1.5wt% of clay, 15% improvement. The flexural strength started to decrease when increasing the clay loading beyond 1.5wt% and the lowest value was found for the nanocomposite containing 5wt% of nanoclay which showed about 12% reduction. The improvement in

the flexural strength can be attributed to the good exfoliation of the nanoclay in the epoxy resin and the reinforcing-ability and interfacial bonding-ability of I30E nanoclay.

The decrease in flexural strength with higher clay loadings can be due to the increase in the dynamic viscosity as shown in Figure 4.3 and the difficulty to properly degas the mixture of clay and epoxy after adding the hardener. The reduction for nanocomposites containing higher clay loadings can also be attributed to the poor dispersion of layered silicate nanoclay in epoxy resin and the formation of voids and clay agglomeration as shown in Figure 4.4.

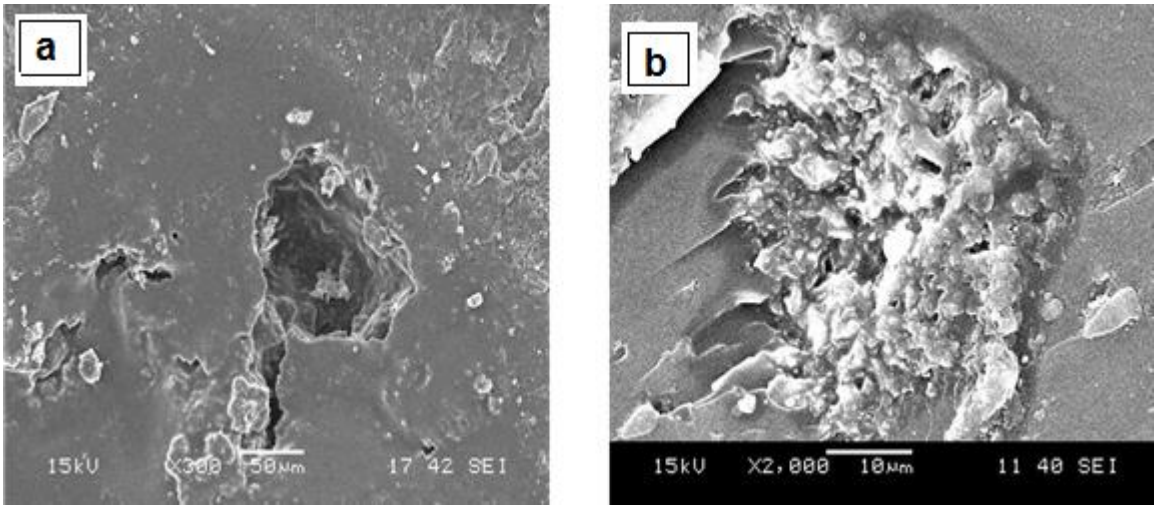

Figure 4.4: SEM image of nanocomposite having (a) voids (X300) and (b) clay aggregate (X2000).

As mentioned in section 2.3.1, The increase in the flexural strength at low percent of clay loading and the strength decrease with increasing clay loading have also been reported by Yuan et al [4], Li et al[11], Zulfli et al [13] and Kusmono et al [22]. Other studies reported that the flexural strength of nanocomposite was lower than that of neat epoxy and decreased with increasing clay concentration [18, 21].

The variations of flexural modulus and fracture strain with clay loading are illustrated in Figure 4.6 and Figure 4.7 respectively. The addition of clay improved the flexural modulus from an average 2.78 GPa for neat epoxy to 3.30 GPa for nanocomposite containing 5 wt% of clay. As can be seen in the figure, the average flexural modulus was found to increase almost linearly with clay loading and showed about 19 % improvement for samples containing 5 wt% of clay. This can be related to the high modulus of the clay as compared with epoxy resin and also to the presence and distribution of clays which restricts the mobility of polymer chains as well as to the good interfacial adhesion between the clay particles and the epoxy matrix. Similar behavior was reported by a number of researchers [5, 44].

It can be seen in Figure 4.7, there was almost a linear reduction in flexural fracture strain as a result of the brittleness of the nanocomposites. Flexure strain dropped by about 65%; from 9.65% for neat epoxy to 3.29% for nanocomposite containing 5wt% clay loading. The improvement in the flexural modulus and reduction in the fracture strain are typical for the polymer-clay nanocomposites [13, 18].

Table 4.3: Average values of flexural strength of neat epoxy and nanocomposites containing different clay loadings.

Sample	Flexural Strength (MPa)	Standard Deviation
Neat Epoxy	100.19	4.71
NC 1% Clay	106.18	3.80
NC 1.5% Clay	114.47	3.91
NC 2% Clay	110.97	5.69
NC 3% Clay	100.25	3.11
NC 5% Clay	88.24	7.61

Table 4.4: Average values of flexural modulus of neat epoxy and nanocomposites containing different clay loadings.

Sample	Flexural Modulus (GPa)	Standard Deviation
Neat Epoxy	2.78	0.07
NC 1% Clay	2.85	0.08
NC 1.5% Clay	2.90	0.06
NC 2% Clay	2.98	0.08
NC 3% Clay	3.15	0.05
NC 5% Clay	3.30	0.09

Table 4.5: Average values of flexural fracture strain of neat epoxy and nanocomposites containing different clay loadings.

Sample	Flexural Strain (%)	Standard Deviation
Neat Epoxy	9.65	0.54
NC 1% Clay	7.56	0.25
NC 1.5% Clay	4.98	0.61
NC 2% Clay	4.23	0.25
NC 3% Clay	3.93	0.61
NC 5% Clay	3.29	0.34

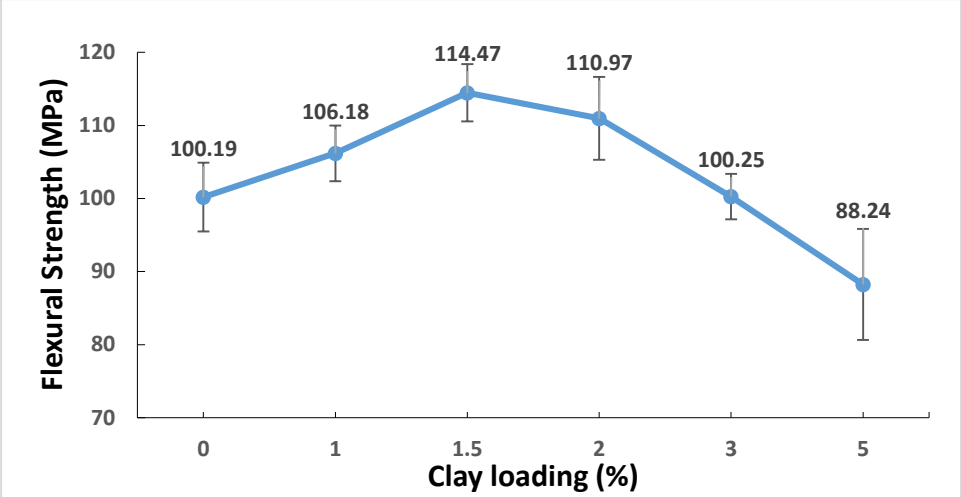

Figure 4.5: Variation of flexural strength with clay loadings.

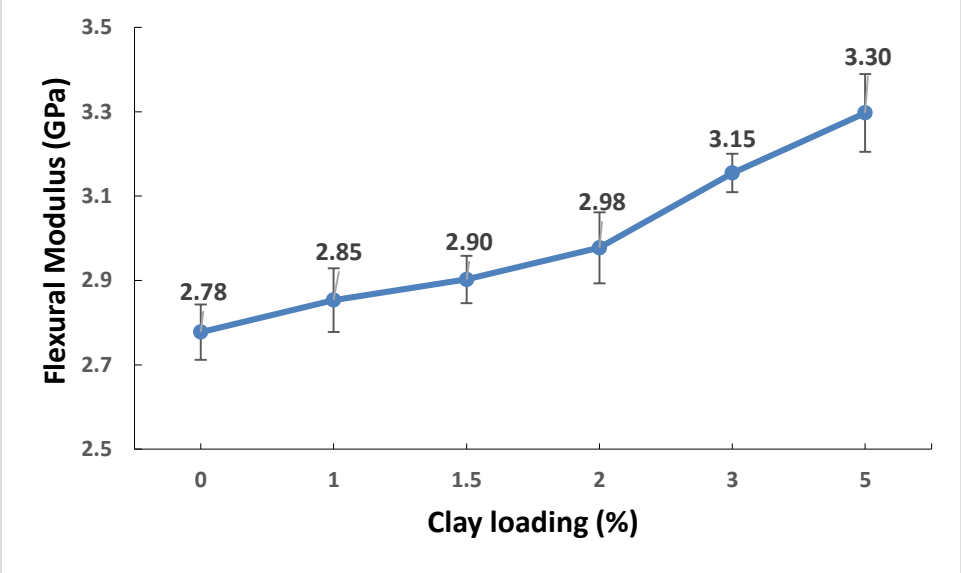

Figure 4.6: Variation of flexural modulus with clay loadings.

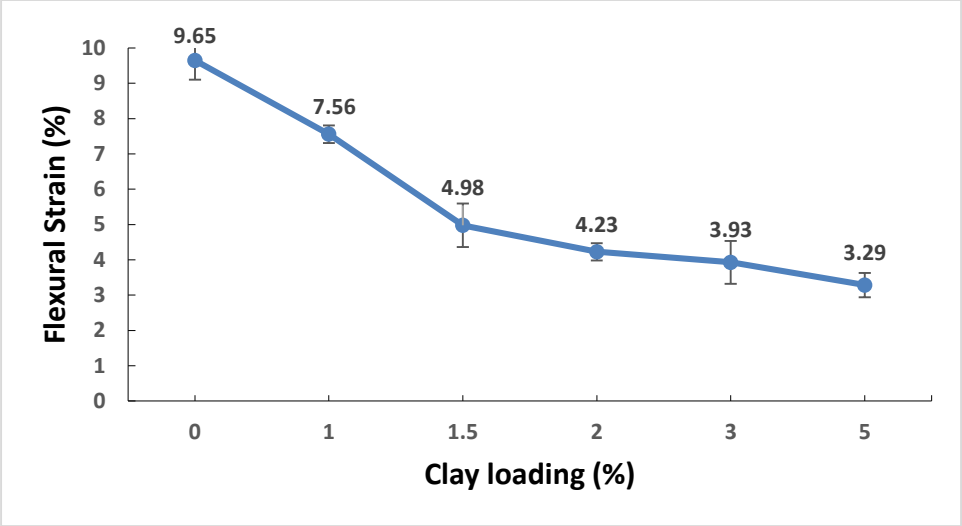

Figure 4.7: The change of flexural strain with clay loadings.

4.3.3 Fractographic Analysis of the Flexural Fracture Surfaces

Morphological characteristics of the fracture surfaces of neat epoxy and nanocomposites fractured under three point bending loading were investigated using SEM. This examination was performed to understand the material's toughness, cracks initiation and propagation and the extent and nature of clay distribution and dispersion within the epoxy matrix. The results will help explain the morphological characteristics effects on the physical and mechanical properties of the resultant nanocomposites. Comparing fractographs of neat epoxy and nanocomposites containing different clay loadings, illustrated in Figure 4.8, demonstrates that the fracture surfaces of the nanocomposites are rough corrugated surfaces displaying a marked departure from the smoother brittle cleavage type fracture for neat epoxy. The rougher fracture surfaces of nanocomposites are indication of higher plastic deformation and hence more energy absorbed during crack propagation [6]. As clear from Figure 4.8, the degree of surface roughness was increased as a result of the gradual increase of nanoclay particles and this can be

attributed to crack deflection due to the presence of clay platelets. The fracture surface of neat epoxy and the effect of nanoclay addition on the fracture surface morphology was studied for nanocomposites samples containing 1%, 1.5%, 2%, 3% and 5wt% and their SEM images are shown in Figure 4.8 to Figure 4.12 at different magnifications. These fractographs reveal that during the flexural test of the nanocomposites, the cracks were often initiated at agglomerated clay clusters and sometimes at micro-voids. This is clear from the magnified micrographs (b) in Figure 4.9, Figure 4.10 and Figure 4.11(d) which show that the cracks were initiated at agglomerated clay clusters, whereas, Figure 4.11(b) illustrates that the crack was initiated at micro-void.

As illustrated in Figure 4.12, the sizes of the agglomerated clay clusters are increasing with raising clay loading. This can explain the reason why the strength of nanocomposites was decreased with increasing nanoclay loading. Figure 4.12(a) shows that the sizes of the largest agglomerated clay clusters are about 25 μm for 1.5wt% of clay loading. For the nanocomposites containing 3% and 5 % of clay loading the sizes of the largest agglomerated clay clusters are about 40 μm and 50 μm as shown in Figure 4.12(b) and (c) respectively.

To ensure that those agglomerated clusters are indeed clay aggregates, energy dispersive spectroscopy (EDS) was used to identify and determine the elemental composition of these clusters. Figure 4.13 displays SEM image of nanocomposite containing 1wt% of clay loading including an expected agglomerated clay cluster. Table 4.6 lists the components of all spectra shown in Figure 4.13. It is found that both spectra 5 and 6 which include the suspected clay aggregates contain 9.12 and 9.94% Si as well as 3.35 and 3.51% Al, respectively proving that it is agglomerated clay cluster.

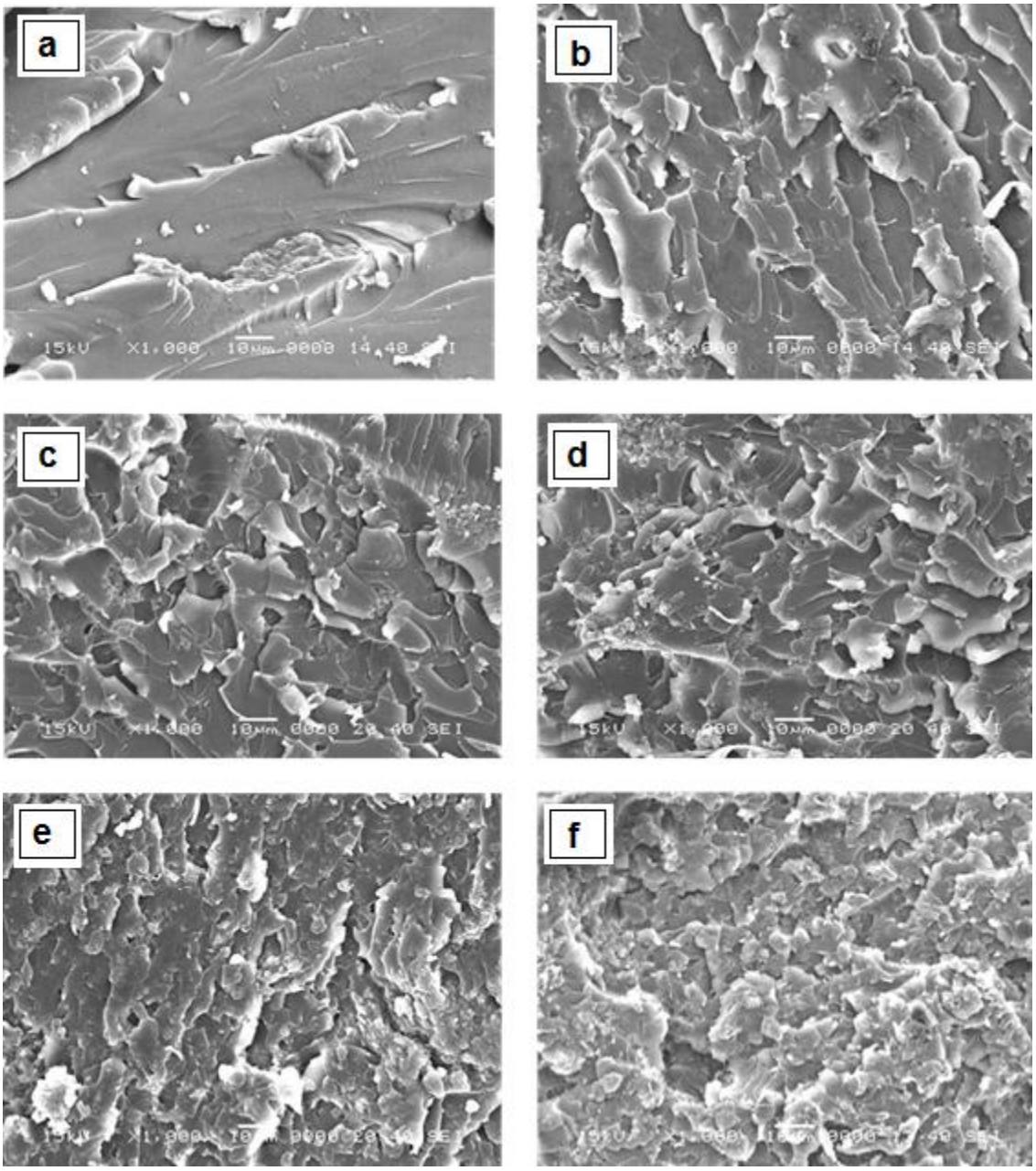

Figure 4.8: SEM fractographs (X1000) of (a) neat epoxy and nanocomposites with different clay loadings (b) 1wt %, (c) 1.5 wt%, (d) 2 wt%, (e) 3 wt% and (f) 5 wt%.

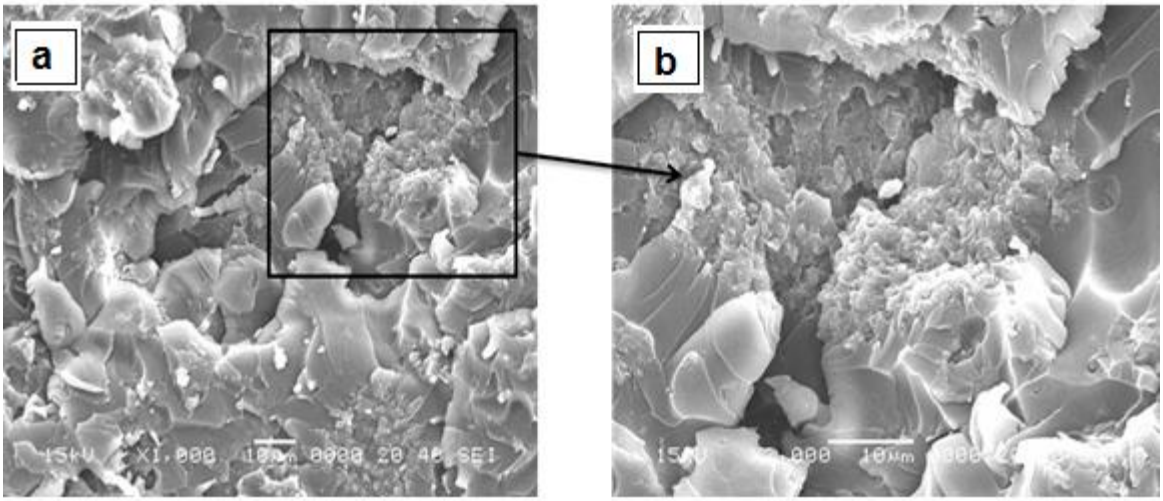

Figure 4.9: SEM fractographs of nanocomposite containing 2 wt% nanoclay at different magnifications (a) 1000X and (b) X2000.

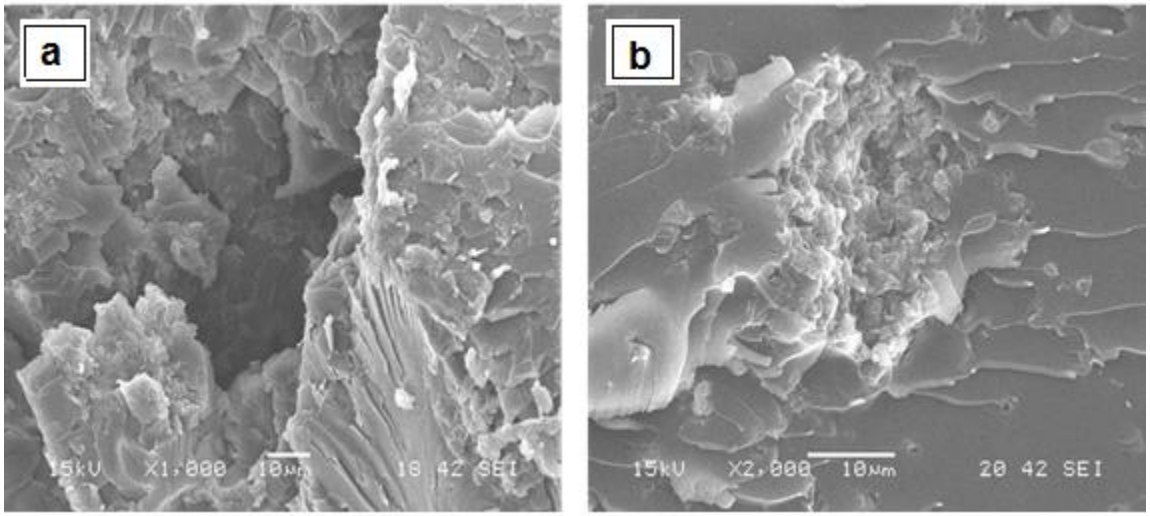

Figure 4.10: SEM fractographs of nanocomposite containing 3 wt% nanoclay at different magnifications (a) 1000X and (b) X2000.

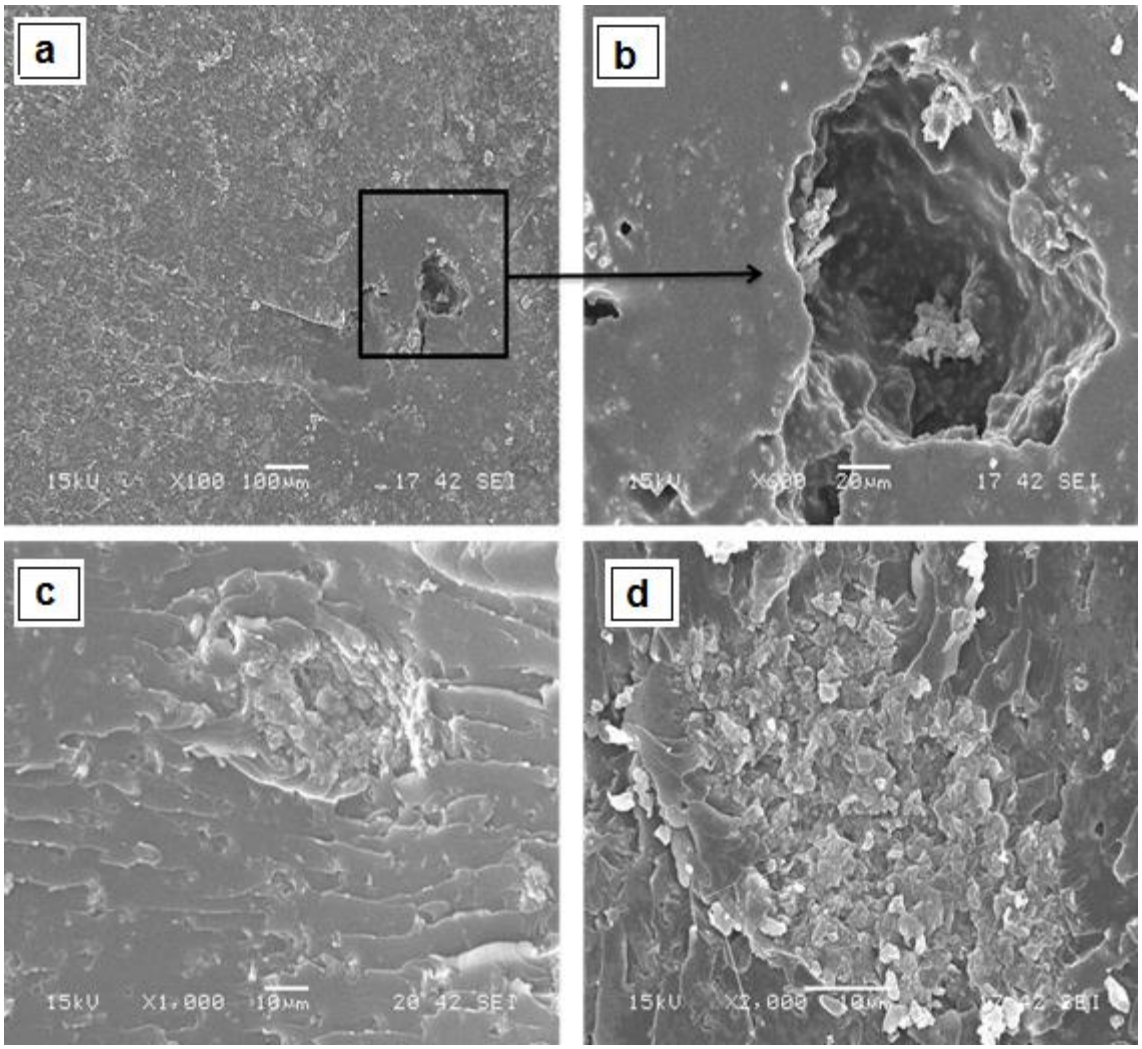

Figure 4.11: SEM fractographs of nanocomposite containing 5 wt% nanoclay at different magnifications (a) 100X, (b) X600, (c) 1000X and (d) X2000.

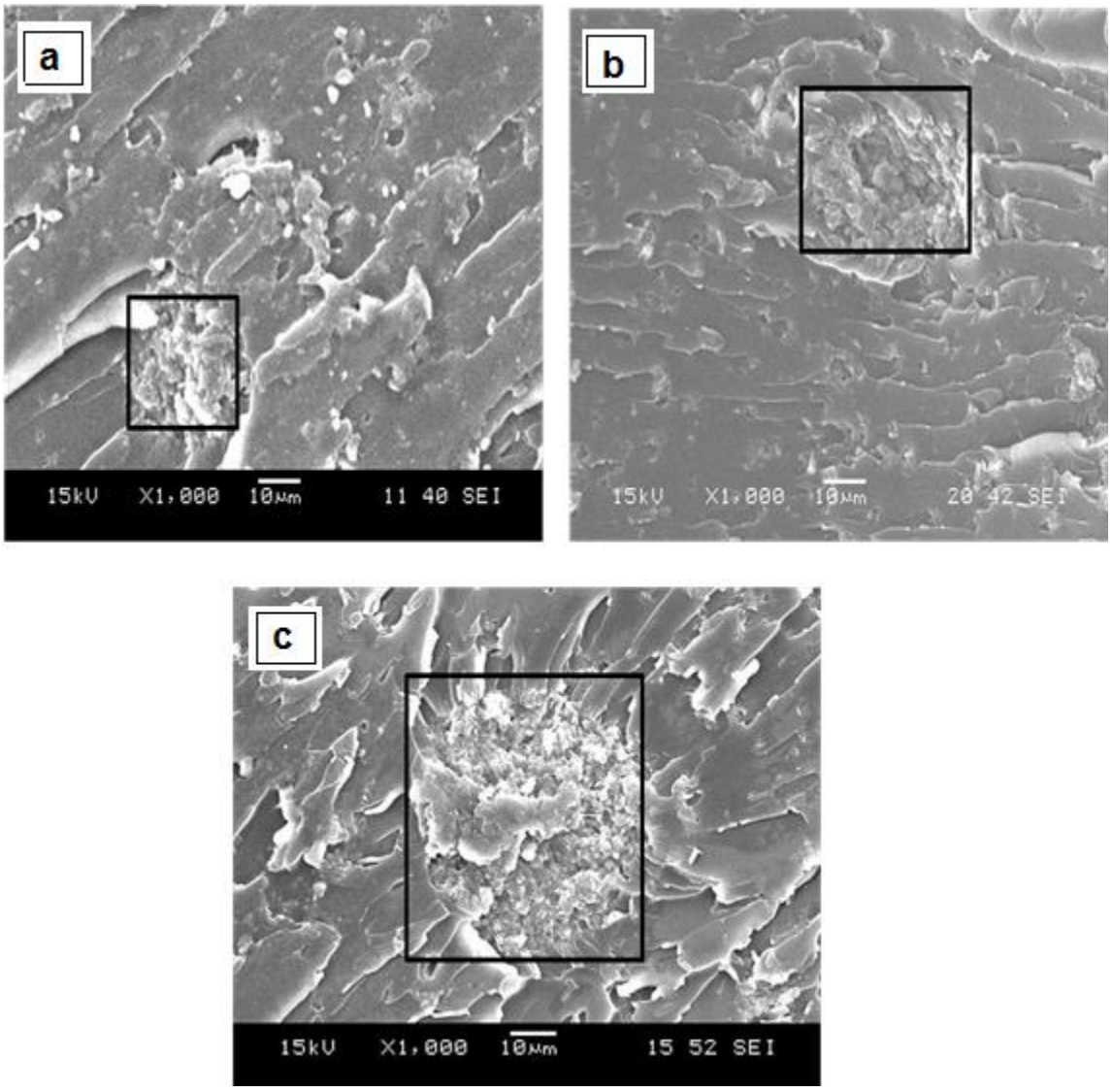

Figure 4.12: SEM fractographs (X1000) showing crack deflection around nanoclay due to clay agglomeration of nanocomposites with different clay loadings (a) 1.5 wt%, (b) 3 wt% and (c) 5 wt%.

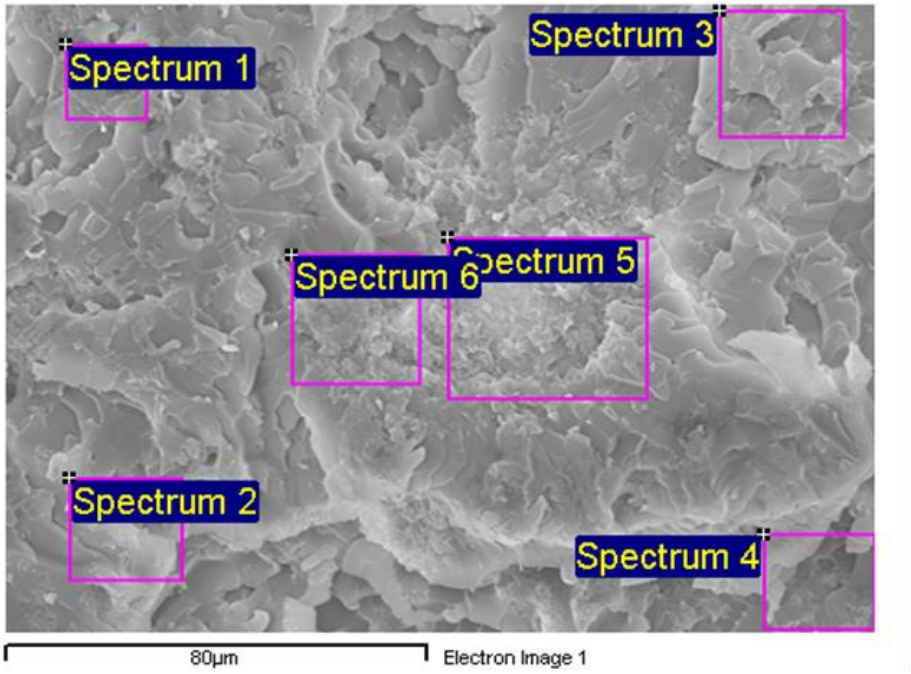

Figure 4.13: SEM image of nanocomposite having clay aggregate used for EDS analysis.

Table 4.6: Elemental composition for the different spectra shown in Figure 4.13.

Spectrum	C %	O %	Mg %	Al %	Si %	Fe %	Total %
Spectrum 1	76.35	23.04	0.04	0.20	0.37	0.00	100.00
Spectrum 2	71.25	26.46	0.30	0.54	1.32	0.13	100.00
Spectrum 3	75.48	23.39	0.13	0.23	0.48	0.28	100.00
Spectrum 4	77.17	21.09	0.12	0.35	0.53	0.74	100.00
Spectrum 5	62.94	23.78	0.53	3.35	9.12	0.30	100.00
Spectrum 6	60.11	25.13	0.61	3.51	9.94	0.70	100.00

4.3.4 Effect of Clay Loading on Fracture Toughness Properties

Fracture Toughness tests were performed to determine the mechanical properties of the neat epoxy and nanocomposites prepared with optimum degassing, mixing and curing parameters. Figure 4.14 displays the fracture load-strain curve for neat epoxy and nanocomposites containing different clay loadings. For neat epoxy it exhibited brittle fracture, as shown in the figure, the brittleness of the nanocomposites increased with increasing the clay loadings. Table 4.7 lists the average values and standard deviations of

the maximum fracture load (P_Q) for neat epoxy and nanocomposites, Figure 4.15 shows typical fracture load (P_Q) for neat epoxy and nanocomposites, as can be seen in the figure, there is a gradual rise in the maximum load with clay loading until 3wt% which showed the highest value (158.66 N) with about 35% improvement in the maximum fracture load as compared with neat epoxy. The maximum fracture load decreased afterwards with 5wt% loading to about (125.37 N).

The Critical Stress Intensity Factor was calculated using the following equations:

$$K_Q = P_Q \times B \times W^{\frac{1}{2}} \times f(a/W) \tag{4.1}$$

$$f(a/W) = 6 \times x^{(1/2)} \left[\frac{1.99 - x(1-x)(2.15-3.93x+2.7x^2)}{(1+2x)(1-x)^{3/2}}\right] \tag{4.2}$$

Where B is the thickness, W is the width of the specimen, P_Q is the maximum load before fracture from the test and x is the ratio between the crack length (a) and the width of the specimen (W).

The value of *f(a/W)* corresponds to the ratio of the crack length over the width of the specimen (a/W) which is equal to 0.5, fracture toughness tests satisfied the plane strain fracture toughness test size criteria.

Using Eq 4.1, the stress intensity factor (K_Q) was calculated and the results are illustrated in Table 4.7 and Figure 4.16. Similar to flexural strength, the fracture toughness increased with increasing clay loading from 0.63 MPa.m$^{1/2}$ for neat epoxy to about 0.86 MPa.m$^{1/2}$ for nanocomposite containing 3 wt% clay loading. However, the value of the fracture toughness for the nanocomposite containing 5 wt% went down due to the formation of voids and clay agglomeration which resulted from the increase in

viscosity. The improvement in fracture toughness may be attributed to the toughening mechanism due to the good dispersion of the nanoclay and to crack deflection around nanoclay tactoids as the fracture surface roughness increased with increasing clay loading. The improvement in K_Q can also be related to the good bonding between the clay and the epoxy resin. Similar findings were reported by a number of researchers [3, 11, 45, 46].

Morphological characteristics of the fracture surfaces of neat epoxy and nanocomposites fractured under three point bending loading were investigated using SEM. Comparing micrographs of neat epoxy and nanocomposites containing different clay loading as illustrated in Figure 4.17, demonstrates that the fracture surfaces of the nanocomposites are rough corrugated surfaces displaying a marked departure from the smoother brittle cleavage type fracture for neat epoxy. The rougher fracture surfaces of nanocomposites are indication of higher plastic deformation and hence more energy absorbed during crack propagation [6]. As clear from Figure 4.17, the degree of surface roughness was increased with raising the clay loading as for the flexural properties.

The fracture surface of neat epoxy and the effect of nanoclay addition on the fracture surface morphology were studied for nanocomposites samples containing 1%, 1.5%, 2%, 3% and 5 wt% and their SEM images are shown in Figure 4.17 to Figure 4.21. These fractographs reveal that during the fracture toughness test of the nanocomposites, the cracks were deflected around the agglomerated clay clusters. This is clear from the magnified micrographs in Figure 4.20(b) and Figure 4.21(a). Similar finding were reported by other researchers [18, 24, 32]. They showed that the fracture surface of pure epoxy was featureless and smooth and the crack was free and easy to propagate. But for

nanocomposite samples the fracture surfaces were corrugated and rougher and more energy were needed for cracks to propagate. The decrease in the fracture toughness for nanocomposite containing 5 wt% of clay can be related to the poor dispersion of nanoclay in epoxy resin, clay aggregation and the formation of microvoids as shown in the magnified micrograph in Figure 4.21(b) due to the high viscosity of the mixture in which higher mixing force was required to properly mix the hardener with the epoxy/clay mixture, these clay aggregation and microvoids acted as stress concentration regions that initiate cracks which led to the premature failure.

The increase in the fracture toughness at low percent of clay loading and the decrease in the fracture toughness with increasing clay loading have also been reported by Zulfli et al [13], Yao et al [15], Kusmono et al [22] and Wang et al [24]. Other studies reported that the fracture toughness of nanocomposite was lower than that of neat epoxy and decreased with increasing clay concentration [19, 20]. Other researchers, however, found continuous improvement in the fracture toughness with raising clay loading [12, 14, 17, 18].

Table 4.7: Average values of the maximum fracture load of neat epoxy and nanocomposites (NC) containing different clay loadings.

Sample	Maximum Fracture Load (N)	Standard Deviation
Neat Epoxy	117.10	3.68
NC 1% Clay	129.32	2.23
NC 1.5% Clay	141.62	3.10
NC 2% Clay	149.07	3.24
NC 3% Clay	158.66	3.56
NC 5% Clay	125.37	3.05

Table 4.8: Average values of the stress intensity factor of neat epoxy and nanocomposites (NC) containing different clay loadings.

Sample	Stress Intensity Factor ($MPa.m^{1/2}$)	Standard Deviation
Neat Epoxy	0.63	0.02
NC 1% Clay	0.70	0.01
NC 1.5% Clay	0.76	0.03
NC 2% Clay	0.80	0.02
NC 3% Clay	0.86	0.01
NC 5% Clay	0.68	0.02

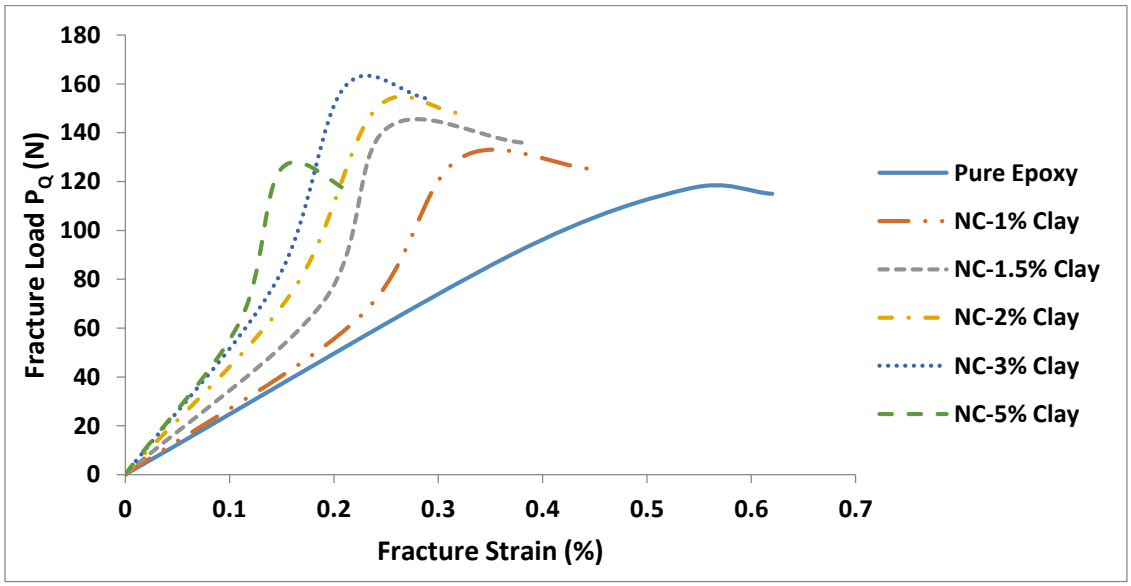

Figure 4.14: Fracture load-Strain curve for neat epoxy and nanocomposites.

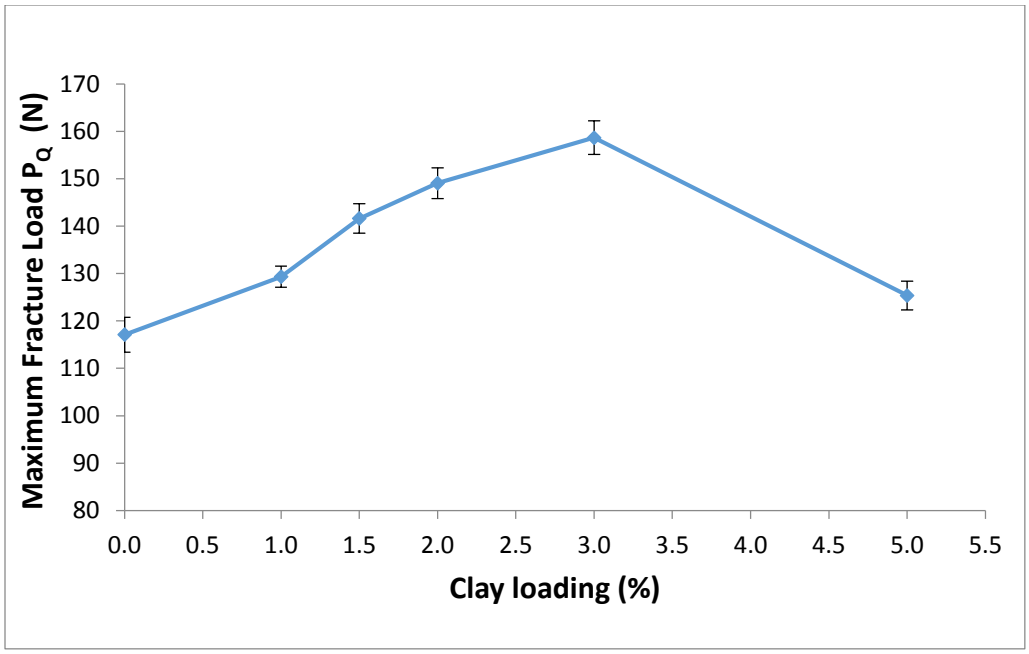

Figure 4.15: Maximum fracture load of Neat Epoxy and nanocomposites with different clay loadings.

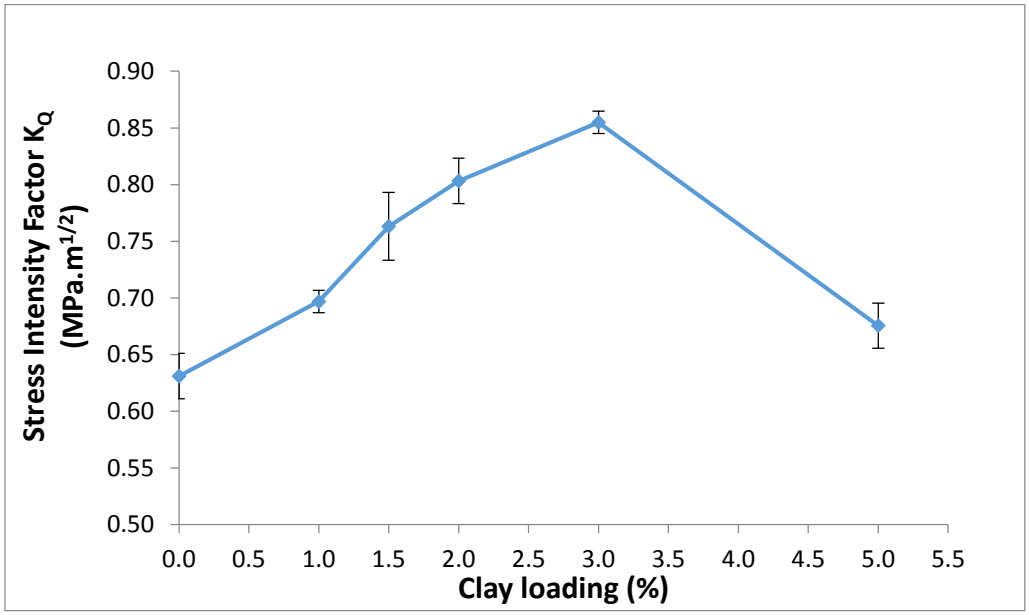

Figure 4.16: Stress Intensity Factor of Neat Epoxy and nanocomposites with different clay loadings.

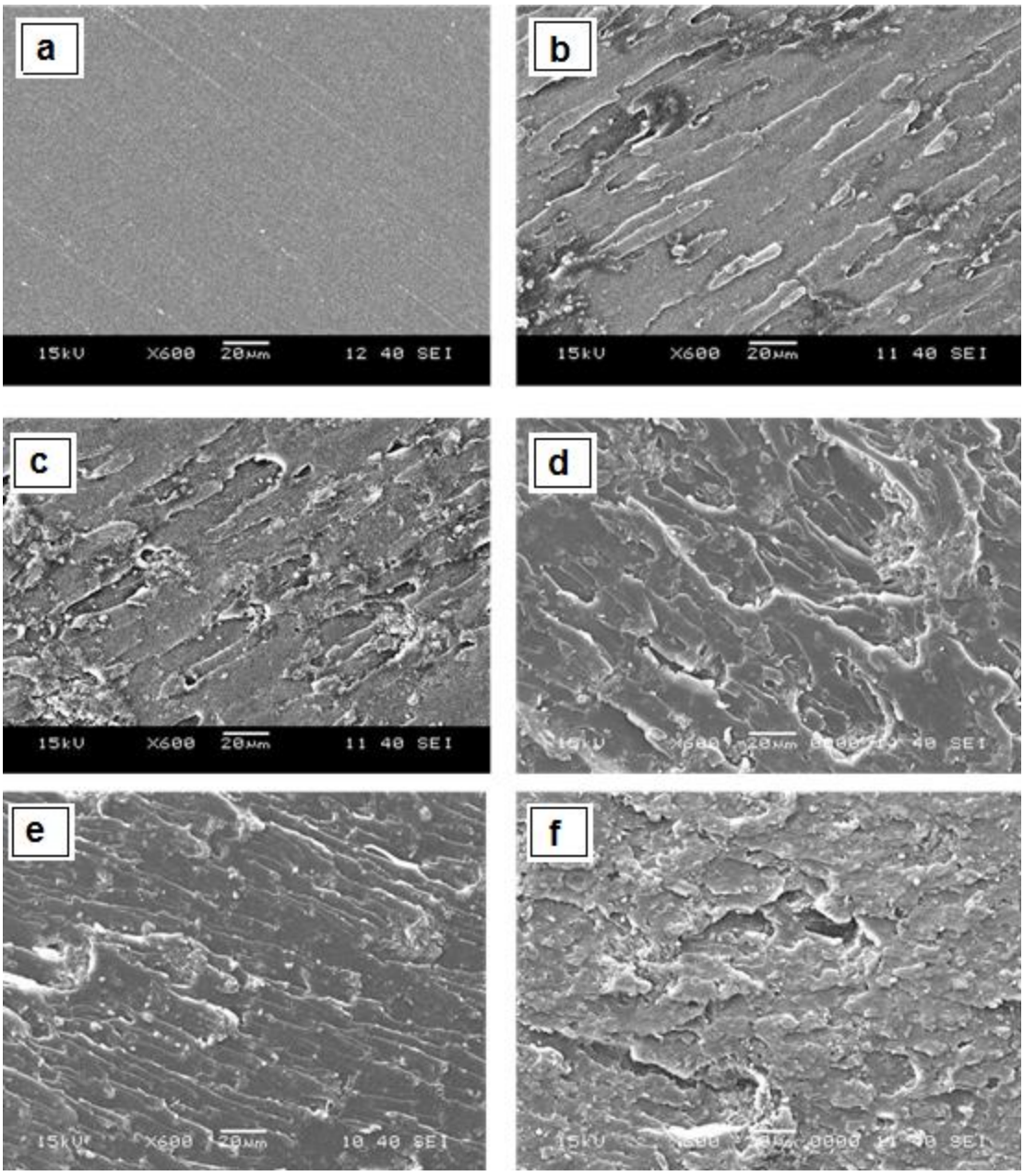

Figure 4.17: SEM fractographs (X600) of (a) neat epoxy and nanocomposite with different clay loadings (b) 1 wt%, (c) 1.5 wt%, (d) 2 wt%, (e) 3 wt% and (f) 5 wt%.

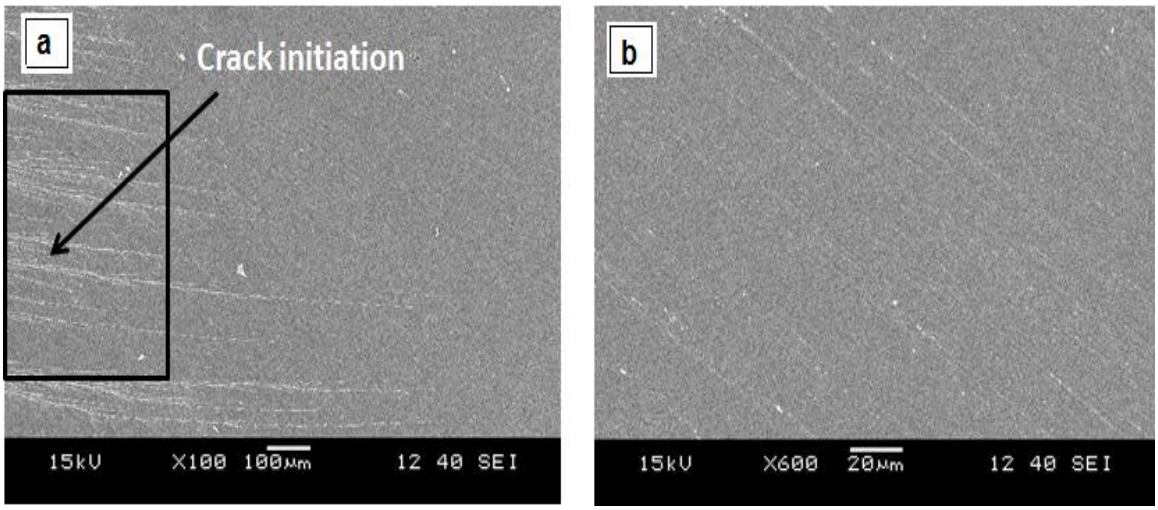

Figure 4.18: SEM fractographs of neat epoxy (a) showing crack initiation and propagation (X100) and (b) propagation region (X600).

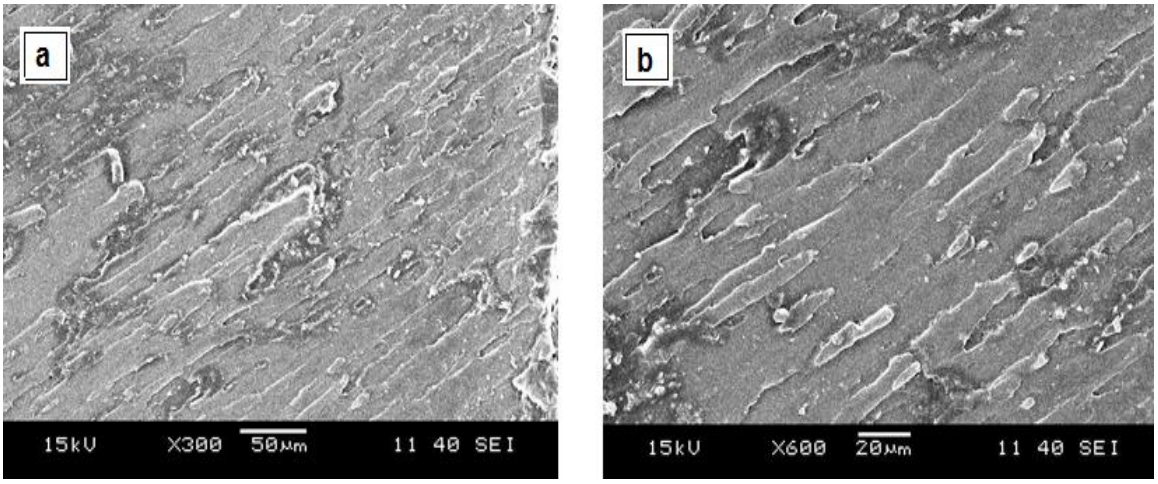

Figure 4.19: SEM fractographs of nanocomposite containing 1wt% nanoclay (a) showing crack initiation and propagation (X300) and (b) propagation region (X600).

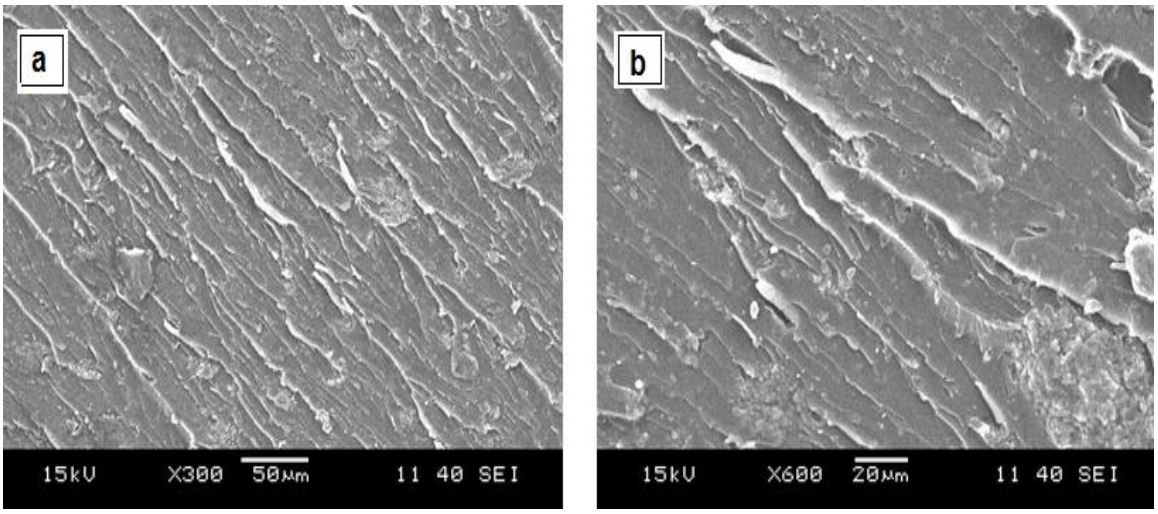

Figure 4.20: SEM fractographs of nanocomposite containing 3wt% nanoclay (a) showing crack initiation and propagation (X300) and (b) propagation region (X600).

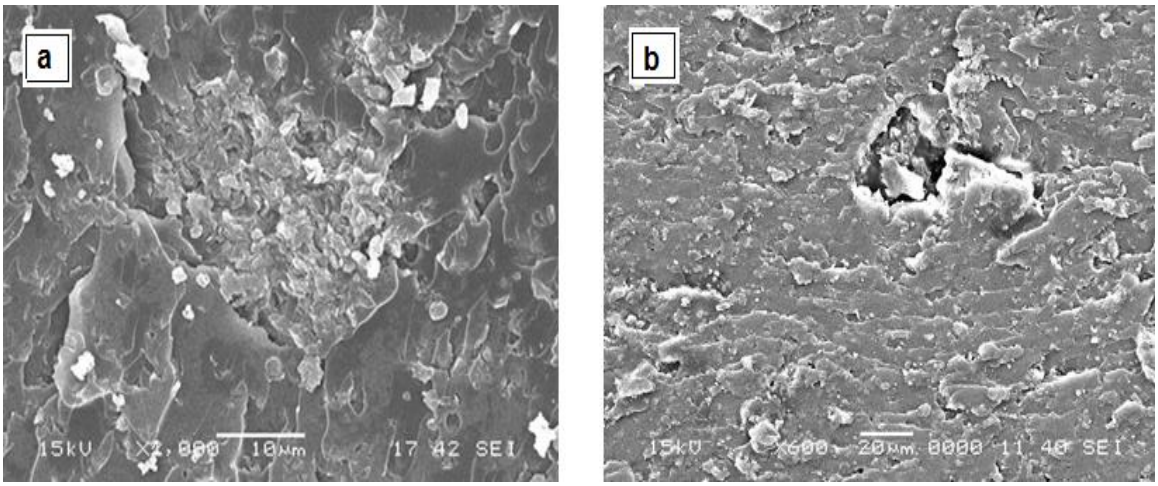

Figure 4.21: SEM fractographs of nanocomposite containing 5wt% nanoclay (a) showing clay agglomeration (X1000) and (b) microvoids (X600).

4.3.5 Effect of Clay Loading on Glass Transition Temperature

DSC was used to investigate the effect of clay loading on the T_g. Midpoint method was used to determine the glass transition temperature. The addition of nanoclay particles did not have a noticeable effect on T_g. As shown in Figure 4.22, T_g decreased slightly with the percent of clay loading; from 160.81ºC for neat epoxy to 150.84ºC for nanocomposite containing 5 wt% of clay loading. The relatively small reduction in T_g can be attributed to

the low crosslinking density in the galleries between the clay layers and to the negative effect of clay layers as a barrier that decreases the crosslinking density during the curing process [5]. Therefore, the decrease of T_g with clay loading can be related to the increase of epoxy molecules having low crosslinking density between the clay layers within the tactoids of clay and the reduction in the crosslinking density outside the tactoids due to barrier properties of the clay layers. The decrease in the glass transition temperature with increasing clay loading has been reported by other researchers [5, 27].The reduction in T_g can also be related to the effect of the organic modifier on curing. Sorina et al [47] observed that the organic modifiers of Cloisite 10 A, Cloisite 15 A and Cloisite 20 A nanoclays affects the degree of crosslinking and not all the hardener groups crosslink with the epoxy monomer and the unreacted quantity of curing agent acts as a plasticizer which leads to decrease T_g.

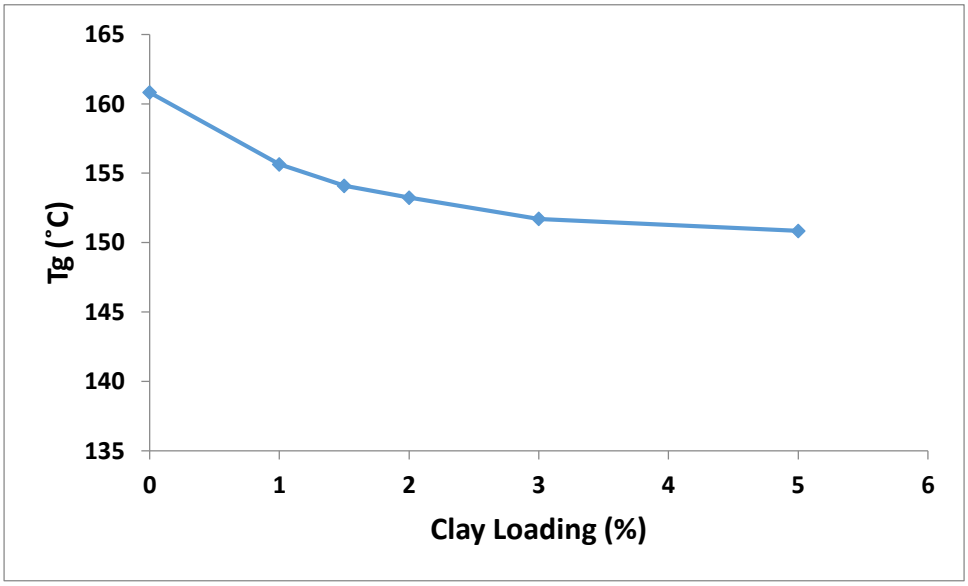

Figure 4.22: Variation of glass transition temperature with clay loading.

4.4 Water-Uptake in Epoxy and Nanocomposites

4.4.1 Experimental Measurements

The maximum water uptake and diffusivity at room temperature and at 80ºC for the neat epoxy and nanocomposites containing different clay loadings are listed in Table 4.9 and Table 4.10, respectively. The total immersion period in tap water was four months at room temperature and 80ºC. The water uptake was determined by periodically measuring the weight gain in all the specimens and the average value of the weight gain from four samples were taken for neat epoxy and nanocomposites.

The variation of the percent weight gains with the square root of exposure time in tap water for neat epoxy and nanocomposites containing different clay loadings of I.30E nanoclay at room temperature and 80ºC have been studied. The percent of weight gain that is considered as a measure of the water uptake is calculated using the following equation

$$M_t(\%) = \frac{(Mi-Mo)}{Mo} X\ 100 \tag{4.3}$$

Where M_t is the percentage weight gain for a given exposure time t, M_i and M_o are the instantaneous and original weights of the exposed specimens, respectively.

The water uptake behavior during the first period is diffusion controlled; hence the diffusion constants for both neat epoxy and nanocomposites have been calculated using the solution of Fick‟s law for short time according to (Eq 4.4)

$$D = \left[\left(\frac{M_t}{\sqrt{t}}\right)^2 \times \frac{\pi h^2}{16 M_s}\right] \tag{4.4}$$

Where M_s represents the relative weight gain at saturation, h is the specimen thickness (mm), t is the exposure time (s), and D is the diffusion coefficient (mm^2/s).

Figure 4.23 presents the change of percentage weight gain at room temperature for neat epoxy and nanocomposites containing different clay loadings with the square root of time ($h^{1/2}$). As can be seen from the figure, there is a linear increase in the percentage of weight gain with time up to 45 $h^{1/2}$. It is clear that the addition of layered silicate nanoclay to neat epoxy decreased the water absorption and diffusivity. The highest water gain percentage decreased from 1.41% for neat epoxy to 1.06% for nanocomposite containing 5% loading which is around 25% reduction in water moisture uptake. The diffusivity also decreased by about 41%; from 6.65×10^{-7} (mm^2/s) for the neat epoxy to 3.91×10^{-7} (mm^2/s) for the nanocomposite containing 5wt% of clay loading. The improvement in barrier properties due to nanoclay addition has been reported by a number of researchers [5, 28, 32-34, 48] as discussed in section 3.6. This improvement can be related to the tortuosity effect where water molecules motion are hindered by the presence of clay layers during the diffusion process so it had longer paths to move in the nanocomposite than in neat epoxy.

Figure 4.24 shows the change in percent weight gain of neat epoxy and nanocomposites containing different clay loadings with the square root of exposure time in tap water at 80ºC, Similar to the water uptake at room temperature, the rate and maximum uptake decreased with increasing clay loading. The higher exposure temperature is seen to enhance the diffusion process.

As can be seen from Figure 4.24, the weight gain first increased linearly with the square root of time ($h^{1/2}$) indicating a diffusion controlled process up to 18 $h^{1/2}$. It is clear that the addition of layered silicate nanoclay to neat epoxy decreased the water absorption. The highest water gain percentage decreased from 2.69% for neat epoxy to 2.12% for nanocomposite containing 5 wt% loading which is around 21.3% reduction in water moisture uptake. The diffusivity also decreased by about 24%; from 9.01×10^{-6} (mm^2/s) for the neat epoxy to 6.86×10^{-6} (mm^2/s) for the nanocomposite containing 5wt% of clay loading.

Table 4.9: Average values of the maximum water uptake, the percentage of water uptake reduction and diffusivity of neat epoxy and nanocomposites (NC) at room temperature.

Sample	Maximum Water Uptake (%)	Percentage of reduction due to Clay addition (%)	Diffusivity×M_s (mm^2/s)
Neat Epoxy	1.41	-	6.65×10^{-7}
NC 1% Clay	1.28	8.76	5.43×10^{-7}
NC 1.5% Clay	1.19	15.67	4.82×10^{-7}
NC 2% Clay	1.14	19.14	4.31×10^{-7}
NC 3% Clay	1.09	22.46	4.13×10^{-7}
NC 5% Clay	1.06	25.00	3.91×10^{-7}

Table 4.10: Average values of the maximum water uptake, the percentage of water uptake reduction and diffusivity of neat epoxy and nanocomposites (NC) at 80°C.

Sample	Maximum Water Uptake (%)	Percentage of reduction due to Clay addition (%)	Diffusivity×M_s (mm^2/s)
Neat Epoxy	2.69	-	9.01×10^{-6}
NC 1% Clay	2.46	8.74	8.34×10^{-6}
NC 1.5% Clay	2.40	10.91	8.22×10^{-6}
NC 2% Clay	2.32	13.95	7.75×10^{-6}
NC 3% Clay	2.24	16.72	7.38×10^{-6}
NC 5% Clay	2.12	21.27	6.86×10^{-6}

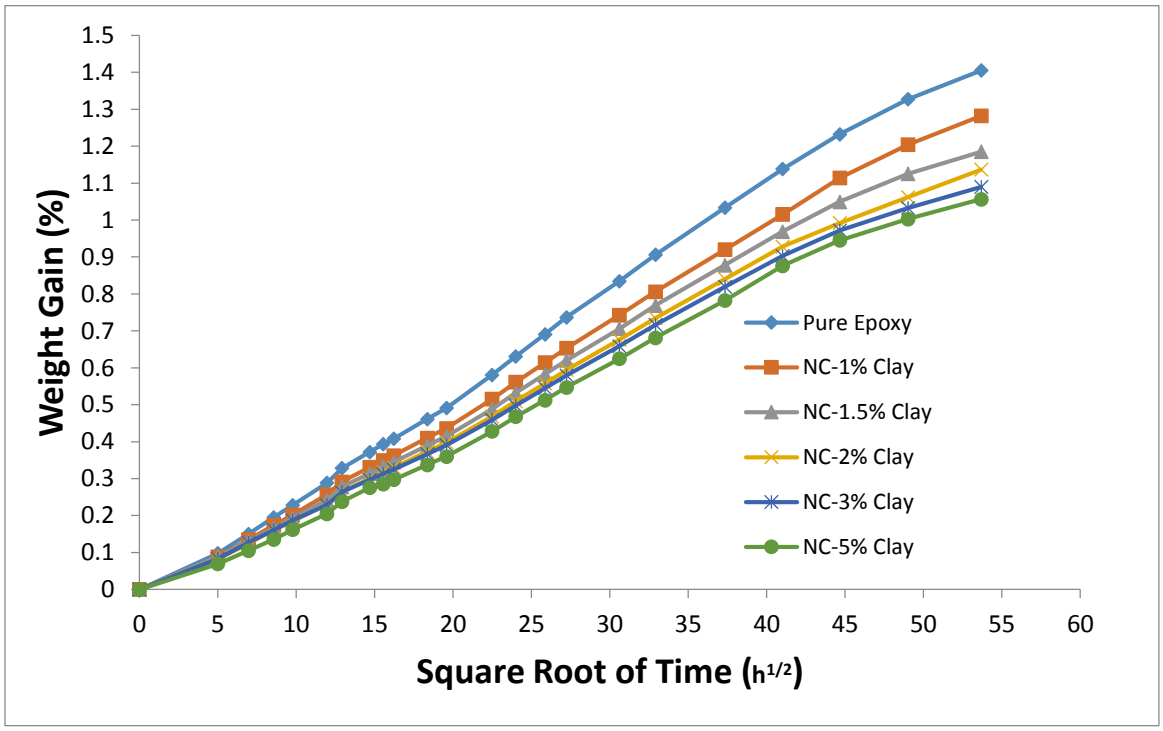

Figure 4.23: Variation in water percentage weight gains for epoxy and nanocomposites having different clay loadings with immersion time at RT.

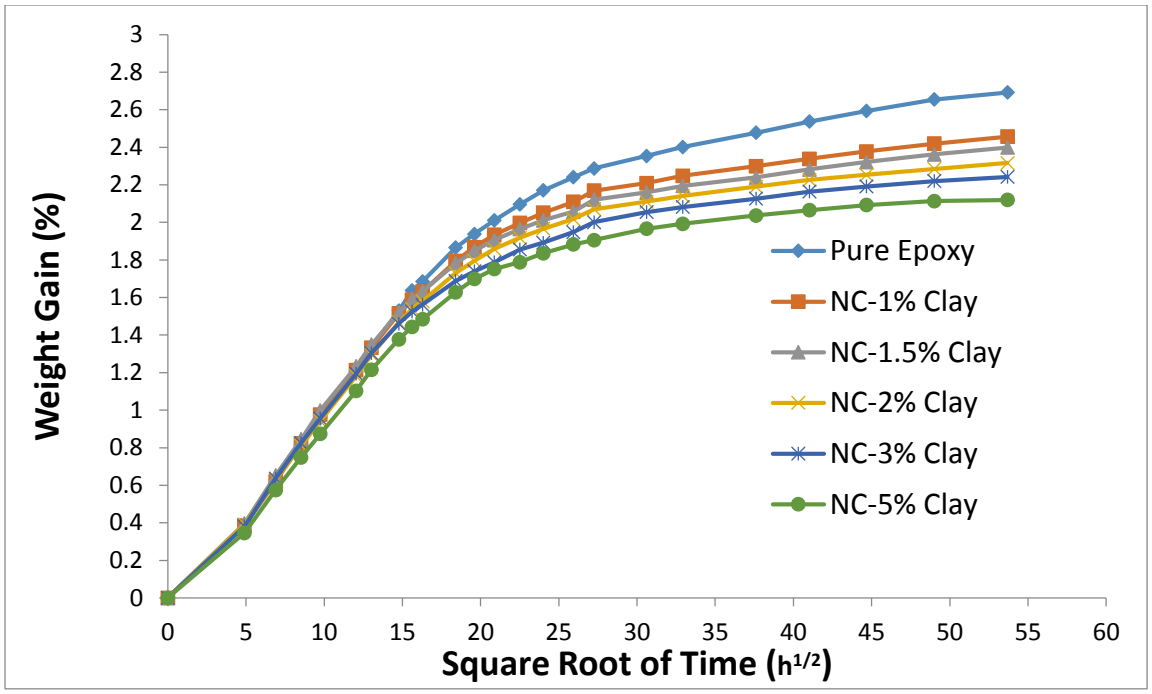

Figure 4.24: Variation in water percentage weight gains for epoxy and nanocomposites having different clay loadings with immersion time at 80°C.

The improvement in barrier properties and the reduction in the diffusivity due to nanoclay addition can be attributed to the tortuosity effect where water molecules have to move around clay layers during the diffusion within the nanocomposites.

Figure 4.25 illustrates the effect of temperature on water uptake of neat epoxy and nanocomposites. Figure 4.26 shows that the maximum water uptake decreased due to clay addition with similar rate for both RT and 80°C. The high increase in water uptake at 80°C as compared with the ones that immersed at room temperature is attributed to the higher immersion temperature (80°C) which indicate that water absorption of pure epoxy and nanocomposites is temperature dependent and water molecules are diffused in accelerated manner in epoxy and nanocomposites specimens at 80°C water temperature than the ones where immersed in tap water at room temperature. The effect of immersion

temperature on increasing the diffusion and weight gain of epoxy and nanocomposites have been also reported by a number of researchers [5, 37, 38, 48].

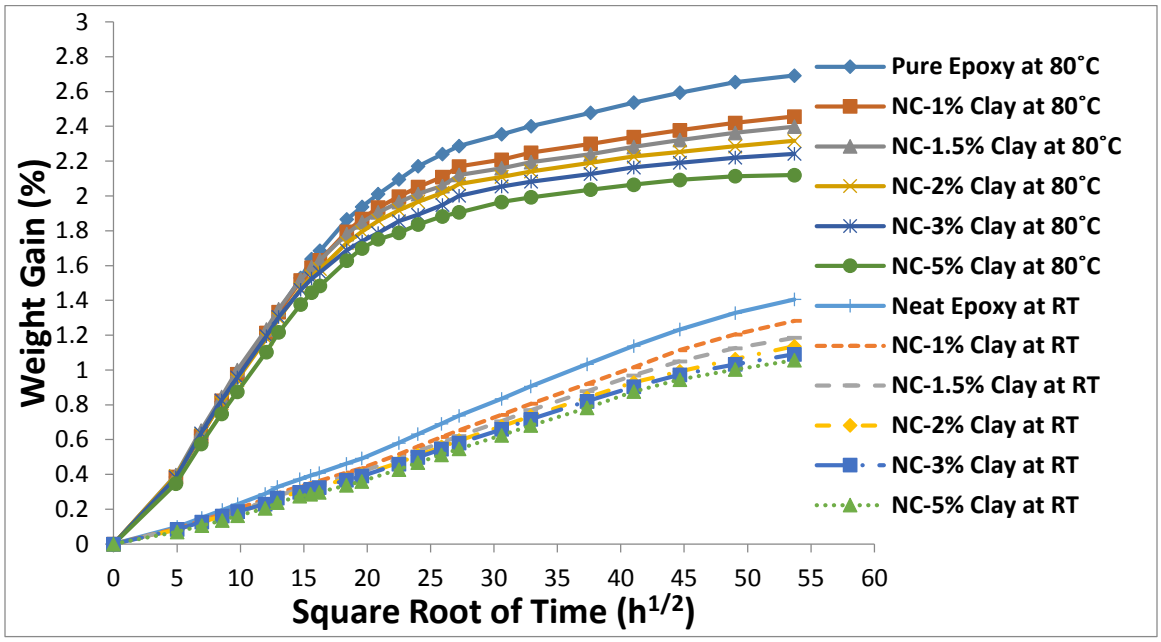

Figure 4.25: Variation in percentage weight gains for epoxy and nanocomposites having different clay loadings with immersion time at RT and 80 ºC.

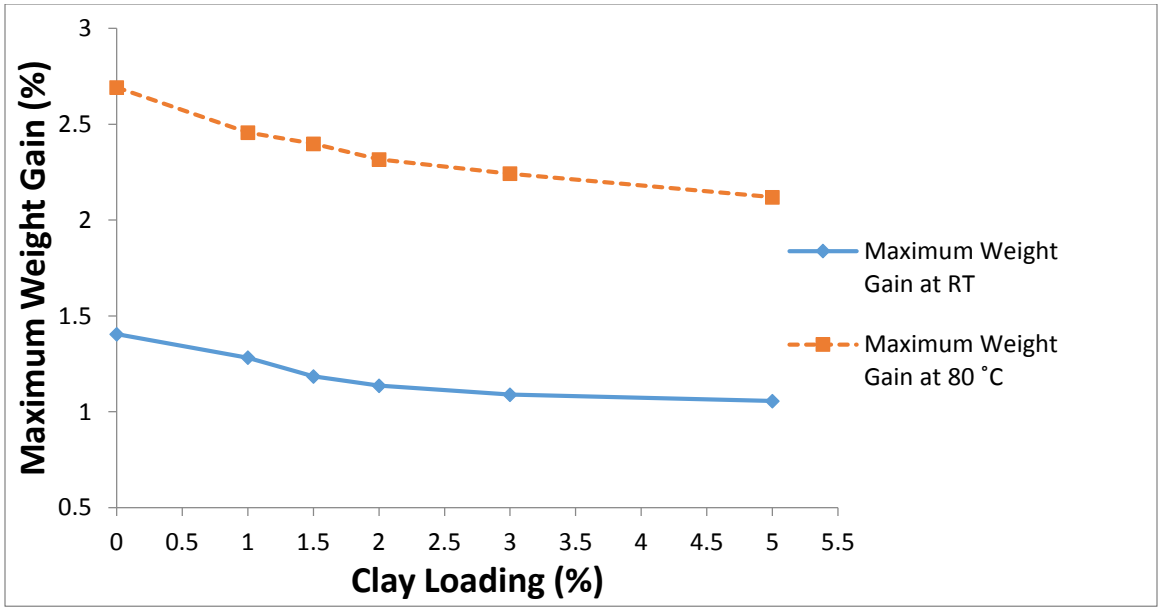

Figure 4.26: Variation of the maximum weight gain for epoxy and nanocomposites with clay loading immersed at room temperature (RT) and 80ºC.

4.4.2 Effect of Water-Uptake on Glass Transition Temperature

Table 4.11 lists the T_g values for neat epoxy and nanocomposites containing different clay loadings of I.30E nanoclay before and after exposure to water at different temperatures. Figure 4.27 displays the variation of T_g with clay loading for neat epoxy and nanocomposites before and after exposure to water at room temperature and at 80ºC. As can be seen in the figure, T_g for neat epoxy and nanocomposites decreased due to water uptake. The reduction in T_g for neat epoxy are 12 and 29% due to water uptake at room temperature and at 80ºC, respectively, while it is 2 and 13%, respectively, for the nanocomposites with 1 wt% clay loading.

The reduction in T_g can be attributed to the plasticizing effect of water molecules which diffused into epoxy matrix. This reduction seems to be proportional to maximum weight gain and this explains the lower reduction in T_g for samples exposed to water at room temperature compared to those exposed to water at 80ºC. The reduction in T_g for neat epoxy and nanocomposites have been reported by other researchers [38, 49]. As explained in section 4.3.5, the slight reduction in T_g for nanocomposites is due to the presence of lower water molecules as compared with neat epoxy [6].

Table 4.11: Water uptake effect at room temperature and 80°C on Tg of epoxy and nanocomposites.

Sample	T_g (°C) Before Exposure	T_g (°C) After Exposure at RT	T_g (°C) After Exposure at 80°C
Neat Epoxy	160.81	141.23	113.81
NC 1% Clay	155.64	152.70	135.52
NC 1.5% Clay	154.09	150.90	130.16
NC 2% Clay	153.24	149.31	128.73
NC 3% Clay	151.71	148.24	127.89
NC 5% Clay	150.84	146.34	125.74

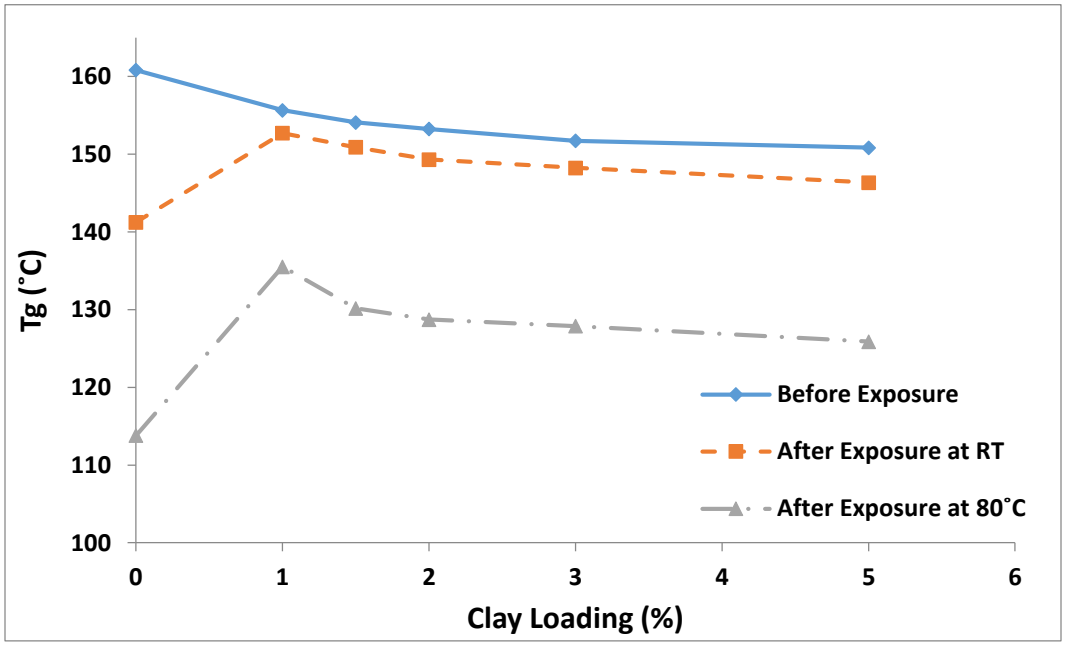

Figure 4.27: T_g for epoxy and nanocomposites containing different clay loadings before and after water exposure at room temperature and at 80°C.

4.4.3 Effect of Water-Uptake on Flexural Properties

Flexural tests were conducted to study the effect of water uptake at different immersion temperatures (room temperature and 80°C) on the flexural properties of neat epoxy and nanocomposites. The effect of water uptake on flexural strength (σ_f), flexural modulus

(E) and flexural strain (ε_f) of neat epoxy and nanocomposites containing different clay loadings is illustrated in Table 4.12. The results showed that both flexural strength and flexural modulus decreased as a result of water uptake, however, obvious improvement in flexural strains are observed. These reductions are proportional to quantity of liquid uptake. Similarly, a clear increase in fracture strain for the samples immersed in water at 80ºC as compared with the samples immersed at room temperature was observed.

The variations of the average values of flexural strength and flexural modulus for the neat epoxy and the nanocomposites before and after immersion in water at both (RT and 80 ºC) are illustrated in Figure 4.28 and Figure 4.29, respectively. The reduction in flexural strength and modulus of the nanocomposites containing 1, 1.5, 2 and 3wt% of nanoclay are seen to be less than that of neat epoxy. The decrease in flexural strength and modulus due to water uptake at room temperature for the nanocomposites containing 1wt% of clay are 9 and 3.5%, respectively while it is about 21 and 9.5%, respectively for 80ºC. The decrease in the flexural strength and modulus for neat epoxy and nanocomposites containing different clay loadings have also been reported by [32, 35, 36]. This drop in the mechanical properties resulted from water uptake and can be attributed to the effect of the water which that acts as plasticizers in the epoxy and nanocomposites.

The effect of water uptake at different immersion temperatures on the flexural strain of neat epoxy and nanocomposites containing different clay loadings is illustrated in Figure 4.30. A clear increase in ductility for neat epoxy is observed due to water uptake at room temperature and at 80ºC; 40 and 62%, respectively. The improvement in the fracture strain after water uptake seems to be proportional to maximum weight gain and this explains the increase in ε_f for samples exposed to water at 80ºC compared to those

exposed to water at room temperature. The addition of nanoclay, however, leads to a decrease in the fracture strain as explained earlier in section 4.3.2. The improvement in flexural strain of the nanocomposites containing 1, 1.5, 2, 3 and 5wt% of nanoclay are seen to be less than that of neat epoxy. This is due to the brittleness of the nanocomposites.

Table 4.12: Effect of water uptake on flexural properties of neat epoxy and nanocomposites at room temperature and 80°C.

Sample	Condition	σ_f (MPa)	SD	E(GPa)	SD	ε_f (%)	SD
Neat Epoxy	Before Exposure	100.19	4.71	2.78	0.07	9.65	0.54
	After Exposure at RT	85.21	3.54	2.60	0.05	13.54	0.23
	After Exposure at 80ºC	66.65	3.62	2.37	0.04	15.67	0.42
NC 1%	Before Exposure	106.18	3.80	2.85	0.08	7.56	0.25
	After Exposure at RT	96.32	4.14	2.75	0.04	9.87	0.41
	After Exposure at 80ºC	83.43	3.54	2.58	0.06	11.32	0.31
NC 1.5%	Before Exposure	114.47	3.91	2.90	0.06	4.98	0.61
	After Exposure at RT	110.12	2.36	2.80	0.03	6.45	0.43
	After Exposure at 80ºC	100.55	4.32	2.65	0.04	7.89	0.21
NC 2%	Before Exposure	110.97	5.69	3.01	0.08	4.23	0.25
	After Exposure at RT	103.47	4.52	2.88	0.06	5.44	0.36
	After Exposure at 80ºC	94.44	2.65	2.76	0.03	6.60	0.31
NC 3%	Before Exposure	100.25	3.11	3.15	0.05	3.93	0.61
	After Exposure at RT	95.13	3.25	3.07	0.02	4.56	0.26
	After Exposure at 80ºC	85.24	3.21	2.98	0.02	5.43	0.11
NC 5%	Before Exposure	88.24	7.61	3.30	0.09	3.29	0.34
	After Exposure at RT	82.59	5.54	3.24	0.04	3.85	0.47
	After Exposure at 80ºC	64.61	3.51	3.18	0.03	4.21	0.13

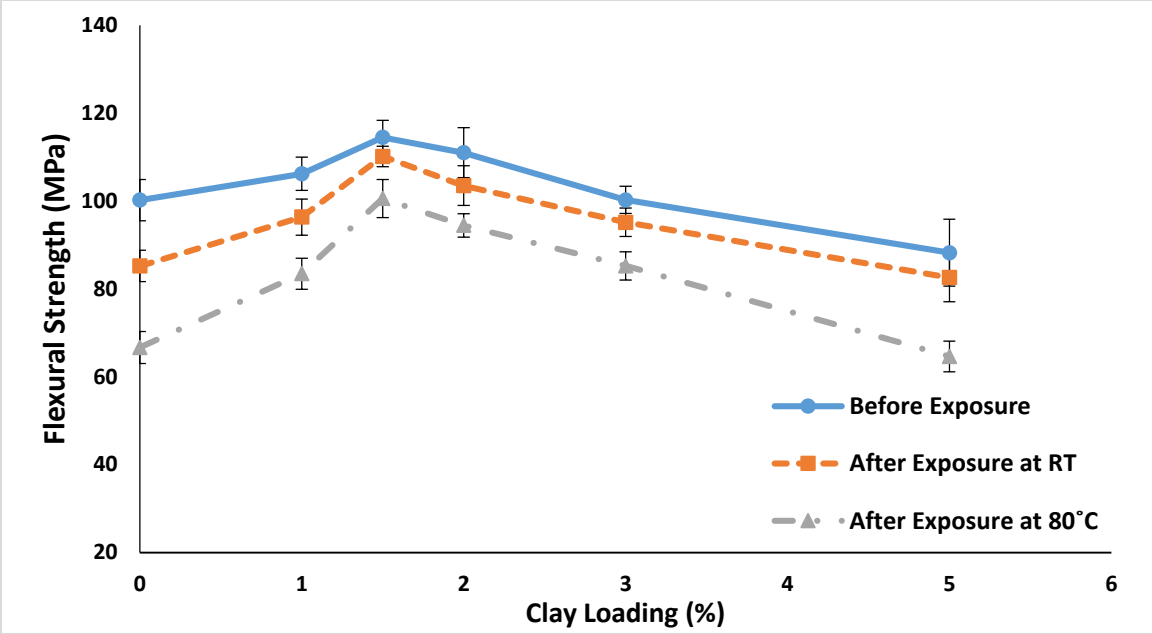

Figure 4.28: Variation of flexural strength with clay loading for neat epoxy and nanocomposites before and after exposure to water at RT and 80°C.

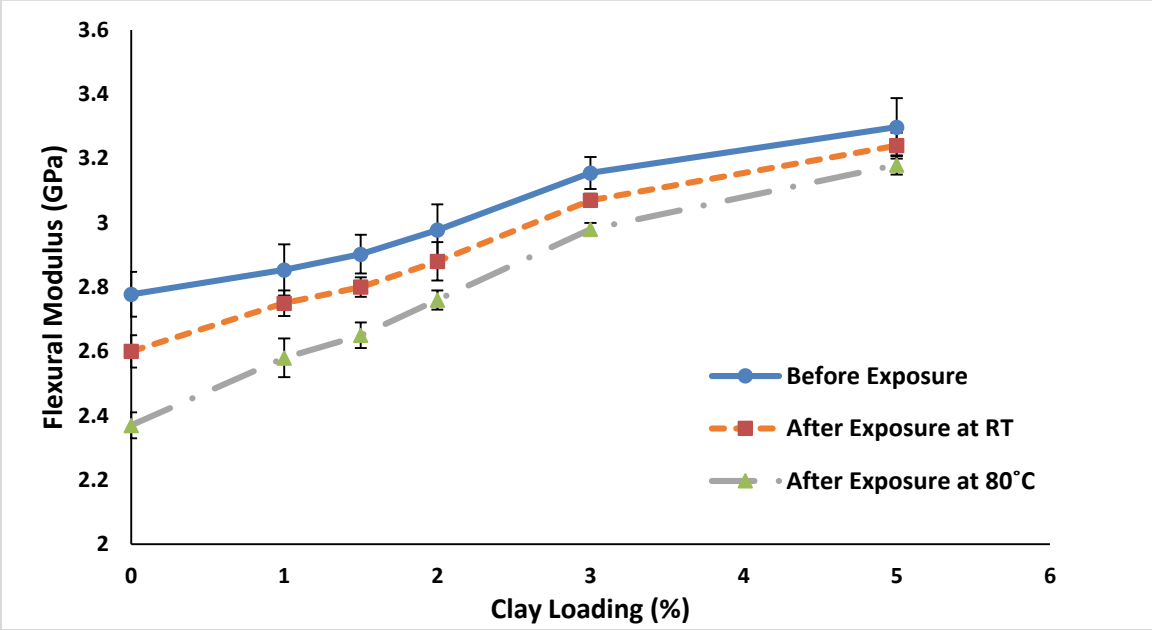

Figure 4.29: Variation of flexural modulus with clay loading for neat epoxy and nanocomposites before and after exposure to water at RT and 80°C.

.

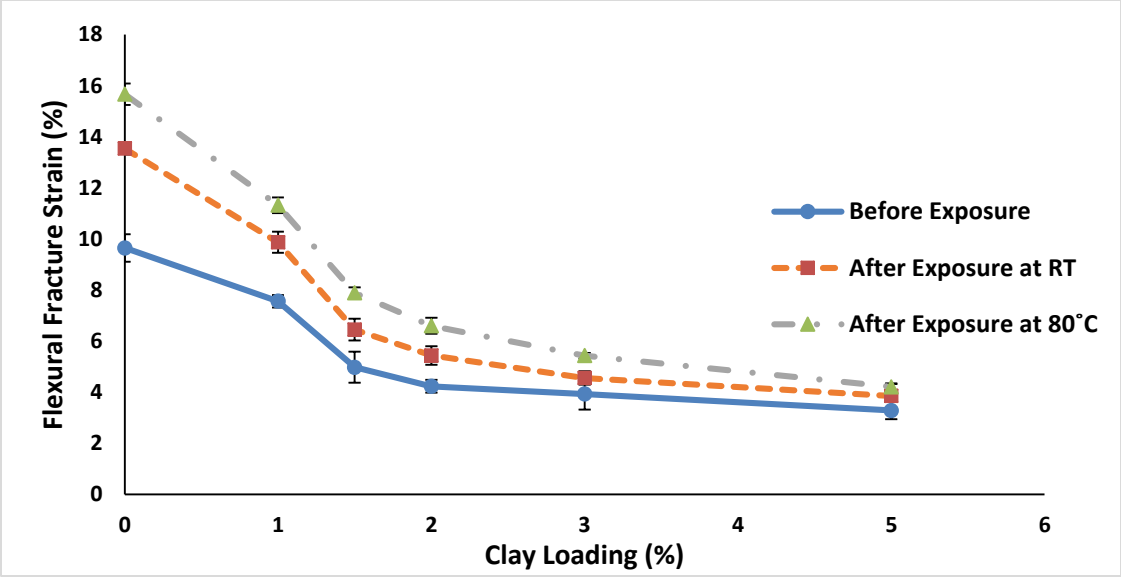

Figure 4.30: Variation of flexural strain with clay loading for neat epoxy and nanocomposites before and after exposure to water at RT and 80ºC.

4.4.4 Effect of Water-Uptake on Fracture Toughness Properties

Single Edge Notch Bending (SENB) fracture toughness tests were conducted as described in section 3.7.2 to study the effect of water uptake at (RT and 80ºC) on fracture toughness of neat epoxy and nanocomposites. Figure 4.31 shows representative fracture load-strain curves for neat epoxy before and after exposure to water at (RT and 80ºC). As can be seen in the figure, the fracture load decreased as a result of water uptake, however, improvement in fracture strains are observed. The reduction in the maximum fracture load, P_Q, and the fracture toughness, K_Q, due to water uptake for neat epoxy and nanocomposites containing different clay loadings are listed in Table 4.13. The variation of the maximum fracture load and the stress intensity factor for neat epoxy and the nanocomposites containing different loadings of nanoclay before and after immersion in water (at both room temperature and 80ºC) are illustrated in Figure 4.32 and Figure 4.33 respectively. As shown in these figures, the stress intensity factor for neat epoxy

decreased as a result of water uptake. As for the flexural properties these reductions were proportional to the degree of moisture content for both the samples immersed in water at room temperature and 80ºC. The reductions in the maximum fracture load and fracture toughness due to water uptake for the nanocomposites containing 1, 1.5, 2 and 3wt% of nanoclay are less than those observed for neat epoxy. The decrease in fracture toughness due to water uptake at room temperature for neat epoxy is around 11% while the reduction resulting from water uptake at 80ºC is about 30%, as listed in Table 4.13. However, the aforementioned percentages of reduction in fracture toughness in the case of nanocomposites were found to decrease. For instance, the decrease in fracture toughness due to water uptake at room temperature for the nanocomposite containing 3wt% clay is around 4.7% while the reduction resulting from water uptake at 80ºC is about 14%.

The reduction in fracture toughness can be attributed to the softening effect due to water moisture uptake specially at 80ºC exposure temperature. Also, it might be related to the decrease in the bonding strength between epoxy and nanoclay due to water immersion and the interfacial adhesion which might be more sensitive to the temperature of water exposure [50-54]. Sekine et al [55] found that with increasing time of exposure to water, the maximum load to failure and the fracture toughness decrease linearly. Schutte [56] suggest that water can not only stress the resin through swelling, but also potentially hydrolyze the functional groups in the resin as well. The hydrophilicity of the resin will be one of the determining factors for the equilibrium content of water, to a first-order approximation. The content of water in the composite will influence the swelling stresses of the resin that can cause microcracking in the matrix. On the other hand, Alamri and

Low [32] observed that the fracture toughness for nanocomposites after water exposure was found to be higher than that the of nanocomposites before water uptake. The authors claimed that the enhancement in fracture toughness can be attributed to the increased resistance to crack propagation due to crack deflection and plastic deformation.

Table 4.13: Average values of the maximum fracture load and the stress intensity factor for neat epoxy and nanocomposites at RT and 80ºC.

Sample	Condition	Maximum Fracture Load(N)	Standard Deviation	Stress Intensity Factor ($MPa.m^{1/2}$)	Standard Deviation
Neat Epoxy	Before Exposure	117.10	3.68	0.63	0.02
	After Exposure at RT	103.21	3.11	0.56	0.03
	After Exposure at 80ºC	82.21	3.11	0.44	0.03
NC 1% Clay	Before Exposure	129.32	2.23	0.70	0.01
	After Exposure at RT	118.21	3.51	0.64	0.01
	After Exposure at 80ºC	98.03	2.52	0.53	0.02
NC 1.5% Clay	Before Exposure	141.62	3.10	0.76	0.03
	After Exposure at RT	132.54	2.45	0.71	0.02
	After Exposure at 80ºC	114.67	4.21	0.62	0.01
NC 2% Clay	Before Exposure	149.04	3.24	0.80	0.02
	After Exposure at RT	141.82	1.62	0.76	0.01
	After Exposure at 80ºC	124.90	2.33	0.67	0.02
NC 3% Clay	Before Exposure	158.66	3.56	0.85	0.01
	After Exposure at RT	151.47	2.87	0.81	0.02
	After Exposure at 80ºC	136.38	2.53	0.73	0.03
NC 5% Clay	Before Exposure	125.37	3.05	0.68	0.02
	After Exposure at RT	114.51	1.41	0.61	0.02
	After Exposure at 80ºC	91.06	3.41	0.49	0.03

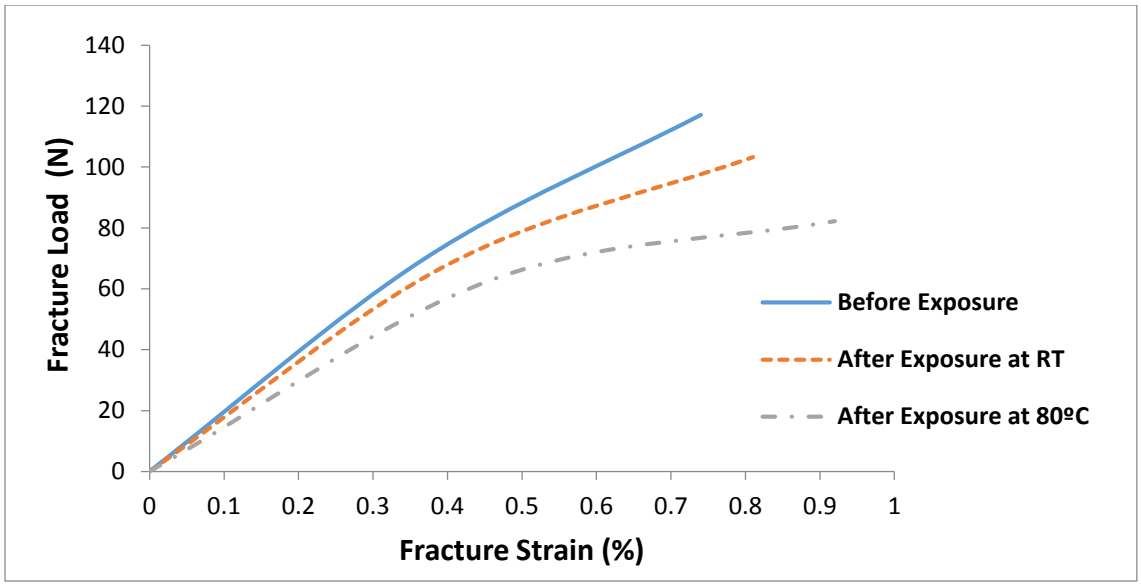

Figure 4.31: Representative load-strain curves for neat epoxy before and after exposure to water.

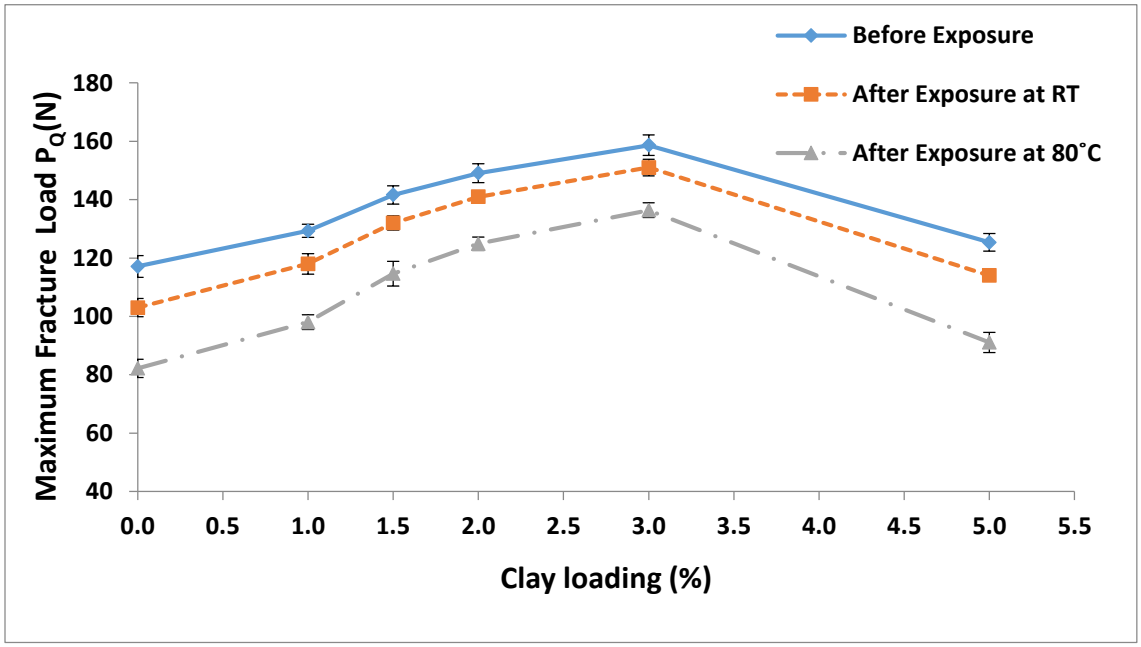

Figure 4.32: Variation of the maximum fracture load with clay loading for neat epoxy and nanocomposites before and after exposure to water at RT and 80°C.

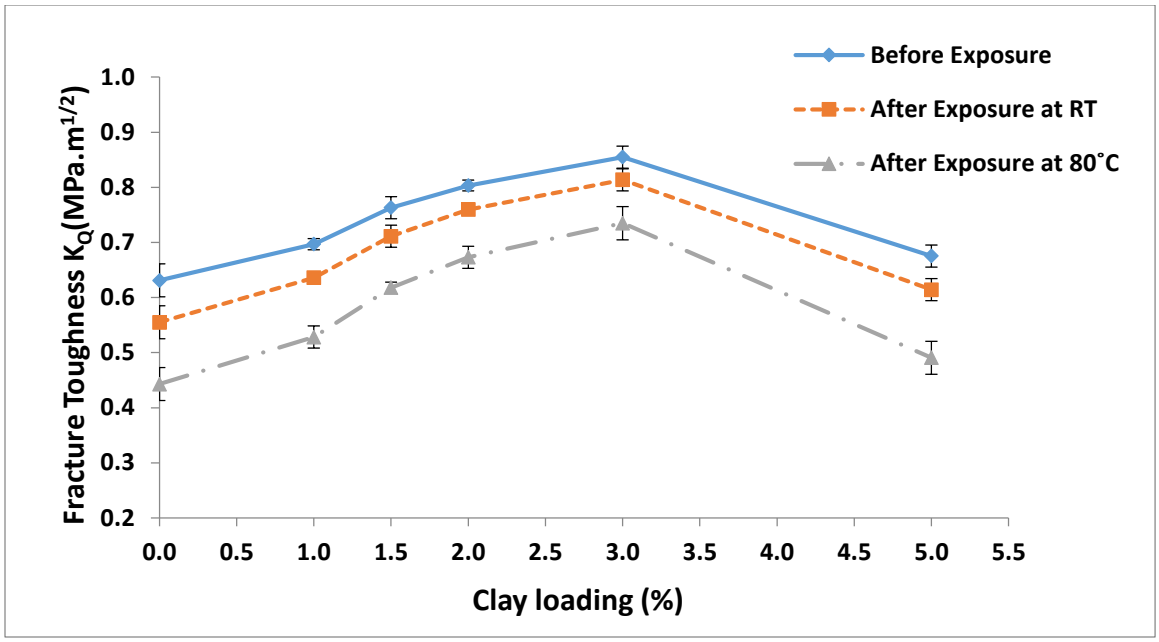

Figure 4.33: Variation of the fracture toughness with clay loading for neat epoxy and nanocomposites before and after exposure to water at RT and 80°C.

CHAPTER 5

CONCLUSIONS AND RECOMMENDATIONS

5.1 Conclusion

In this work, DGEBA epoxy resin was reinforced with I.30E organoclay to synthesize epoxy-clay nanocomposites.

Nanocomposites containing 3 wt% loading of I.30E clay were synthesized by high shear mixing technique to study the effect of degassing parameters on the degree of clay dispersion and distribution within epoxy matrix. It was observed that the degree of clay dispersion was improved with increasing the degassing temperature and time. XRD analyses confirmed that the optimum degassing temperature and time were 120ºC and 4 hours, respectively. Also, XRD analyses showed that the morphology of the resultant nanocomposites was either disordered intercalation or exfoliated structure.

The results, also, showed a shift to the left in the peaks as the degassing time increased from 2 to 4 hours indicating an increase in the inter-planar spacing. This improvement in interlayer spacing and the absence of peak at the degassing temperature of 120ºC are indications that not only the higher degassing temperature and time do reduce the air bubbles due to HSM, they also enhance the diffusion of epoxy into the intergallery of nanoclay platelets.

Nanocomposites containing 1, 1.5, 2, 3 and 5 wt% of I.30E nanoclay were then fabricated using the optimum high shear mixing and optimum curing parameters determined in earlier work. Also, the optimized degassing parameters were used in nanocomposites

fabrication to investigate the effect of clay loading on the mechanical and physical properties of the resultant nanocomposites. The dynamic viscometer was used to measure the viscosity of the nanocomposites after hand and high shear mixing of nanoclay with epoxy. It was observed that there was a linear increase in viscosity with clay loading addition. The dynamic viscosity, after hand mixing, was found to rise with clay loading and showed about 33 % increase for sample containing 5 wt% of clay. Similar trend was observed for the dynamic viscosity after high shear mixing with about 120% increase for sample containing 5 wt% of clay as compared with neat epoxy sample. The increase in the dynamic viscosity is related to the existence and dispersion of nanoclay in epoxy resin.

The flexural test results showed a 15% improvement in the flexural strength for the nanocomposite containing 1.5 wt% of clay. This increase in flexural strength can be attributed to the good dispersion of nanoclay. Higher nanoclay loading resulted in lower flexural strength. The later reduction in flexural strength with clay loading can be related to the voids that formed during mixing of the hardener with epoxy-clay mixture because of the high mixture viscosity at higher clay loadings, in which considerable amounts of air bubbles were observed to form during mixing and some of these bubbles were not eliminated even after degassing. These micro-voids may have acted as stress concentration regions. Another reason for flexural strength reduction might be the existence of clay agglomeration especially at higher clay loadings. These clay clusters act as preferred sites for crack initiation and resulted in premature failure of the nanocomposites. Therefore, nanoclay loading between 1 wt% and 2 wt% is considered to be the optimum clay loading that had the highest flexural strength. Unlike strength, the

flexural modulus increased almost linearly with clay mainly due to the stiffening effect of the clay layers. The results of flexural strain revealed that the addition of clay led to a semi-linear decrease in the fracture strain. Again, this is due to the fact that voids and clay agglomerations increased with clay loading addition because of the increase in viscosity of epoxy-clay mixture. It was observed through fractographic analysis that flexural fracture surface of neat epoxy was featureless and smooth indicating brittle fracture, while nanocomposites displayed rough corrugated surfaces, indicating an improvement in the flexural strength due to the presence of nanoclay particles.

The fracture toughness test results showed a 35% improvement in the stress intensity factor for the nanocomposite containing 3 wt% of clay. This improvement in fracture toughness can be attributed to the good dispersion of nanoclay in epoxy resin and the toughening mechanism due to crack deflection around nanoclay tactoids as the fracture surface roughness increased with increasing clay loading. Also, it can be related to the good bonding between the clay and the epoxy resin so the addition of clays had a positive impact on fracture toughness. Nanocomposite containing 5 wt% nanoclay resulted in lower fracture toughness with only 7% enhancement as compared with neat epoxy. The later reduction in fracture toughness with clay loading can be related to the voids that formed during mixing of the hardener with epoxy-clay mixture.

The DSC results showed that the addition of I.30E clay led to slight reduction in glass transition temperature (Tg) with about 6% reduction for nanocomposite containing 5 wt% nanoclay. The decrease of T_g with clay loading can be related to the increase of epoxy molecules having low crosslinking density between the clay layers within the tactoids of

clay and the reduction in the crosslinking density outside the tactoids due to barrier properties of the clay layers.

The results of exposure to water at room temperature and 80ºC showed that the addition of I.30E nanoclay enhanced the barrier properties of epoxy matrix and the maximum water uptake was decreased due to nanoclay addition, too.

This improvement can be related to the tortuosity effect where water molecules motion were hindered by the presence of clay layers during the diffusion process so it had longer paths to move in the nanocomposite than neat epoxy. The nanoclay addition also decreased the maximum water uptake and diffusivity at room temperature by about 25% and 41%, respectively for nanocomposite containing 5 wt% of clay loading. The maximum water uptake at 80ºC and diffusivity also decreased by about 21% and 24%, respectively with for nanocomposite containing 5 wt% of clay. It was observed that for epoxy and the nanocomposites immersed at higher environmental conditions (80ºC) were nearer to full saturation than those at room temperature for the same immersion time. Also the maximum weight gain for epoxy and nanocomposites immersed at 80ºC where higher than those which were immersed at room temperature (RT).

T_g for neat epoxy and nanocomposites decreased due to water uptake. The reduction in T_g for neat epoxy are 12 and 29% due to water uptake at room temperature and at 80ºC, respectively, while it is 2 and 13%, respectively, for the nanocomposites with 1 wt% clay loading. The reduction in T_g can be attributed to the plasticizing effect of water molecules which diffused into epoxy matrix

The flexural results showed that both flexural strength and flexural modulus decreased as a result of water uptake at room temperature and at 80ºC, while noticeable enhancement in flexural strains is observed. It is noticed that the reduction in flexural strength and flexural modulus and the increase in flexural strain are proportional to quantity of water absorbed. This change on the mechanical properties resulted from water moisture can be attributed to the effect of the water molecules that act as plasticizers in the epoxy matrix.

The fracture toughness results showed that the stress intensity factor decreased as a result of water uptake at room temperature and at 80ºC due to softening effect because chemical degradation might occurred specially at 80ºC exposure temperature. Also it might be related to the decrease in the bonding strength between epoxy and nanoclay due to water immersion and the interfacial adhesion might be more sensitive to the temperature of water exposure.

In conclusion, epoxy-clay nanocomposites containing different clay loadings were synthesized using high shear mixing techniques. The optimum degassing parameters were determined and characterization of nanocomposites was performed using XRD, SEM, DSC and the Dynamic viscometer .The effectiveness of nanoclay in improving the mechanical and barrier properties was studied. The optimum clay loading that have the best flexural, fracture toughness and barrier properties was mentioned in each case.

5.2 Recommendations

The different process parameters (mixing, degassing and curing) have been studied in the present work and earlier work that used the same materials, also the optimum clay loadings that improve the mechanical and physical properties have been investigated. The

next step is reinforce this epoxy-clay nanocomposite with different fiber glass types and using various fabrication techniques such as hand lay-up, hand lay-up with hot pressing, vacuum bagging, resin transfer moulding (RTM),vacuum assisted risen transfer moulding (VARTM) and filament winding to synthesize hybrid composites.

The feasibility of Epoxy-clay nanocomposites as anticorrosion coating materials should be investigated. For instance, it might be used to protect carbon steel pipes that transport oil and water from corrosion especially in harsh environments with both higher temperatures and relative humidity.

The main objective in developing these Epoxy-clay nanocomposites was to use them later on as matrix materials for Glass Fiber Reinforced pipes (GFRP) in the synthesizing process small scale experiments set up were conducted to optimize the different process parameters. So, more research is required to know how to apply the laboratory work to the real industrial applications. For example, many local companies such as Amiantit Bondstrand and Future Pipe are interested to in this kind of research and they are willing to apply it in their own industries.

.

REFERENCES

[1] F. Kreith, "Mechanical engineering handbook: CRCnetBASE 1999," 1999.

[2] E. Bozkurt, E. Kaya, and M. Tanoğlu, "Mechanical and thermal behavior of non-crimp glass fiber reinforced layered clay/epoxy nanocomposites," *Composites Science and Technology,* vol. 67, pp. 3394-3403, 2007.

[3] N. H. M. Zulfli and C. W. Shyang, "Flexural and Morphological Properties of Epoxy/Glass Fibre/Silane-Treated Organo-montmorillonite Composites," *Journal of Physical Science,* vol. 21, pp. 41-50, 2010.

[4] Y. Xu and S. V. Hoa, "Mechanical properties of carbon fiber reinforced epoxy/clay nanocomposites," *Composites Science and Technology,* vol. 68, pp. 854-861, 2008.

[5] M. Al-Qadhi, N. Merah, and Z. Gasem, "Mechanical properties and water uptake of epoxy–clay nanocomposites containing different clay loadings," *Journal of Materials Science,* pp. 1-7, 2013.

[6] M. Al-Qadhi, "Development and characterization of epoxy-clay nanocomposites " 2012.

[7] J.-J. Luo and I. M. Daniel, "Characterization and modeling of mechanical behavior of polymer/clay nanocomposites," *Composites Science and Technology,* vol. 63, pp. 1607-1616, 2003.

[8] C. Chen and T. B. Tolle, "Fully exfoliated layered silicate epoxy nanocomposites," *Journal of Polymer Science Part B: Polymer Physics,* vol. 42, pp. 3981-3986, 2004.

[9] B. Qi, Q. Zhang, M. Bannister, and Y.-W. Mai, "Investigation of the mechanical properties of DGEBA-based epoxy resin with nanoclay additives," *Composite structures,* vol. 75, pp. 514-519, 2006.

[10] T.-K. Oh, "The effect of shear force on microstructure and mechanical property of epoxy/clay nanocomposite," University of Florida, 2004.

[11] X. Li, Z.-J. Zhan, G.-R. Peng, and W.-K. Wang, "Nano-disassembling method—A new method for preparing completely exfoliated epoxy/clay nanocomposites," *Applied Clay Science,* vol. 55, pp. 168-172, 2012.

[12] H.-Y. Liu, G.-T. Wang, Y.-W. Mai, and Y. Zeng, "On fracture toughness of nano-particle modified epoxy," *Composites Part B: Engineering,* vol. 42, pp. 2170-2175, 2011.

[13] M. Zulfli and W. Chow, "MECHANICAL AND THERMAL BEHAVIOURS OF GLASS FIBER REINFORCED EPOXY HYBRID COMPOSITES CONTAINING ORGANO-MONTMORILLONITE CLAY," *Malaysian Polymer Journal,* vol. 7, pp. 8-15, 2012.

[14] I. Zaman, Q.-H. Le, H.-C. Kuan, N. Kawashima, L. Luong, A. Gerson, *et al.*, "Interface-tuned epoxy/clay nanocomposites," *Polymer,* vol. 52, pp. 497-504, 2011.

[15] X. Yao, D. Zhou, and H. Yeh, "Macro/microscopic fracture characterizations of SiO< sub> 2</sub>/epoxy nanocomposites," *Aerospace science and technology,* vol. 12, pp. 223-230, 2008.

[16] A. Brunner, A. Necola, M. Rees, P. Gasser, X. Kornmann, R. Thomann, *et al.*, "The influence of silicate-based nano-filler on the fracture toughness of epoxy resin," *Engineering fracture mechanics,* vol. 73, pp. 2336-2345, 2006.

[17] J. Ma, M.-S. Mo, X.-S. Du, P. Rosso, K. Friedrich, and H.-C. Kuan, "Effect of inorganic nanoparticles on mechanical property, fracture toughness and toughening mechanism of two epoxy systems," *Polymer,* vol. 49, pp. 3510-3523, 2008.

[18] M. M. Shokrieh, A. R. Kefayati, and M. Chitsazzadeh, "Fabrication and mechanical properties of clay/epoxy nanocomposite and its polymer concrete," *Materials & Design,* vol. 40, pp. 443-452, 2012.

[19] A. K. Subramaniyan and C. Sun, "Toughening polymeric composites using nanoclay: crack tip scale effects on fracture toughness," *Composites Part A: Applied Science and Manufacturing,* vol. 38, pp. 34-43, 2007.

[20] S. R. Ha, K. Y. Rhee, H. C. Kim, and J. T. Kim, "Fracture performance of clay/epoxy nanocomposites with clay surface-modified using 3-aminopropyltriethoxysilane," *Colloids and Surfaces A: Physicochemical and Engineering Aspects,* vol. 313, pp. 112-115, 2008.

[21] B. Akbari and R. Bagheri, "Deformation mechanism of epoxy/clay nanocomposite," *European polymer journal,* vol. 43, pp. 782-788, 2007.

[22] Kusmono, M. W. Wildan, and Z. A. Mohd Ishak, "Preparation and Properties of Clay-Reinforced Epoxy Nanocomposites," *International Journal of Polymer Science,* vol. 2013, p. 7, 2013.

[23] M. Quaresimin, M. Salviato, and M. Zappalorto, "Fracture and interlaminar properties of clay-modified epoxies and their glass reinforced laminates," *Engineering Fracture Mechanics,* vol. 81, pp. 80-93, 2012.

[24] L. Wang, K. Wang, L. Chen, Y. Zhang, and C. He, "Preparation, morphology and thermal/mechanical properties of epoxy/nanoclay composite," *Composites Part A: Applied Science and Manufacturing,* vol. 37, pp. 1890-1896, 2006.

[25] J. Golebiewski and A. Galeski, "Thermal stability of nanoclay polypropylene composites by simultaneous DSC and TGA," *Composites Science and Technology,* vol. 67, pp. 3442-3447, 2007.

[26] A. Lee and J. D. Lichtenhan, "Thermal and viscoelastic property of epoxy–clay and hybrid inorganic–organic epoxy nanocomposites," *Journal of Applied Polymer Science,* vol. 73, pp. 1993-2001, 1999.

[27] C. Zilg, R. Mülhaupt, and J. Finter, "Morphology and toughness/stiffness balance of nanocomposites based upon anhydride-cured epoxy resins and layered silicates," *Macromolecular Chemistry and Physics,* vol. 200, pp. 661-670, 1999.

[28] D. C. Lee and L. W. Jang, "Characterization of epoxy–clay hybrid composite prepared by emulsion polymerization," *Journal of applied polymer science,* vol. 68, pp. 1997-2005, 1998.

[29] T. Mohan, M. Ramesh Kumar, and R. Velmurugan, "Rheology and curing characteristics of epoxy–clay nanocomposites," *Polymer international,* vol. 54, pp. 1653-1659, 2005.

[30] T.-D. Ngo, M.-T. Ton-That, S. Hoa, and K. Cole, "Effect of temperature, duration and speed of pre-mixing on the dispersion of clay/epoxy nanocomposites," *Composites Science and Technology,* vol. 69, pp. 1831-1840, 2009.

[31] W. Liu, S. V. Hoa, and M. Pugh, "Fracture toughness and water uptake of high-performance epoxy/nanoclay nanocomposites," *Composites Science and Technology,* vol. 65, pp. 2364-2373, 2005.
[32] H. Alamri and I. M. Low, "Effect of water absorption on the mechanical properties of nano-filler reinforced epoxy nanocomposites," *Materials & Design,* vol. 42, pp. 214-222, 2012.
[33] J.-K. Kim, C. Hu, R. S. Woo, and M.-L. Sham, "Moisture barrier characteristics of organoclay–epoxy nanocomposites," *Composites Science and Technology,* vol. 65, pp. 805-813, 2005.
[34] O. Becker, R. J. Varley, and G. P. Simon, "Thermal stability and water uptake of high performance epoxy layered silicate nanocomposites," *European polymer journal,* vol. 40, pp. 187-195, 2004.
[35] N. Abacha, M. Kubouchi, K. Tsuda, and T. Sakai, "Performance of epoxy-nanocomposite under corrosive environment," *Express Polymer Letters,* vol. 1, pp. 364-369, 2007.
[36] F. Buehler and J. Seferis, "Effect of reinforcement and solvent content on moisture absorption in epoxy composite materials," *Composites Part A: Applied Science and Manufacturing,* vol. 31, pp. 741-748, 2000.
[37] S. Zainuddin, M. Hosur, Y. Zhou, A. Kumar, and S. Jeelani, "Durability studies of montmorillonite clay filled epoxy composites under different environmental conditions," *Materials Science and Engineering: A,* vol. 507, pp. 117-123, 2009.
[38] X. Kornmann, M. Rees, Y. Thomann, A. Necola, M. Barbezat, and R. Thomann, "Epoxy-layered silicate nanocomposites as matrix in glass fibre-reinforced composites," *Composites Science and Technology,* vol. 65, pp. 2259-2268, 2005.
[39] M. Al-Qadhi, N. Merah, and K. Mezghani, "Optimizing the Curing Process of Epoxy-Clay Nanocomposites," *Key Engineering Materials,* vol. 471, pp. 415-419, 2011.
[40] N. Merah and M. Al-Qadhi, "Effects of Processing Techniques on Morphology and Mechanical Properties of Epoxy-Clay Nanocomposites," *Advanced Materials Research,* vol. 652, pp. 167-174, 2013.
[41] "Annual Book of ASTM Standards, Plastics Materials," 1995.
[42] A. Yasmin, J. L. Abot, and I. M. Daniel, "Processing of clay/epoxy nanocomposites by shear mixing," *Scripta Materialia,* vol. 49, pp. 81-86, 2003.
[43] R. Velmurugan and T. Mohan, "Epoxy-clay nanocomposites and hybrids: synthesis and characterization," *Journal of Reinforced Plastics and Composites,* vol. 28, pp. 17-37, 2009.
[44] H. Miyagawa and L. T. Drzal, "The effect of chemical modification on the fracture toughness of montmorillonite clay/epoxy nanocomposites," *Journal of adhesion science and technology,* vol. 18, pp. 1571-1588, 2004.
[45] G. Swaminathan and K. Shivakumar, "Thermomechanical and fracture properties of exfoliated nanoclay nanocomposites," *Journal of reinforced plastics and composites,* vol. 30, pp. 256-268, 2011.
[46] S. Zunjarrao, R. Sriraman, and R. Singh, "Effect of processing parameters and clay volume fraction on the mechanical properties of epoxy-clay nanocomposites," *Journal of materials science,* vol. 41, pp. 2219-2228, 2006.

[47] S.-A. Gârea, H. Iovu, and A. Bulearca, "New organophilic agents of montmorillonite used as reinforcing agent in epoxy nanocomposites," *Polymer Testing,* vol. 27, pp. 100-113, 2008.
[48] W. Liu, S. Hoa, and M. Pugh, "Water uptake of epoxy–clay nanocomposites: Experiments and model validation," *Composites Science and Technology,* vol. 68, pp. 2066-2072, 2008.
[49] X. Kornmann, L. Berglund, R. Thomann, R. Mulhaupt, and J. Finter, "High performance epoxy-layered silicate nanocomposites," *Polymer Engineering & Science,* vol. 42, pp. 1815-1826, 2002.
[50] M. Li, "Temperature and moisture effects on composite materials for wind turbine blades," MONTANA STATE UNIVERSITY-BOZEMAN, 2000.
[51] M. M. Thwe and K. Liao, "Durability of bamboo-glass fiber reinforced polymer matrix hybrid composites," *Composites Science and Technology,* vol. 63, pp. 375-387, 2003.
[52] P. Joseph, M. S. Rabello, L. Mattoso, K. Joseph, and S. Thomas, "Environmental effects on the degradation behaviour of sisal fibre reinforced polypropylene composites," *Composites Science and Technology,* vol. 62, pp. 1357-1372, 2002.
[53] B. Ray, "Temperature effect during humid ageing on interfaces of glass and carbon fibers reinforced epoxy composites," *Journal of Colloid and Interface Science,* vol. 298, pp. 111-117, 2006.
[54] R. Selzer and K. Friedrich, "Mechanical properties and failure behaviour of carbon fibre-reinforced polymer composites under the influence of moisture," *Composites Part A: Applied Science and Manufacturing,* vol. 28, pp. 595-604, 1997.
[55] H. SEKINE, K. SHIMOMURA, and N. HAMANA, "Strength deterioration and degradation mechanism of glass chopped reinforced plastics in water environment," *JSME international journal. Ser. 1, Solid mechanics, strength of materials,* vol. 31, pp. 619-626, 1988.
[56] C. L. Schutte, "Environmental durability of glass-fiber composites," *Materials Science and Engineering: R: Reports,* vol. 13, pp. 265-323, 1994.

VITAE

Yasir Abdelhafiz Ali Elnaiem

Saudi Arabia, Dhahran, KFUPM Campus, 31261

+966540204223

+249918222336

yasirelnaiem1987@gmail.com

Date of Birth: 31/05/1987

Gender: Male.

Marital Status: Single.

Nationality: Sudanese.

Education

***M.S. in Mechanical Engineering,* May 2014**

King Fahd University of Petroleum and Minerals

Dhahran, Saudi Arabia.

Thesis Title: ***Enhancement of Mechanical and Physical properties of Silicate based Epoxy Nanocomposites.***

CGPA: 3.964 out of 4 scale

***B.S. in Mechanical Engineering,* June 2009**

University of Khartoum, *Khartoum, Sudan.*

Thesis Title: Design and Rehabilitation of Khartoum Refinery Pipeline (80Kilometers Long) and Estimating the permissible flow rate amounts.

Graduated with First Class (Honors), CGPA: 7.78 out of 10 scale

Publications

- Ahmad Rafiq, Muneer Al-Qadhi, Nesar Merah and Yasir Ali. Mechanical Behavior of Hybrid Glass Fibre/Epoxy clay Nanocomposites. 2014, Advanced Materials Research, 894, 336.
- Yasir Ali, Muneer Al-Qadhi, Nesar Merah and Ahmad Rafiq. Influence of Degassing and nanoclay Loading on Physical and Flexural Properties of Epoxy. Defect And Diffusion Forum.(Available July 2014).

Computer Skills

Ansys software for structural and thermal analysis

Minitab software for quality control/ quality assurance

Automatic computer aided drawing (**AutoCAD**)

Solid works

Mat lab

p3 (primavera project planning)

Microsoft office (word , excel , power point)

Experimental Techniques

XRD (X-Ray Diffraction).

OM (Optical Microscope).

SEM (Scanning Electron Microscope).

DSC (Differential Scanning Calorimetry) .

TGA (Thermal gravimetric analysis).

Universal Instron Testing Machine (for Mechanical Tests).

US (Ultra Sonication) Technique

HSM (High Shear Mixing) Technique.

Experience

Design Engineer (in Research and Development Center), 2010-2012

Marble Engineering Co., *Khartoum, Sudan*

Teacher Assistant 2009-2010

University of Khartoum, Mechanical Engineering Department.

Activities:

Conducting Thermodynamics/Fluids Mechanics tutorials.

Conducting Engineering Drawing tutorials

Teacher Assistant 2012-2014

King Fahd University of Petroleum And Minerals, Mechanical Engineering Department.

Activities:

work as a Teaching Assistant in Design and Manufacturing Lab for undergraduate students in which they learn how to work in teams and how to develop new ideas, brainstorming techniques, design and manufacturing stages.

References

Nesar Merah

King Fahd University of Petroleum & Minerals

Dhahran 31261, Saudi Arabia

nesar@kfupm.edu.sa

AbdelRahman N.Shuaib

King Fahd University of Petroleum & Minerals

Dhahran 31261, Saudi Arabia

arshuaib@kfupm.edu.sa

Omer Elfarouq Elbadawi

Khartoum University

Khartoum,Sudan

oeelbadawi@uofk.edu